Syntheses and Characterizations of Carbazole-Based Conjugated Polymers for Blue-light Emitting and Photovoltaic Applications

ZhongMin Geng

February 2016

Syntheses and Characterizations of Carbazole-Based Conjugated Polymers for Blue-light Emitting and Photovoltaic Applications

ZhongMin Geng

Doctoral Program in Materials Science

Submitted to the Graduate School of

Pure and Applied Sciences

in Partial Fulfillment of the Requirements

for the Degree of Doctor of Philosophy in Engineering

at the University of Tsukuba

CONTENTS

Chapter 1 Introduction 1
Reference 10
Chapter 2 Syntheses and characterizations of blue-light emitting π-conjugated polymers 12
Preface 12
2.1 N-substituted poly(4*H*-benzo[*def*]carbazole)s for blue photoluminescence 13
2.1.1 Background 13
2.1.2 Results and discussion 16
2.1.2.1 Synthesis 16
2.1.2.2 Solubility and thermal stability 17
2.1.2.3 Optical properties 18
2.1.2.4 Electrochemical properties 22
2.1.2.5 X-ray diffraction analysis 23
2.1.3 Summary 24
2.1.4 Experimental 25
2.1.4.1 General methods and instrumentations 25
2.1.4.2 Materials 25
2.1.4.3 Synthesises of monomers and polymers 25
2.2 Synthesis and characterization of D-A polymers having azine unit for blue light emission 35
2.2.1 Background 35
2.2.2 Results and discussion 35
2.2.2.1 Synthesis 35
2.2.2.2 Solubility and thermal stability 36
2.2.2.3 Optical properties 37
2.2.2.4 Electrochemical properties 39
2.2.4.5 Electroluminescence properties 40
2.2.3 Summary 42
2.2.4 Experimental 42
2.2.4.1 Fabrication and Measurement of OLED Devices 42
2.2.4.2 Materials 42
2.2.4.3 Synthesises of monomers and polymers 42
2.3 Efficient blue luminescence D-π-A type copolymers having sulfone/phosphine oxide unit 50
2.3.1 Background 50
2.3.2 Results and discussion 53
2.3.2.1 Synthesis 53
2.3.2.2 Solubility and thermal stability 55
2.3.2.3 Optical properties 55
2.3.2.4 Electrochemical properties 58
2.3.2.5 Electroluminescence properties 60
2.3.3 Summary 63

2.3.4 Experimental……...63
2.3.4.1 Fabrication and measurement of LEC devices ……..63
2.3.4.2 Materials and synthesis of monomers and polymers ……..64
Reference ……..……73
Chapter 3 Synthesis and photovoltaic performance of D-A structure narrow bandgap copolymers based on benzo[def]carbazole ……..……..76
3.1 Background ……..……...76
3.2 Results and discussion ……..…78
3.2.1 Synthesis ……..……78
3.2.2 Solubility and thermal stability ……..80
3.2.3 Optical properties ……..…81
3.2.4 Photovoltaic Properties ……..……...82
3.3 Summary ……..……86
3.4 Experimental ……..…87
3.4.1 General methods and instrumentations ……..….87
3.4.2 Fabrication and measurement of solar cell devices ……..…87
3.4.3 Materials ……..…88
3.4.4 Synthesis of monomers and polymers ……..……88
References ……..…92
Chapter 4 Conclusion..93
Publications ……..……..95
Acknowledgement ……..96

Chapter 1

Introduction

1.1 Background

Conjugated organic polymers are basically long chain macromolecules that have alternating carbon-carbon single and multiple bonds (might have cumulative double bonds) along the backbone. Electrons delocalized along the π-conjugated backbone contribute electrical conductivity of the polymers. Shirakawa, MacDiarmid, and Heeger have discovered electrical conductivity of a polyacetylene film upon chemically doping with bromine in 1977 [1, 2]. For the last few decades, conjugated polymers have attracted considerable interest around the world and considerable developments have been made. Many different conjugated polymers have been extensively studied, such as polythiophenes and polypyrroles, among others, as shown in Fig. 1-1 [3-9].

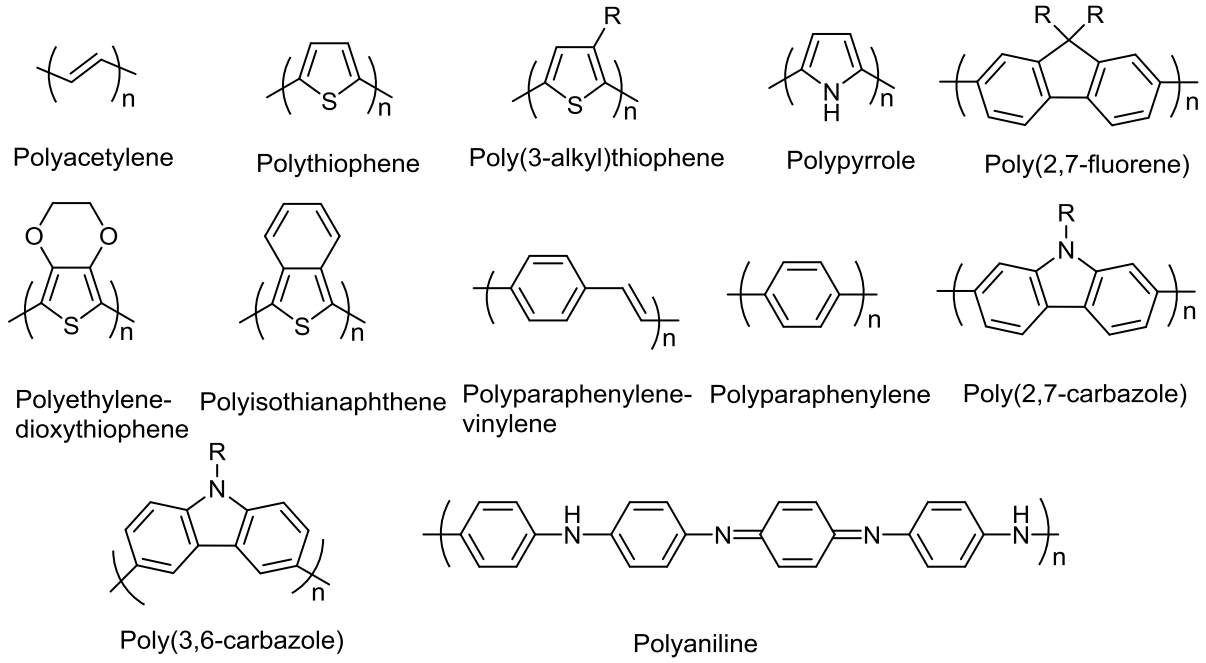

Fig. 1-1 Chemical structures of several commonly used conjugated polymers

Originally it was thought these types of polymer systems would serve as substitution for highly conductive metals, such as copper and aluminum. However, the conjugated polymers were chemically unstable in atmospheric conditions. In 1990, the first polymer light-emitting diodes (PLED) was reported by Burroughes and co-workers [10], which was a demonstration of practical applications in the field of conjugated polymers. Subsequently, conjugated polymers have been successfully used in a wide range of applications including thin film transistors [11], chemical sensors for massive analyses [12, 13], light emitting electrochemical cells (LEC) [14-16] and organic photovoltaic cells (OPV) [17, 18]. Electronic devices, such as organic light-emitting devices and photovoltaic cells are currently under development for practical uses. Conjugated polymers are not only unique materials for basic researches on organic semiconductors but also promising materials for industrial applications, since they can be easier to make devices for energy conservation and energy generation than alternative materials. These electroactive and photoactive conjugated polymers have an advantage of easy tuning their properties through simple chemical

modifications [19, 20].

Carbazole is a heterocyclic aromatic organic compound having a dibenzopyrrole structure. The structure and numbering of positions in carbazole (**Cz**) are shown in Fig. 1-2. Conjugated polymers with carbazole unit have interesting optical and electronic properties such as photoconductivity and photorefractivity [21, 22]. A number of carbazole derivatives have been synthesized and electrochemical and spectroscopic properties of them have been extensively investigated [23-25]. Carbazole has been widely used as a functional building unit of conjugated polymers for light-emitting layers in OLED and LEC devices utilized as active layer components because they are thermally stable and show blue photo- and electroluminescence due to the large bang gap of the biphenyl unit. The optical and electrical properties of polymers based on carbazole can be easily tuned by substitution on the 2-, 3-, 6-, 7- and 9*H*-positions.

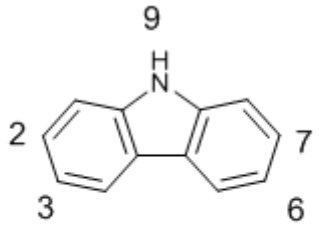

Cz

Fig. 1-2 The structures and numbering system of **Cz**

In this thesis, two different research issues in the field of organic electronics were studied. New materials based on carbazole for blue-light emitting and photovoltaic applications are developed and their basic properties and prospect in applications are described.

Three major objectives of the present study are listed hereunder:

1. Synthesis and characterization of deep-blue light emitting and photovoltaic materials
2. Study on structural and physical properties of synthesized polymers
3. Exploration of the suitability of these polymers in the field of optoelectronic devices

1.2 Syntheses and characterizations of blue-light emitting π-conjugated polymers.

Blue light-emitting materials are of great significance for their unique applications in flat-panel displays and high-density information storage. Especially in full-color displays, the short-wavelength emission can serve as an excitation source for emission over the whole visible range [26]. Therefore, development of high-efficiency blue emitting materials is important. However, to develop stable pure blue polymeric emitters for PLEDs and LECs with their color coordinates in the Commission Internationale de L'Eclairage (CIE) chromaticity diagram within the standard blue (CIE: x< 0.15; y< 0.15) are still rare, It is also difficult to achieve high efficiency and good charge balance due to the large energy bandgap (E_g) of these materials [27]. In chapter 2, the design, syntheses and properties of new blue-light emitting π-conjugated materials are discussed.

1.2.1 N-substituted poly(4*H*-benzo[*def*]carbazole)s for blue photoluminescence

Since the first report on blue PLEDs device fabricated with poly(*p*-phenylene) (PPP) in 1992 [28], a large

number of blue-light-emitting materials have been developed. Among the vast kinds of blue-light-emitting polymers, fluorene-based conjugated polymers have been recognized as a promising class of them, because of their good processability for making thin film devices and high fluorescent performances in the solid state [29]. Unfortunately, polyfluorenes have usually emitted impure blue colors due to emissions from contaminants such as excimers and keto-defects in addition to principal emission from β-phase, when they are applied as emitting layer materials in PLEDs [30]. Since early in this century, poly(2,7-carbazole)s regarded as a strained planner poly(4,4'-biphenylylene) with an imino-bridge have been considered as a new candidate for blue light emitting materials comparable to the fluorene-based polymers, because they have band gaps appropriate for blue light emissions and smaller ionization potentials compared to polyfluorenes [25].

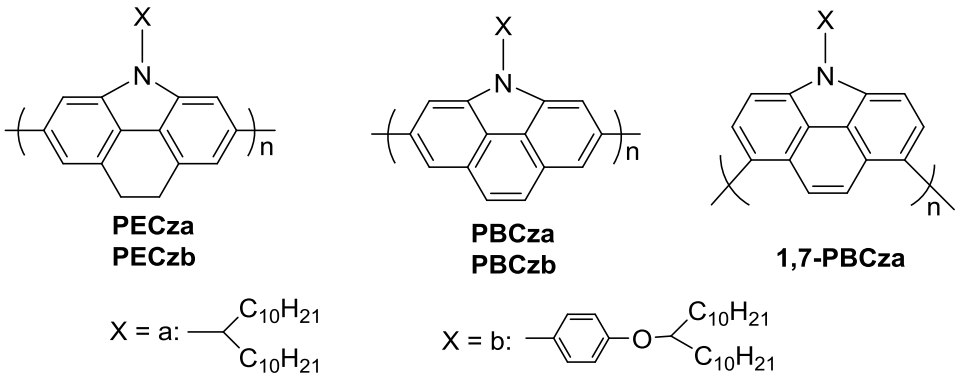

Fig. 1-3 The structures of **PECza, PECzb, PBCza, PBCzb** and **1,7-PBCza**

In this section, a new series of N-alkyl and N-phenyl substituted poly(carbazole)s having a 4,5-ethenylene bridge, poly(4*H*-benzo[*def*]carbazole)s (**PBCza, PBCzb** and **1,7-PBCza**) (Fig. 1-3), were synthesized. Derivatives of 4,5-ethylene bridged poly(carbazole) (**PECza** and **PECzb**) were also synthesized for comparison. Basic properties of these polymers were compared with those of poly(2,7-carbazole)s and poly(3,6-carbazole)s.

This new series of carbazole-based homopolymers had enough high molecular weights, good solubility in common organic solvents, amorphous nature in the film state, and good thermal stability showing about 400 °C of temperature at 5 wt% loss in TGA. The band gaps of these polymers were in the range of 2.77-3.15 eV that were appropriate for bluish light emissions. The fluorescence maxima of these polymers in $CHCl_3$ and in film state were in the ranges of 419-456 and 426-495 nm, respectively (Fig. 1-4). The CIE(*x*, *y*) values of **PECza**, **PECzb**, **PBCza** and **PBCzb** in $CHCl_3$ were almost identical to (0.15, 0.05) in the region of deep blue. In film state, CIE values for **PECz** (0.16, 0.15) were in the region of blue, while CIE values for **PBCz** (0.19, 0.21) shifted toward greenish blue but in the region of blue. The shift of the PL color is ascribed to the stronger intermolecular interaction between the larger planar units of **PBCz** as suggested in the XRD results. Poly(2,6-benzocarbazole)s (**PBCza** and **PBCzb**) showed unexpectedly blue-shifted absorption bands, the shallower E_{HOMO}, and the wider E_g compared with those of poly(2,7-carbazole) regardless of having the larger π-conjugation in the monomer unit. It is considered that **PECz** and **PBCz** have potential to be applied in PLEDs as blue-light emitting materials.

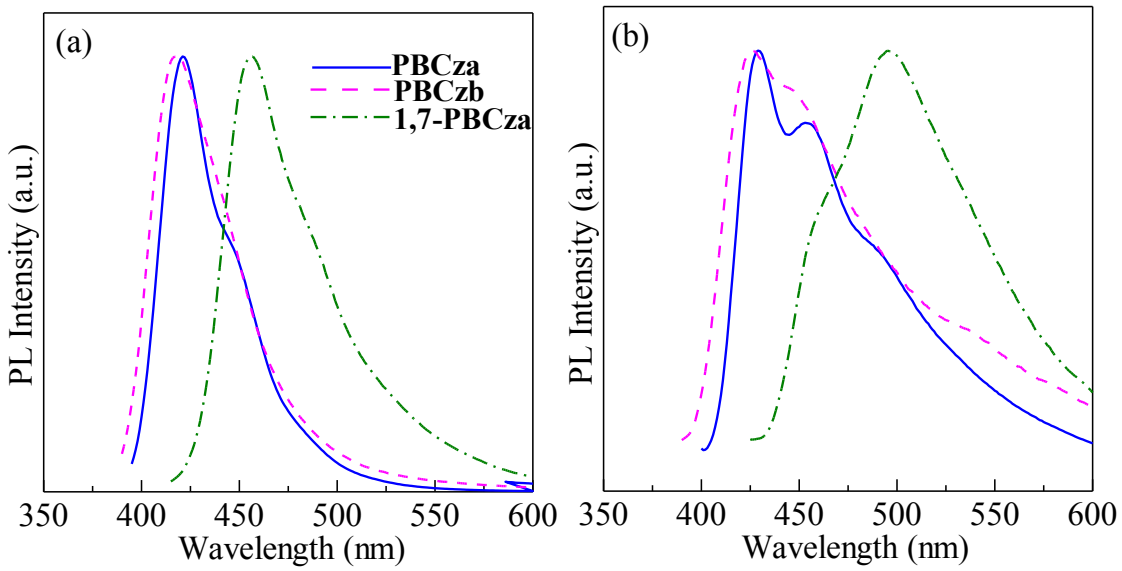

Fig.1-4 PL spectra of **PBCza**, **PBCzb** and **1,7-PBCza** in $CHCl_3$ (a) and flim state (b).

On the other hand, **1,7-PBCz** is found to have unique properties that the absorption and emission bands were observed in considerable longer region in wavelength with moderate Φ_{fl}, which were quite different from those of poly(3,6-carbazole)s. **1,7-PBCza** showed the shallow E_{HOMO} and narrow E_g, fluorescing in blue green color (CIE (0.20, 0.33)) in the film state. Therefore, the **1,7-BCz** unit would rather be applied in a donor component of donor-acceptor-type narrow band gap polymers for organic solar cells.

1.2.2 Synthesis and characterization of D-A polymers having azine unit for blue light emission.

In this part, the design of p-type conjugated polymers by incorporating electron-withdrawing groups, such as azine unit, seems to be a straightforward strategy to tune carrier injection and transporting properties of known materials. A new D-A system has been designed, which is expected to heighten both the energy levels of the E_{LUMO}, giving rise to a series of intriguing properties such as improved resistance to oxidation, facilitated electron injection, and ambipolar characteristics.

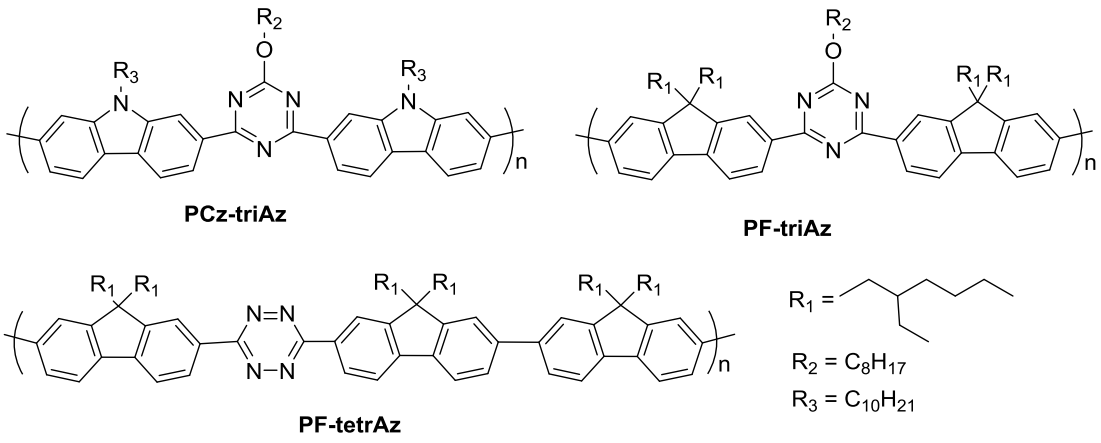

Fig. 1-5 The structures of **PCz-triAz**, **PF-tetrAz** and **PF-triAz**

The synthesises, characterizations and photoluminescence properties of these polymers, **PCz-triAz**, **PF-tetrAz** and **PF-triAz,** shown in Fig. 1-5 were investigated. Herein, the carbazole/fluorene sequences were selected as D for the reason of good thermal and electrochemical stability, high fluorescence yield and facile chemical functionalization, while 1,2,4,5-tetrazine (**tetrAz**) and 1,3,5-triazine (**triAz**) were chosen as A for their electron deficiency.

Three types of D-A copolymers were designed and synthesized by combination of an electron donor unit of carbazole/fluorene sequences and an electron acceptor azine unit such as 1,2,4,5-tetrazine and 1,3,5-triazine. They have good thermal stability showing about at 360 °C with 5 wt% loss in TGA. Three copolymers exhibited intense blue photoluminescence with emission peak maxima at 438, 437 and 421 nm in $CHCl_3$, respectively (Fig. 1-6). In the film state, the emission peak of **PCz-triAz** was observed at 495 nm, while the emission peak maxima at 451 nm for **PF-tetrAz** and 422 nm for **PF-triAz**. The CIE values for **PF-tetrAz** (0.16, 0.12) and **PF-triAz** (0.16, 0.07) were in the region of blue, while CIE values for **PCz-triAz** (0.2, 0.32) shifted toward blueish green. These polymers exhibited good fluorescence quantum efficiencies in $CHCl_3$ (Φ_{fl} = 0.62, 0.63, 0.97).

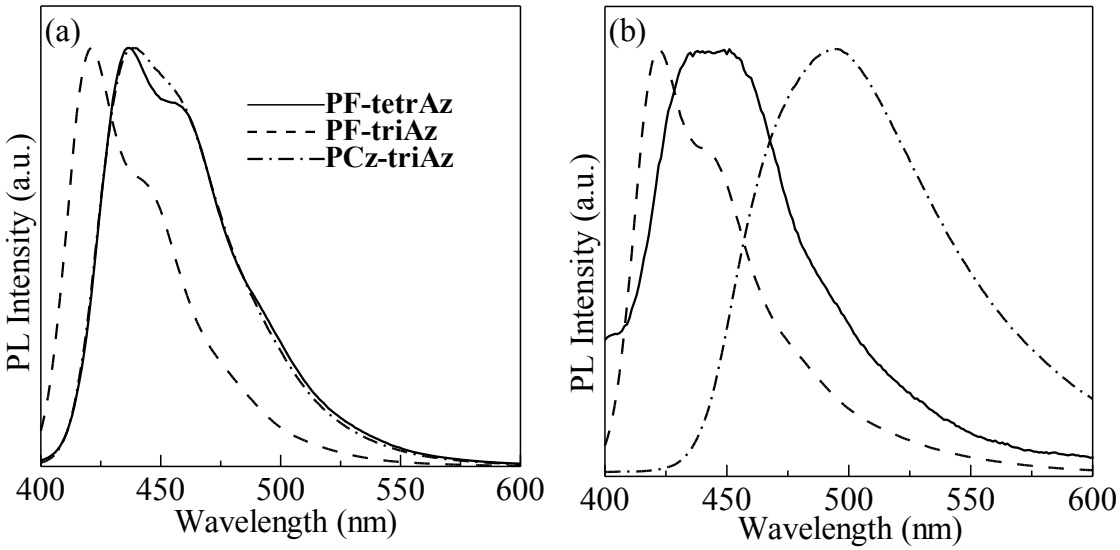

Fig. 1-6 PL spectra of **PCz-triAz**, **PF-tetrAz** and **PF-triAz** in $CHCl_3$ (a) and flim state (b)

Compared to **PCz-triAz (**E_{HOMO} = –5.47eV, E_g = 2.77 eV**), PF-tetrAz** and **PF-triAz** showed deep E_{HOMO} (–5.83, –6.0 eV) for hole transport and proper E_g (2.96, 3.12 eV) for blue emission. According to above results, these D-A copolymers have a great potential to be applied in PLED as the blue-light emitting materials.

1.2.3 Efficient blue luminescence D-π-A type copolymers having sulfone/phosphine oxide unit

Donor-π-acceptor (D-π-A) type copolymers have aroused much interest because they show high fluorescent quantum yields and good charge carrier transport properties for using as hole- and electron-transporting moieties [31]. It has been proved that use of D-π-A type molecules can enhance the electroluminescence efficiencies of PLEDs [32, 33]. However, the D-π-A structure can enlarge π conjugation and lead the intramolecular charge transfer trend to fluorescence red shifts [34]. In this work, to design

efficiencies pure blue electroluminescence materials, it is important to suitably control the enlargement of π-conjugation and trend of the intramolecular charge-transfer inside the molecules.

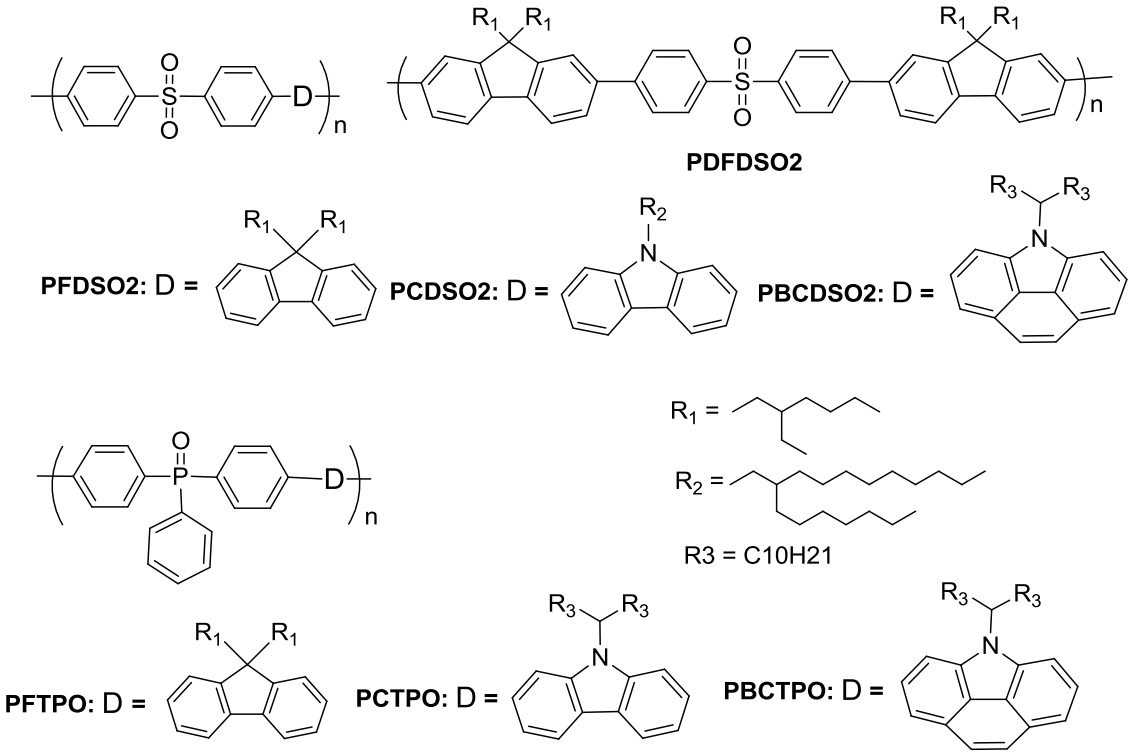

Fig. 1-7 The structures of **PFDSO2**, **PCDSO2**, **PBCDSO2**, **PDFDSO2**, **PFTPO**, **PCTPO** and **PBCTPO**

Herein, a series of D-π-A type copolymers were designed and synthesized (Fig. 1-7). The widely used hole-transporting moiety, fluorene/carbazole, was selected as the electron-donor for its relatively mild electron-donating ability, the sulfone/phosphine oxide unit as an acceptor unit for these excellent electron injection properties. Moreover, the sulfone and phosphine oxide with two rotatable phenyl rings, serve as a breaker of π-conjugation, because of their conformations of tetrahedral (sulfone)/ trigonal-pyramidal (phosphine oxide), which could effectively confine the π-conjugation of the molecules. All of these copolymers were fabricated simple LECs devises with structure of ITO/ PEDOT:PSS (40 nm)/ emission layer + ionic liquid/ Al (100 nm). The electroluminescence properties of these materials were investigated.

A new series of D-π-A type copolymers were designed and synthesized. They have good thermal stability showing at about 400 °C with 5 wt% loss in TGA. These copolymers exhibited intense blue photoluminescence with emission peak maxima at 380 ~ 447 nm in $CHCl_3$. In the film state, the emission peaks of polymers were observed at 404 ~ 449 nm. All the polymers exhibited good fluorescence quantum efficiencies in $CHCl_3$. The polymers basically have good molecular weights, good solubility in common organic solvents, deep HOMO levels (5.58-6.05 eV) (Fig. 1-8), a conjugated polymers that shows excellent fluorescence quantum efficiency, and proper bandgaps (E_g) for blue emission. These polymers have been used as emitting layer materials of LECs devices that have a configuration of ITO/ PEDOT:PSS/ polymer+ionic liquid /Al. The LEC device embedded with **PDFDSO2** shows intense luminance of about 1080 cd m^{-2}, while the devices embedded with **PFDSO2** and **PCDSO2** show less luminance.

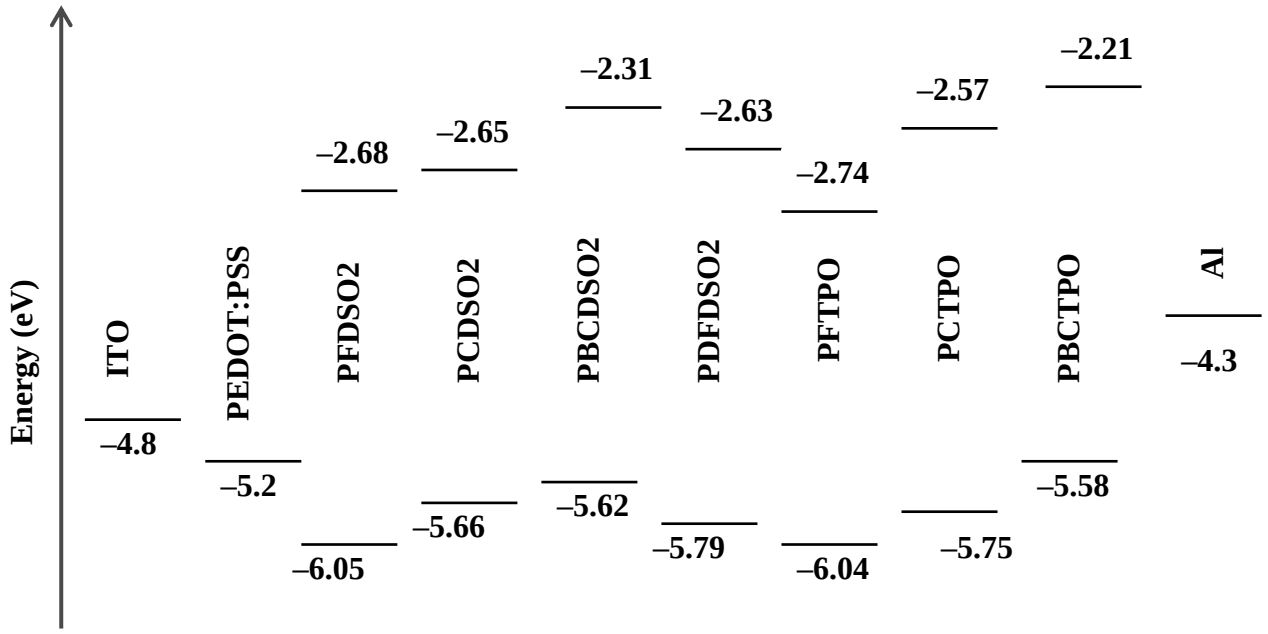

Fig. 1-8 Energy band diagrams of the polymers

1.3 Synthesises and photovoltaic performance of D-A structure narrow bandgap copolymers based on benzo[*def*]carbazoles

The bulk heterojunction (BHJ) OPV as renewable energy system has attracted much attention because of their many unique features such as low cost, easy fabrication, light weight and good flexibility [35, 36]. To obtain high-performance OPV, it is necessary to design and synthesize conjugated polymers with desired properties, such as (1) sufficient solubility for uniforming thin film, (2) miscibility with an n-type material, (3) narrow band gap for matching the high photon flux region of the solar spectrum to ensure enough light harvesting and (4) high hole mobility for efficient charge transport [37, 38]. Narrow-bandgap π-conjugated polymers can harvest sunlight and increase the exciton concentration in the active layers, leading to an increase of short-circuit current (J_{sc}) [39]. Therefore, new polymers with proper properties of photoabsorption, semiconducting, energy levels, and stability have been attempted to be developed up to date.

In this section, a simple strategy, synthesize D-A type narrow-bandgap copolymers was used. Benzo[*def*]carbazole is chosen as the donor unit for this new attempt for synthesis of the D-A type copolymers. Because this π-extended planar fused aromatic ring, benzo[*def*]carbazole, will be helpful for intensifying intermolecular π overlap and thus narrowing π-π stacking, which can contribute to enhancing charge carrier mobility. Moreover, the bridging nitrogen-atom in benzo[*def*]carbazole offer a center for solubilizing functionality and tuning of energy levels of molecular orbitals by introducing appropriate substituents.

Three D-A type benzo[*def*]carbazole-based copolymers, **PBCDTBT**, **PBCDTTPD** and **PBCBTDPP,** shown in Fig. 1-9 were synthesized and characterized. Herein, benzothiadiazole (**BT**), thienopyrrole-4,6-dione (**TPD**) and 1,4-diketopyrrolopyrrole (**DPP**) were chosen as the typical A unit. The effects of the different segments on the absorption spectra, energy levels, and the photovoltaic performances of the copolymers are also studied.

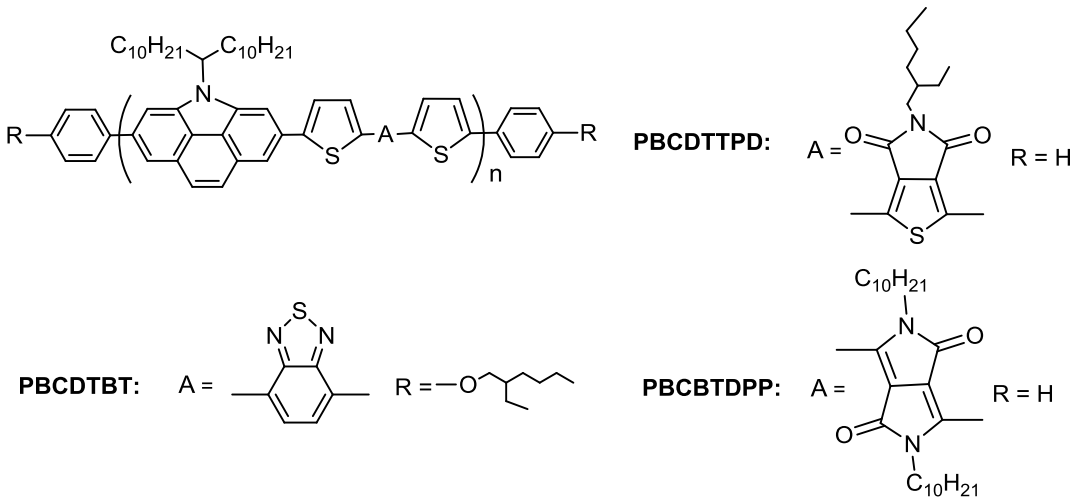

Fig. 1-9 The structures of **PBCDTBT**, **PBCDTTPD** and **PBCBTDPP**

Three copolymers exhibited broad absorption bands in UV and visible regions from 350 to 700 nm with optical band gaps in the range of 1.68-2.11 eV, which overlapped with the major region of the solar spectrum. Photoelectron yield spectroscopy revealed that these copolymers showed energy levels of the highest occupied molecular orbital in the range of –5.22 eV to –5.34 eV, which could provide good air stability and high open circuit voltages in photovoltaic applications. The BHJ OPV using **PBCDTBT** exhibited the PCE value of 1.42 % with J_{sc} of 6.41 mA cm^{-2}, FF of 0.33, and V_{oc} of 0.67 V (Fig. 1-10), while those using **PBCDTTPD** and **PBCBTDPP** showed PCE of 0.98 % (with J_{sc} = 2.52 mA cm^{-2}, FF = 0.50, V_{oc} = 0.77 V), and 0.75 % (with J_{sc} = 2.10 mA cm^{-2}, FF = 0.51, V_{oc} = 0.70 V, respectively. The higher performance of **PBCDTBT**:$PC_{70}BM$ (1:3) than **PBCDTTPD**:$PC_{70}BM$ (1:3), and **PBCBTDPP**:$PC_{70}BM$ (1:4) was almost ascribed to the higher J_{sc} of the former device, because the blend films of **PBCDTBT**:$PC_{70}BM$ showed a rather smooth surface and more intimate mixing, which certainly increased the heterojunction interface area for exciton dissociation and consequently led to the higher J_{sc} of OPV.

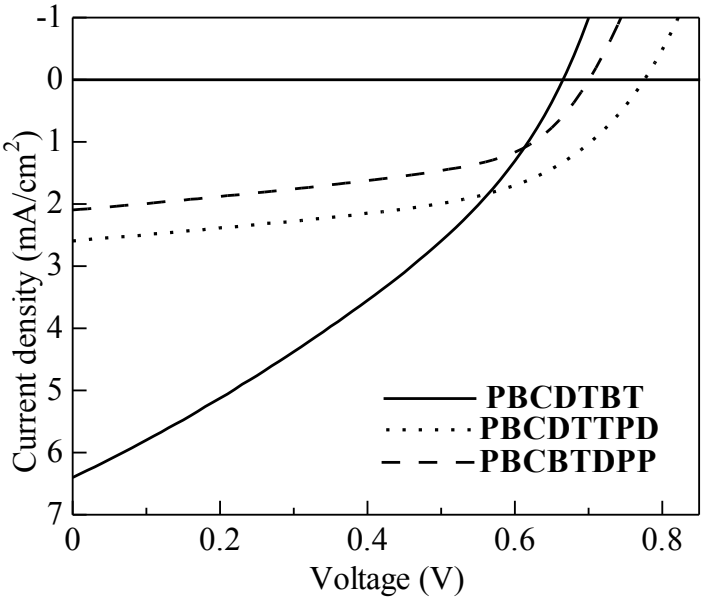

Fig. 1-10 *J*−*V* curves of BHJ solar cell of **PBCDTBT:**$PC_{70}BM$ (1:3), **PBCDTTPD:**$PC_{70}BM$ (1:3) and **PBCBTDPP:**$PC_{70}BM$ (1:4) under illumination of AM 1.5 G.

1.4 Summary

This thesis majors in the synthesis, characterization and the testing of new, environmentally stable materials based on carbazole for blue-light emitting and photovoltaic applications.

The chapter 2, firstly, new type of poly(carbazole)s for blue light emitting are succeeded to synthesize by bridging of 4,5-ethenylene to a carbazole unit to construct benzo[*def*]carbazole. These homopolymers exhibited high molecular weights, good solubility in common organic solvents, amorphous nature in the film state and good thermal stability. The CIE (*x*, *y*) values of them in film state were almost showed in the region of blue. The properties of poly(carbazole)s were studied to be applied in PLEDs as blue-light emitting materials. In second part, new D-A coplymers have been designed and synthesized using carbazole/fluorene sequences as the electron donor unit and azine unit as electron acceptor. These polymers showed intense blue photoluminescence with CIE values in the region of blue and showed good fluorescence quantum efficiencies in $CHCl_3$. Polyfluorenes having electron accepting azine units (**PF-tetrAz** and **PF-triAz)** showed shallow E_{HOMO} for hole transport and proper E_g for blue emission. These D-A copolymers will be applied in the blue-light emitting materials. In third part, a series of D-π-A type copolymers were designed and synthesized. The sulfone/phosphine oxide with rotatable phenyl rings served as controlling of the π-conjugation to well-preserve blue emission. The polyfluorenes with electron accepting sulfone units **(PDFDSO2)** based LECs devices showed intense luminance of about 1080 cd m^{-2}.

Chapter 3 presented synthesis, characterization and OPV study of a novel benzo[*def*]carbazole based polymers with the D-A architecture with three different electron acceptors. These copolymers exhibited broad absorption bands in UV and visible regions with narrow optical band gaps. The absorption bands overlapped with the major region of the solar spectrum. Compared with **PBCDTTPD** and **PBCBTDPP** based BHJ OPV, The OPV using poly(benzo[*def*]carbazole) having electron accepting benzothiadiazole units **(PBCDTBT)** exhibited the highest PCE, which ascribed to the high J_{sc} of the device. The mixing morphology of film **PBCDTBT**:$PC_{70}BM$ showed a rather smooth surface and more intimate mixing led to the high J_{sc} of OPV. Benzo[*def*]carbazole is a kind of effective donor segment for the D-A type OPV according to initial performances of these copolymers.

Reference

[1] H. Shirakawa, E. J. Louis, A. G. MacDiarmid, C. K. Chiang, A. Heeger, Chem. Commun. 578 (1977).

[2] J. Kim, D. T. McQuade, A. Rose, Z. Zhu, T. M. Swager, J. Am. Chem. Soc. 123 (2001) 11488-11489.

[3] H. S. O. Chan, S. C. Ng, Prog. Polym. Sci. 23 (1998) 1167-1231.

[4] R. D. McCullough, Adv. Mater. 10 (1998) 93-116.

[5] L. Dall'Acqua, C. Tonin, R. Peila, F. Ferrero, M. Catellani, Synth. Met. 146 (2004) 213-221.

[6] L. Groenendaal, F. Jonas, D. Freitag, H. Pielartzik, J. R. Reynolds, Adv. Mater. 2000, 12, 481-494.

[7] F. Carpi, D. De Rossi, Opt. Laser Technol. 38 (2006) 292-305.

[8] L. J. Rothberg, M. Yan, F. Papadimitrakopoulos, M. E. Galvin, E. W. Kwock, T. M. Miller, Synth. Met. 80 (1996) 41-58.

[9] S. J. Pomfret, P. N. Adams, N. P. Comfort, A. P. Monkman, Polymer. 41(2000) 2265-2269.

[10] J. H. Burroughes, D. D. C. Bradley, A. R. Brown, R. N. Marks, K. Mackay, R. H. Friend, P. L. Burns, A. B. Holmes, Nature. 347 (1990) 539-541.

[11] J. J. M. Halls, C. A. Walsh, N. C. Greenham, E. A. Marseglia, R. H. Friend, S. C. Moratti, A. B. Holmes, Nature. 376 (1995) 498-500.

[12] D. L. Ellis, M. R. Zakin, L. W. Bernstein, M. F. Rubner, Anal. Chem. (1996) 68 807-816.

[13] K. J. Albert, N. S. Lewis, C. L. Schauer, G. A. Sotzing, S. E. Stitzel, T. P. Vaid, D. R. Walt, Chem. Rev. 100 (2000) 2595-2626.

[14] Q. Pei, G. Yu, C. Zhang, Y. Yang, A.J. Heeger, Science. 269 (1995) 1086-1088.

[15] A. Pertegas, D. Tordera, J. J. Serrano-Pérez, E. Ortí, H. J. Bolink, J. Am. Chem. Soc. 135 (2013) 18008-18011.

[16] Z. B. Yu, L. Li, H. Gao, Q. Pei, Sci. China: Chem. 56 (2013) 1075-1086.

[17] E. Bundgaard, F. C. Krebs, Sol. Energy Mater. Sol. Cells. 91 (2007) 954-985.

[18] S. Gunes, H. Neugebauer, N. S. Sariciftci, Chem. ReV. 107 (2007) 1324-1338.

[19] J. F. Morin, N. Drolet, Y. Tao, M. Leclerc, Chem. Mater. 16 (2004) 4619-4626.

[20] N. Leclerc, S. Sanaur, L. Galmiche, F. Mathevet, A. J. Attias, J. L. Fave, J. Roussel, P. Hapiot, N. Lemaître, B. Geffroy, Chem. Mater. 17 (2005) 502-513.

[21] R. M. Adhikari, R. Mondal, B. K. Shah, D. C. Neckers, J. Org. Chem. 72 (2007) 4727-4732.

[22] J. X. Yang, X. T. Tao, C. X. Yuan, Y. X. Yan, L. Wang, Z. Liu, Y. Ren, M. H. Jiang, J. Am. Chem. Soc. 127 (2005) 3278-3279.

[23] M. Kijima, R. Koguchi, S. Abe, Chem. Lett. 34 (2005) 900-901.

[24] R. Koguchi, N. Kobayashi, M. Kijima, Macromolecules. 42 (2009) 5946-5952.

[25] M. Kijima, IOP Conf. Series: Materials Science and Engineering. 54 (2014) 012017.

[26] J. Ye, Z. Chen, M. K. Fung, C. J. Zheng, X. M. Ou, X. H. Zhang, Y. Yuan, C. S. Lee, Chem. Mater. 25 (2013) 2630-2637.

[27] T. Horii, T. Shinnai, K. Tsuchiya, T. Mori, M. Kijima, J. Polym. Sci. Polym. Chem. 50 (2012) 4557-4562.

[28] G. Grem, G. Leditzky, B. Ullrich, G. Leising, Adv. Mater. 4 (1992) 36-37.

[29] D. Neher, Macromol. Rapid. Commun. 22 (2001) 1365-1385.

[30] F. B. Dias, J. Morgado, A. L. Macanita, F. P. da Costa, H. D. Burrows, A. P. Monkman, Macromolecules. 39 (2006) 5854-5864.

[31] J. Ye, Z. Chen, M. K. Fung, C. J. Zheng, X. M. Ou, X. H. Zhang, Y. Yuan, C. S. Lee, Chem. Mater. 25 (2013) 2630-2637.

[32] Q. S. Zhang, J. Li, K. Shizu, S. P. Huang, S. Hirata, H. Miyazaki, C. Adachi, J. Am. Chem. Soc. 134 (2012) 14706-14709.
[33] C. Liu, Y. Gu, Q. Fu, N. Sun, C. Zhong, D. G. Ma, J. G. Qin, C. L. Yang, Chem. Eur. J., 18 (2012) 13828-13835.
[34] S. L. Lin, L. H. Chan, R. H. Lee, M. Y. Yen, W. J. Kuo, C. T. Chen, R. J. Jeng, Adv. Mater. 20 (2008) 3947-3952.
[35] K. M. Coakley, M. D. McGehee, Chem. Mater. 16 (2004) 4533-4542.
[36] A. Heeger, J. Chem. Soc. Rev., 39 (2010) 2354-2371.
[37] Z. Deng, L. Chen, F. Wu, Y. Chen, J. Phys. Chem. C., 118 (2014) 6038-6045.
[38] J. S. Wu, Y. J. Cheng, M. Dubosc, C. H. Hsieh, C. Y. Chang, C. S. Hsu, Chem. Commun. 46 (2010) 3259-3261.
[39] H. Zhou, L. Yang, S. Stoneking, W. You, ACS Applied Materials & Interfaces. 2 (2010) 1377-1383.

Chapter 2

Syntheses and Characterizations of Blue-light Emitting π-Conjugated Polymers

Preface

Organic electronics are considered to play an important role in our lives due to the development and increased understanding of organic semiconductors. Organic semiconductors offer a wide variety of advantages such as low cost, emission in visible (Vis) range, and tunability compared to the traditional inorganic semiconductors and conductors. Organic semiconductors have found many application areas for photo- and electro- active organic materials including organic light emitting diodes (OLEDs) [1-3], light emitting electrochemical cells (LECs) [4-6], organic solar cells [7, 8], organic thin-film transistors [9] and high-density information storage (Fig.1).

Fig.2-1 a) OLEDs [10]; b) organic solar cells [11]; c) organic thin-film transistors [12].

In the past decades, blue light-emitting materials have attracted considerable scientific and commercial interest for their potential utility in full-color displays and high-density information storage. Especially in full-color displays, development of high-efficiency blue-light-emitting materials is important among three basic colors of blue, green, and red. Because the short-wavelength emission can serve as an excitation source for emissions over the whole visible range [13]. However, to develop pure blue polymeric emitters with their color coordinates in the Commission Internationale de L'Eclairage (CIE) chromaticity diagram within the standard blue (CIE: x< 0.15; y< 0.15) (Fig.2-2) are still rare since wide bandgap (E_g) of these materials makes the achievement of high efficiency and pure blue light emission have been incompatible in the OLED

devices difficult [14]. In this chapter, the design, syntheses and properties of new blue-light emitting π-conjugated materials are discussed.

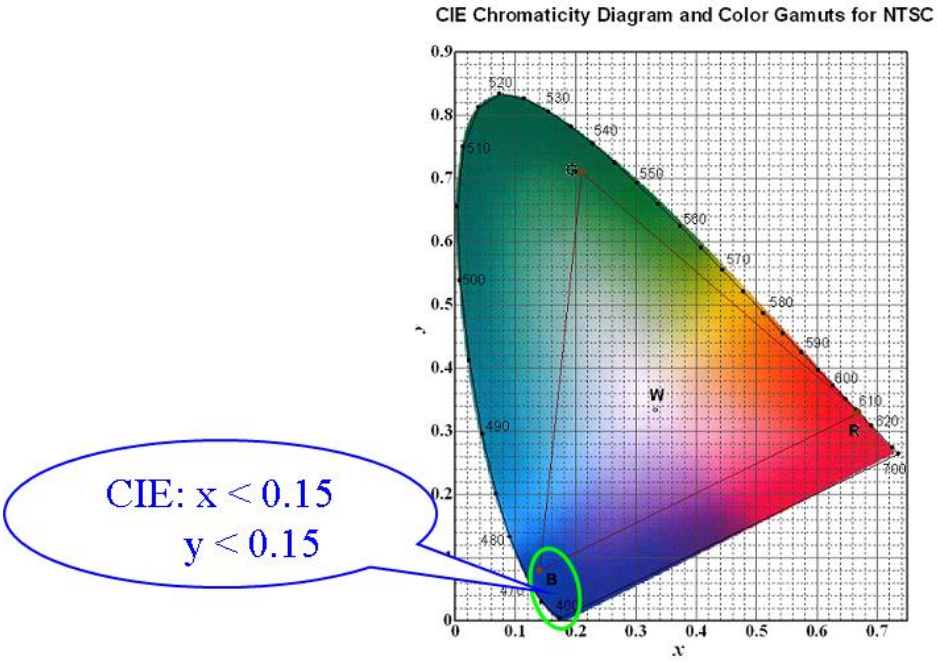

Fig. 2-2 CIE diagram.

The main objectives of this work are as follows:

1. Design and synthesize pure blue emission materials with high the brightness, efficiency and color stability
2. 4,5-Ethenylene bridged poly(carbazole)s synthesized for blue photoluminescence
3. Synthesis of new D-A type of copolymers for blue light emission having azine unit
4. Design of D-π-A structure copolymers having sulfone/phosphine oxide unit for blue luminescence

2.1 N-substituted poly(4*H*-benzo[*def*]carbazole)s for blue photoluminescence

2.1.1 Background

Polymer light emitting diodes (PLEDs) are type of solid state light-emitting devices. The basic PLEDs consists of a stack of thin organic layers sandwiched between a transparent anode and a metallic cathode (Fig. 2-3). The organic layers comprise an emissive layer and a conductive layer. When an appropriate voltage is applied to the device, electrons are injected from the cathode and holes are injected from the anode. To enhance electron injection, cathodes are often made of disadvanced work function materials, such as aluminum or calcium. Conversely, to enhance hole injection, anodes are constructed from advanced high work function materials. The typical anode material is indium/tin oxide (ITO).

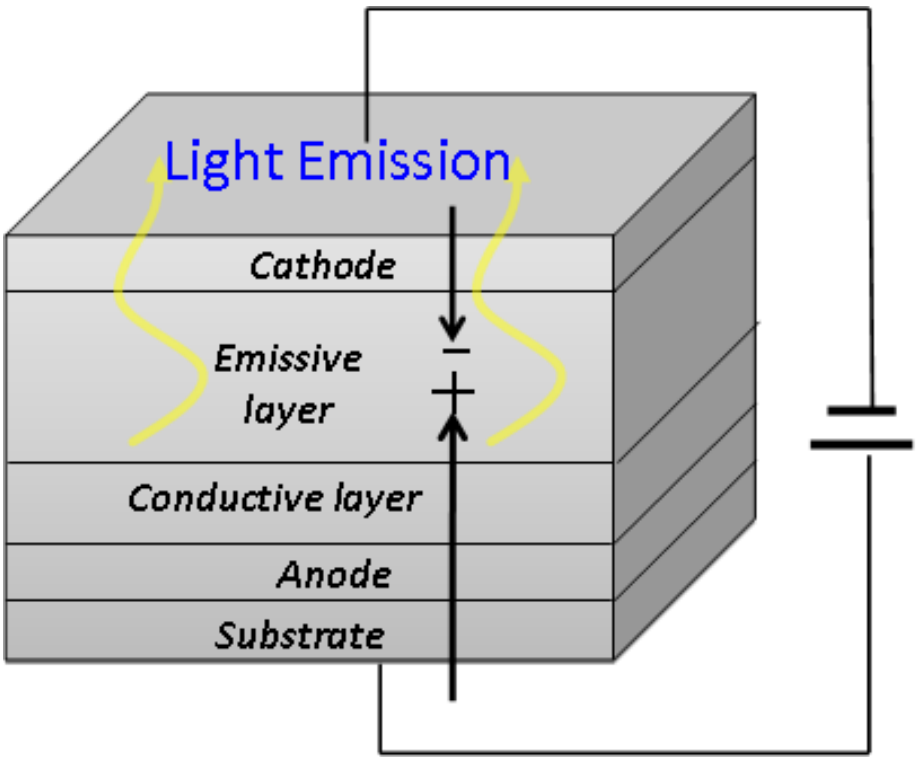

Fig. 2-3 Structure of PLED device

The process of light emission creation by PLED is as follows (Fig. 2-4):

When voltage is applied to PLED device, electrical current flows from the cathode to the anode through the organic layers. The cathode gives electrons to emissive layer and the anode removes electrons from the conductive layer. The holes leaved by removing electrons from the conductive layer need to be filled with the electrons in the emissive layer. The holes jump to emissive layer and recombine with the electrons. As the electrons drop into the holes, they release their extra energy in the form of a photon of light. The PLED emit light.

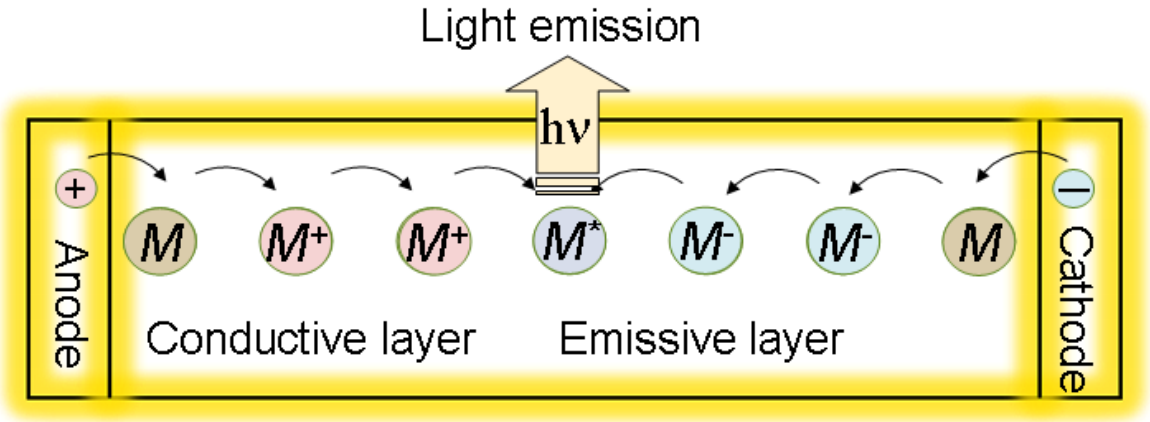

Fig. 2-4 Light creation by PLED

Organic semiconductors used for PLED show many advantages. First of all, compare to inorganic semiconductors, PLED are more cost-effective due to the nearly unlimited synthetic abundance of organic

materials and nomally thinner film thickness, typically ~ 100 nm thick. Secondly, PLEDs are compatible with low-cost and large-area manufacturing processes. The organic layers of PLEDs can be processed by wet procession without high vacuum environment such as roll-to-roll process [15,16], casting, spin coating, and ink-jet printing [17-19]. These processes only require at room temperature, which fabricates significantly easier than most inorganic materials. Moreover, the extremely flexibility of organic materials makes them intrinsically compatible with flexible substrates. Hence, various low-cost substrates, such as glass, plastic, and stainless steel foils, can be used for PLED devices. Furthermore, PLEDs also have excellent display performances such as a fast response time, a wide viewing angle, a high contrast, and low power consumption, compared to the properties of inorganic semiconductors.

In 1992, the first blue PLED device was reported, which was fabricated with poly(*p*-phenylene) (PPP) (as shown in Fig. 2-5). After that, a large number of materials for blue-light-emitting have been developed [20-24]. Fluorene-based (Fig.2-5) conjugated polymers have been recognized as a promising class among the blue-light-emitting polymers, because they are good processable and show rarely high fluorescent performances in the solid states [25, 26]. Unfortunately, the PLEDs used polyfluorene as a emitting layer emitted impure blue colors due to emissions from contaminates such as excimers and keto-defects in addition to principal emission from β-phase [27].

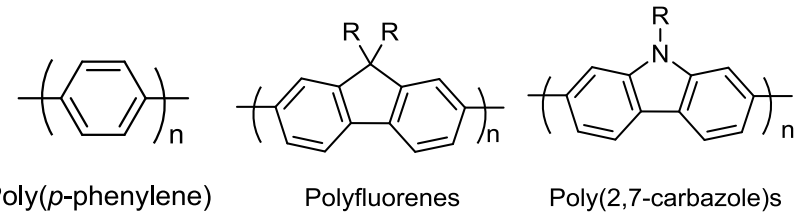

Fig. 2-5 The structures of poly(*p*-phenylene), polyfluorene and poly(2,7-carbazole)s

Carbazole is a heterocyclic aromatic organic compound with a tricyclic structure, which consisting of two six-membered benzene rings fused on either side of a five-membered nitrogen-containing ring. Carbazole is a conjugated unit that can construct materials with interesting optical and electronic properties such as photoconductivity and photorefractivity [28, 29], which has attracted significant attention for the application. Since early in this century, poly(2,7-carbazole)s (Fig.2-5) regarded as a poly(4,4'-biphenylylene) consisting of the strained planner unit of imino-bridged biphenylylene, have been considered as a new candidate for blue light emitting materials comparable to the fluorene-based polymers, because they have wide band gaps appropriate for blue light emissions, sharp emission bands in the solid film state, and smaller ionization potentials compared to polyfluorenes [30-34]. Furthermore, poly(2,7-carbazole) derivatives showed shallower highest occupied molecular orbital (HOMO) level around –5.5 eV [35, 36], which might be more advantageous than polyfluorenes for hole injection from the ITO anode in the PLEDs device.

In this section, a new series of poly(carbazole)s for stable light emitting material are attempted to synthesize by bridging of 4,5-ethylene and 4,5-ethenylene to carbazole (**Cz**) unit to construct ethylenecarbazole (**ECz**) and benzo[*def*]carbazole (**BCz**) structures as shown in Fig. 2-6. The corresponding poly(benzo[*def*]carbazole)s (**PBCz**) were obtained by dehalogenative polyconsensation of 2,6-dibrominated and 1,7-dibrominated **BCz** monomers. In parallel, for comparison, poly(8,9-dihydro-2,6-benzo[*def*] carbazole)s (**PECz**), were also synthesized from the precursor derivatives of the ethylene bridged carbazoles (**ECz**). Basic properties of these polymers were compared with those of corresponding poly(2,7-carbazole)s and poly(3,6-carbazole)s.

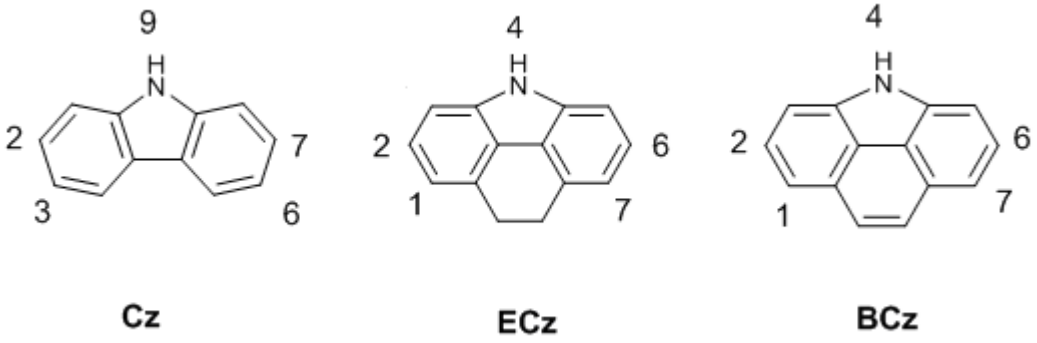

Fig. 2-6 The structures and numbering system of **Cz**, **ECz** and **BCz**

2.1.2 Results and discussion

2.1.2.1. Synthesis

The general synthetic routes toward the monomers and polymers are shown in Scheme 2-1**,** Scheme 2-2 and Scheme 2-3. The 1-decylundecyl group was introduced into N-position of **3** by the procedure reported previously [37], giving **4a**. The introduction of the *p*-(1-decylundecyloxy)phenyl group at N-position of **3** was carried out according to the procedure in our previous report [38], giving **4b.** The oxidation of **4a** and **4b** with DDQ were carried out to give monomers **5a** and **5b**, respectively. The debromination of **5a** and successive bromination of **6a** were performed to obtain **7a.** In order to obtain **PECza**, **PECzb**, **PBCza**, **PBCzb** and **1,7-PBCza,** the homopolymerizations of **4a**, **4b**, **5a**, **5b** and **7a** by Yamamoto reaction [39] were carried out, respectively.

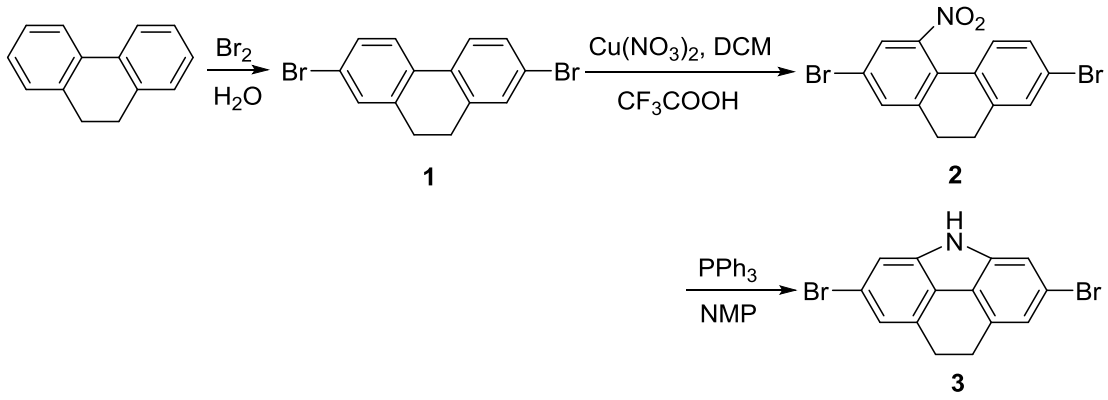

Scheme 2-1. Synthetic route of 2,6-dibromo-8,9-dihydrobenzo[*def*] carbazole

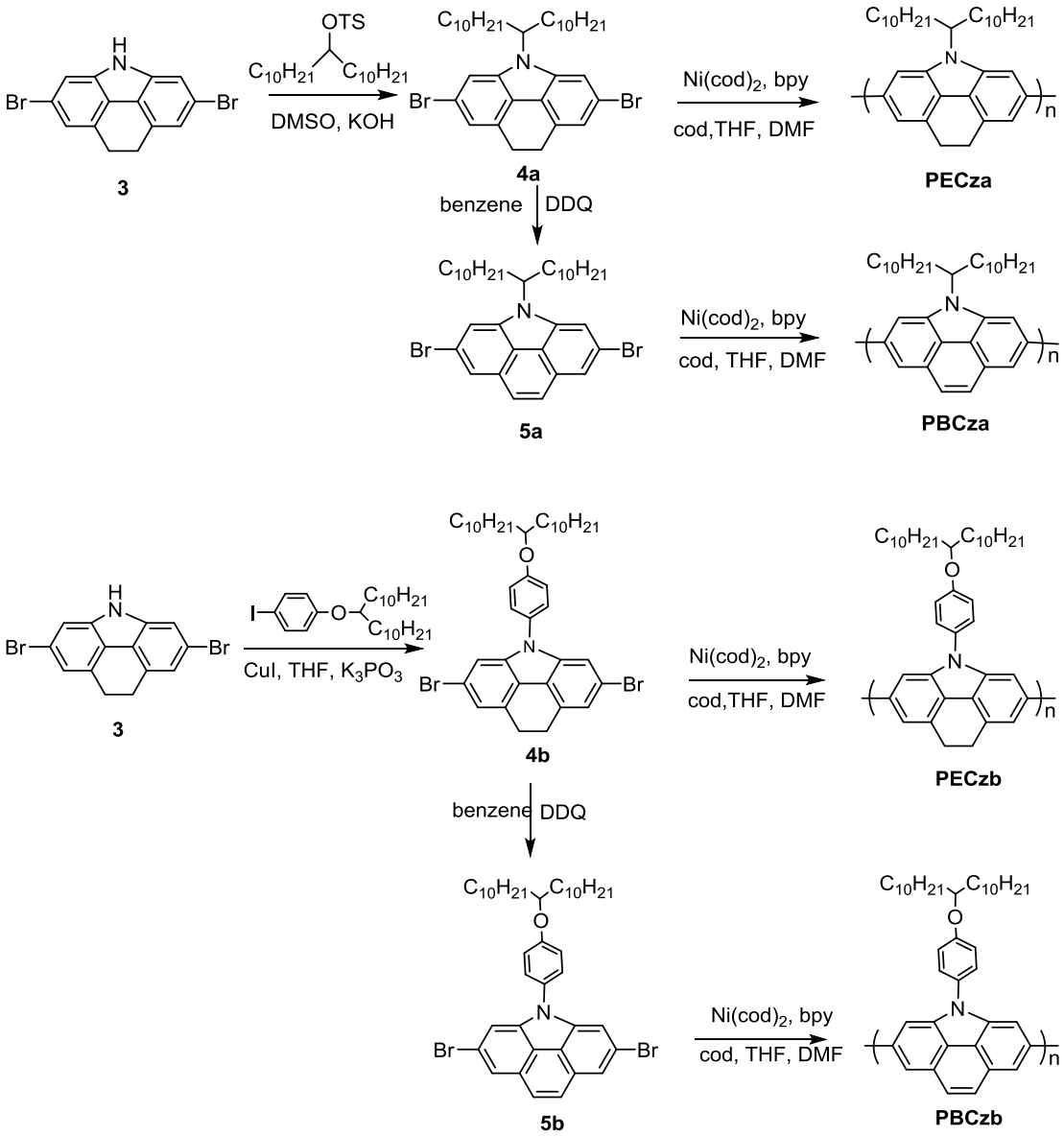

Scheme 2-2 Synthetic routes of **PECz** and **PBCz**

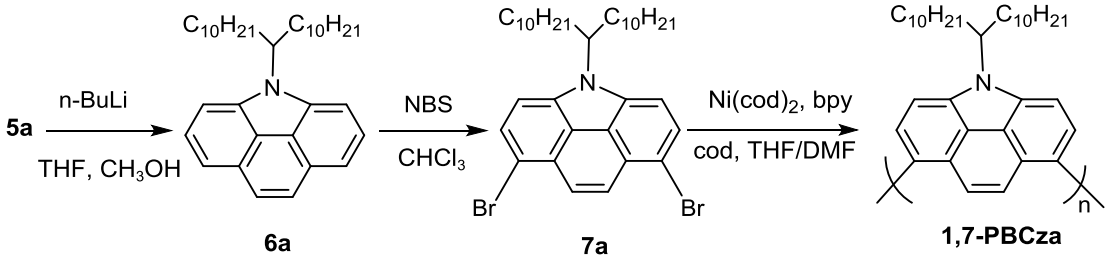

Scheme 2-3 Synthetic route of **1,7-PBCza**

2.1.2.2. Solubility and thermal stability

All of the polymers have a good solubility in usual organic solvents such as toluene, THF, $CHCl_3$, and so forth. The gel permeation chromatography (GPC) results were summarized in Table 2-1. They showed good

processability to make thin cast films. The number-average molecular weight (M_w) of the polymers were larger than 10 kg mol^{-1}, the polydispersities (M_w/M_n) about 1.5, and the degree of polymerization (DP) higher than 27. The thermal gravimetric analysis (TGA) results are shown in Fig. 2-7. These polymers had a good thermal stability, and their temperatures of 5wt % loss in TGA (T_d) were around 400 °C, respectively. According to T_d results, it is easy find that the polymers with N-phenyl side group showed lower T_d values. This result suggests that thermal stabilities of N-phenyl side group substituted polymers (**PECzb** and **PBCzb**) are lower than those of N-alkyl substituted ones (**PECza**, **PBCza**, **and 1,7-PBCza**), which might be due to suppression of intimate interaction among polymer chains by steric effect of the rigid N-phenyl group.

Table 2-1 GPC and TGA results of the polymers.

Polymer	M_n (kg mol^{-1})	M_w (kg mol^{-1})	M_w/M_n	DP[a]	T_d (°C)[b]
PECza	78.3	107.7	1.38	161.4	464
PECzb	121.1	229.7	1.89	209.8	377
PBCza	13.3	18.9	1.42	27.6	422
PBCzb	299.2	528.2	1.76	520.3	366
1,7-PBCza	13.0	19.9	1.57	27.0	436

[a]DP was estimated from M_n.

[b]Temperature of 5 % weight loss determined by TGA under an argon atmosphere.

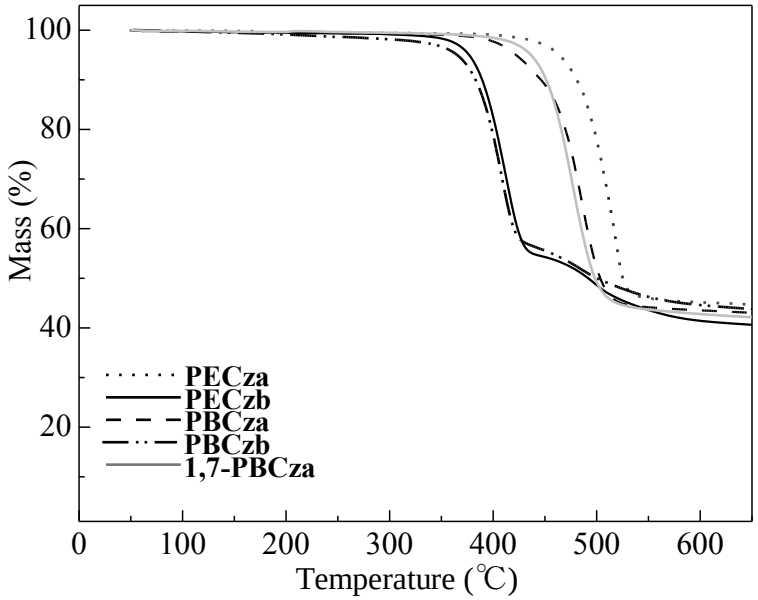

Fig. 2-7 TGA curves of the polymers.

2.1.2.3. Optical properties.

The UV-vis absorption and photoluminescence (PL) spectra of dilute solution and thin films of **PECza**, **PECzb**, **PBCza**, **PBCzb** and **1,7-PBCza** were investigated, and the results are shown in Fig. 2-8 and Fig. 2-9. The UV-vis and PL spectra data for all polymers are summarized in Table 2-2.

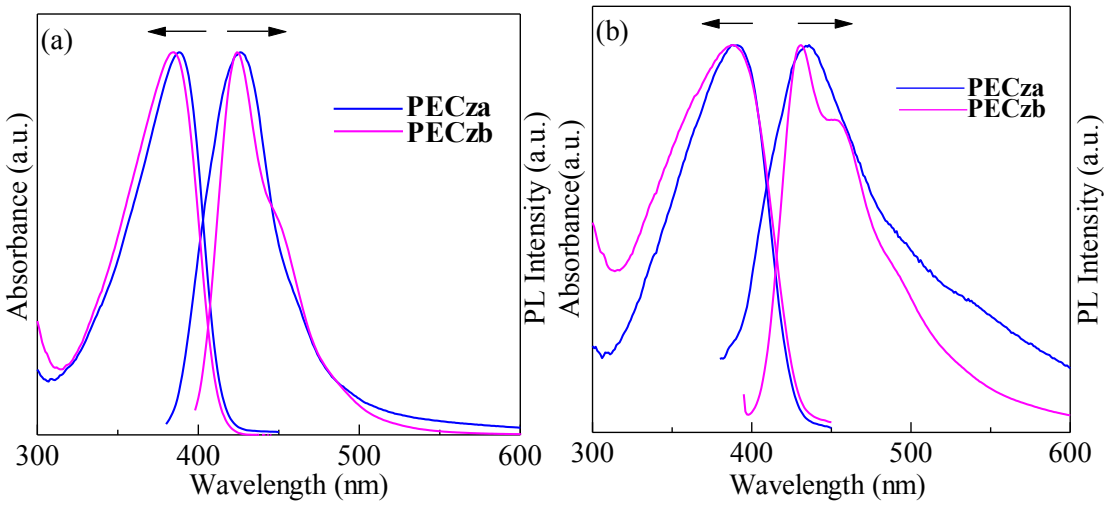

Fig. 2-8 UV-vis and PL spectra of **PECza** and **PECzb** in $CHCl_3$ (a) and film state (b).

The absorption and PL spectra of **PECza** and **PECzb** in $CHCl_3$ are depicted in Fig. 2-8a. The absorption maxima ($\lambda_{max,\ Abs}$) in wavelength at 388 nm for **PECza** and 385 nm for **PECzb** are due to π-π* transition of the conjugated main chains. The $\lambda_{max,\ Abs}$ of the series of **PECz** were similar with those of poly(2,7-carbazole)s (**PCz**) ($\lambda_{max,\ Abs}$ = 387 nm) [40, 41]. The PL emission peak maxima ($\lambda_{max,\ Em}$) in $CHCl_3$ were observed at 426 nm for **PECza** and 424 nm for **PECzb**. The fluorescence quantum yields (Φ_{fl}) of **PECza** and **PECzb** (Φ_{fl} =0.45, 0.67) were lower than those of **PCz** (Φ_{fl} ≈1) in $CHCl_3$. The Stokes shifts ($\Delta\lambda = (\lambda_{max,\ Em}) - (\lambda_{max,\ Abs})$) in $CHCl_3$ were 38 nm for **PECza** and 39 nm for **PECzb,** which were slightly larger than those of **PCz** (ca. 35 nm) [42]. These larger Δλ is due to the lager structural change between ground and excited states, which might affect lowering Φ_{fl}.

Table 2-2 Optical properties, HOMO-LUMO energy gaps, and the energy levels of the polymers.

Polymer	$\lambda_{max,\ Abs}$ (nm)		$\lambda_{max,\ Em}$ (nm)		$\Delta\lambda^a$ (nm)	Φ_{fl}	E_g (eV)	E_{HOMO} (eV)	E_{LOMO} (eV)
	in $CHCl_3$	film	in $CHCl_3$	film					
PECza	388	388	426	436	38	0.45	2.96	–5.59	–2.54
PECzb	385	389	424	431	39	0.67	2.94	–5.53	–2.59
PBCza	358	361	421	429	63	0.30	3.15	–5.50	–2.44
PBCzb	361	361	419	426	58	0.48	3.05	–5.49	–2.44
1,7-PBCza	396	398	456	495	60	0.45	2.77	–5.37	–2.60

[a]Stokes shifts measured in $CHCl_3$.

The absorption and PL spectra of **PECza** and **PECzb** in thin solid film state are shown in Fig. 2-8b. The absorption spectra of **PECza** and **PECzb** were almost the same each other, and their energy gaps (E_g) estimated from the onset of the absorption spectra in the film state were 2.94 and 2.96 eV, respectively, which were almost the same with those of **PCz** (2.92 eV).

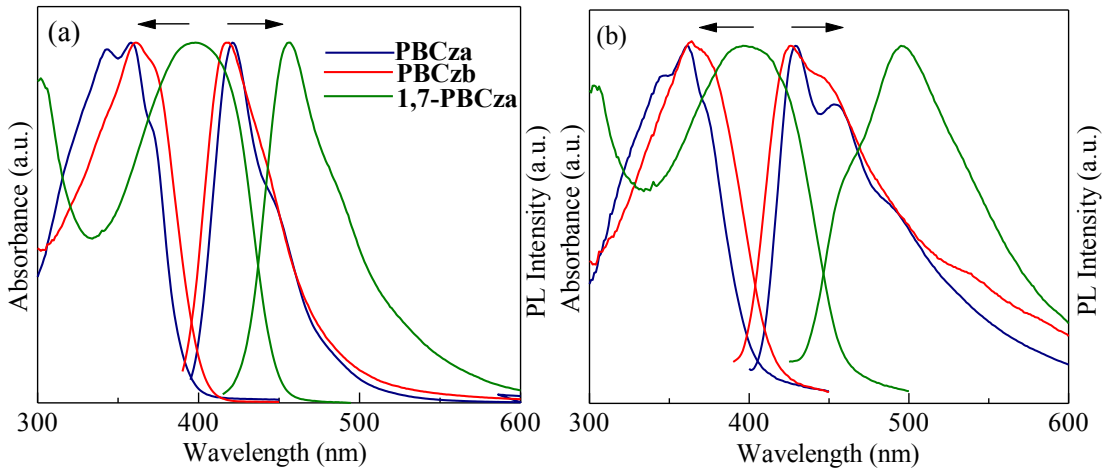

Fig. 2-9 UV-vis and PL spectra of **PBCza**, **PBCzb** and **1,7-PBCza** in $CHCl_3$ (a) and film state (b).

The absorption and PL spectra of **PBCz** in $CHCl_3$ are shown in Fig. 2-9a. The $\lambda_{max,\ Abs}$ were observed at 358 nm for **PBCza** and 361 nm for **PBCzb** owing to π-π* transition of conjugated polymer main chains. Unexpectedly, the $\lambda_{max,\ Abs}$ showed a blue-shifted in comparison to **PCz** and poly(2,7-phenanthrene)s [43, 44], although they include an extended π-conjugated structure of phenanthrene in the unit. Consequently, both of **PBCza** and **PBCzb** fluoresced in deep-blue color in $CHCl_3$, and the $\lambda_{max,\ Em}$ of them were observed at 421 nm and 419 nm, respectively. The Δλ of **PBCza** and **PBCzb** in $CHCl_3$ were 63 and 58 nm, which were larger than those of **PECz** and **PCz** (35-39 nm). The larger Δλ of **PBCza** and **PBCzb** might be lead to the lower Φ_{fl} than those of of **PECz** and **PCz.** According these results, the 4,5-ethenylene bridge and the N-bridge cooperatively control each ring strain and 2,7-conjugation of polycarbazole and polyphenanthrene i.e., an optimized structure of **BCz** calculated by DFT showed both features of an elongated C-N linked **Cz** and a strained phenanthrene with the imino bridge as shown in Fig. 2-10, Table 2-3 and Table 2-4.

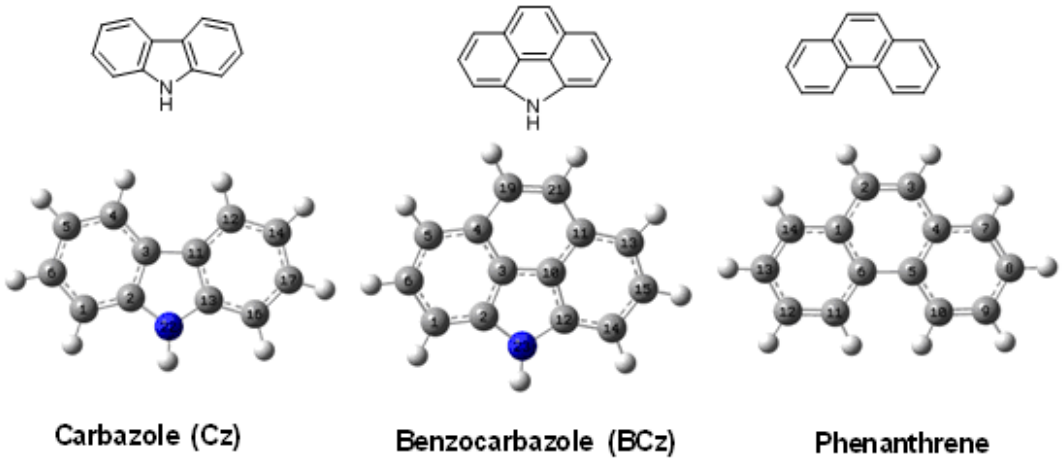

Fig. 2-10 Optimized geometric structures with numbering atoms of **Cz**, **BCz** and **Phenanthrene** obtained by DFT/B3LYP/6–31G*.

Table 2-3 Selected optimized bond angles of **Cz**, **BCz** and Phenanthrene obtained by DFT/B3LYP/6–31G*

	Cz	**BCz**	**Phenanthrene**
Bond angle(°)[a]			
C_1-C_2-C_3	121.9	117.4	
C_2-C_3-C_{11}	106.7		
C_{11}-C_{13}-N_{22}	108.4		
C_4-C_3-C_{11}	134.1		
C_2-C_3-C_{10}		108.8	
C_{10}-C_{12}-N_{23}		106.4	
C_4-C_3-C_{10}		123.8	
C_5-C_6-C_{11}			123.0
C_4-C_5-C_6			119.1
C_6-C_{11}-C_{12}			121.4

[a]The data for comparison are in the same color rows.

Table 2-4 Selected optimized bond lengths of **Cz**, **BCz** and Phenanthrene obtained by DFT/B3LYP/6–31G*

	Cz	**BCz**	**Phenanthrene**
Bond length (Å)[a]			
C_1-C_2	1.3967	1.3906	
C_2-C_3	1.42078	1.4079	
C_3-C_{11}	1.45038		
C_{13}-N_{22}	1.38663		
C_3-C_{10}		1.3883	
C_{12}-N_{23}		1.4055	
C_{11}-C_{12}			1.4045
C_5-C_6			1.4614
C_6-C_{11}			1.4104

[a]The data for comparison are in the same color rows.

The absorption and PL spectra of **PBCza** and **PBCzb** in the thin film state were shown in Fig. 2-9b. The $\lambda_{max,\ Abs}$ of **PBCza** and **PBCzb** were slightly red-shifted than those in $CHCl_3$, because of some aggregations or interactions between the polymer chains in the thin film state. The E_g of **PBCza** and **PBCzb** were 3.15 and 3.05 eV, respectively, which were larger than those of **PECz** and **PCz**. The large E_g values of **PBCz** were lead to the blue shifts of $\lambda_{max,\ Abs}$ in solution. Moreover, the PL spectra of **PBCz** showed tailing bands in the thin film state that might involve vibronic feature and excimeric emissions in the longer wavelength region.

Fig. 2-9a also shows the absorption and PL spectra of **1,7-PBCza** in $CHCl_3$. Comparison with $\lambda_{max,\ Abs}$ of poly(3,6-carbazole)s ($\lambda_{max,\ Abs}$ = ca. 310 nm), the $\lambda_{max,\ Abs}$ of **1,7-PBCza** in $CHCl_3$ was observed at 396 nm, which was considerably red-shifted [45, 46]. This large red-shift is owing to effect of the 4,5-ethenylene bridging at the **Cz** ring with extension of extend π-conjugation along the main chain through the 1,7-linkage and the bridge. The $\lambda_{max,\ Em}$ of **1,7-PBCza** was observed at 456 nm, and the Δλ was 60 nm. Interestingly, The **1,7-PBCza** showed surprisingly high Φ_{fl} (= 0.45) compared with those (Φ_{fl} = 0.04 to 0.06) for poly(3,6-carbazole)s in dichloromethane [46]. This result suggests that the stabilization of energy states of

1,7-PBCza by the extended π-conjugation might be responsible for the enhancement of quantum yields. The absorption and PL spectra of **1,7-PBCza** in the thin film state are also shown in Fig. 2-9b. The $\lambda_{max,\ Abs}$ of **1,7-PBCza** showed larger red-shifted compared with those of **PECz**, **PBCz**, and **PCz**. Compared with E_g of poly(3,6-carbazole)s (3.2 eV) [46], the E_g of **1,7-PBCza** is exceptionally narrow. The emission band of **1,7-PBCza** showed much broader and shifted to lower energy compared with thatof poly(3,6-carbazole)s ($\lambda_{max,\ Em}$ = 426 nm) [46]. According to these photophysical results, we can find that **1,7-PBCza** is a potential polymer having light-emitting as well as hole transporting functions to be applied in PLEDs.

2.1.2.4. Electrochemical properties

Electrochemical properties of **PECza**, **PECzb**, **PBCza**, **PBCzb** and **1,7-PBCza** were investigated by cyclic voltammetry (CV) and their voltammograms are shown in Fig. 2-11 and related data are summarized in Table 2-2. The energy levels of HOMO (E_{HOMO}) of **PECza** (–5.59 eV) and **PECzb** (–5.53 eV) were estimated from the onset potential of an oxidation peak, which were similar to those of **PCz** (ca. –5.6 eV) [42]. The E_{HOMO} of **PBCza** and **PBCzb** were –5.50 and –5.49 eV, respectively, which were shallower than those of **PECz**. **1,7-PBCza** showed the shallowest E_{HOMO} (–5.37 eV), although it was deeper than those of the comparison poly(3,6-carbazole)s (ca. –5.10 eV) [46].

Because it was difficult to recognize the position of onset potentials in the reduction waves of the homopolymers in the film state, the energy levels of the LUMO (E_{LUMO}) were determined from the E_{HOMO} and E_g using the equation, $E_{LUMO} = E_{HOMO} + E_g$. The E_{LUMO} of **PECza**, **PECzb**, **PBCza**, **PBCzb** and **1,7-PBCza** were estimated to be –2.54, –2.59, –2.44, –2.44 and –2.60 eV, respectively.

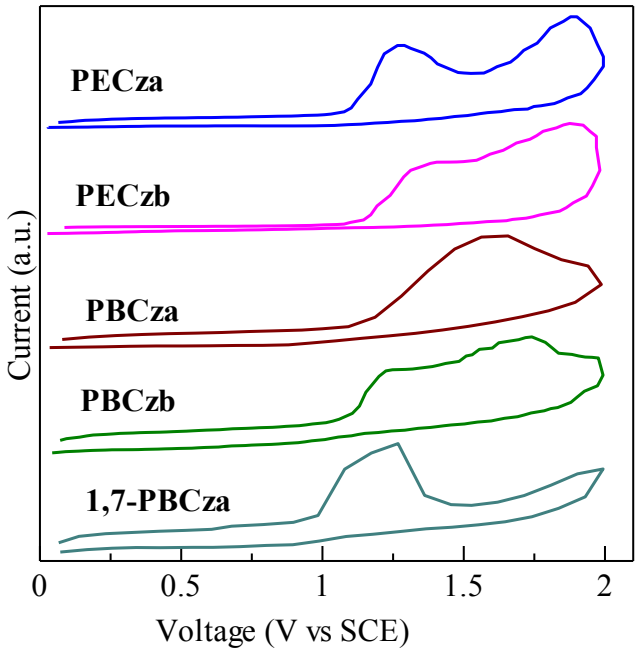

Fig. 2-11 Cyclic voltammograms of **PECza**, **PECzb**, **PBCza**, **PBCzb** and **1,7-PBCza**.

In order to understand the difference of E_{HOMO} between **PCz** and **PBCz,** density functional theory (DFT) in the Gaussian 09 program at the B3LYP/6-31G(d) basis set was used to investigate the electronic structures of **Cz** and **BCz.** The optimized geometry and electron density distributions in the HOMO and LUMO for the different building blocks were shown in Fig.2-12. It is easy to find that electrons delocalize along the whole rings well on both the HOMO and LUMO of **Cz** and **BCz**, therefore the scope of delocalization in the **BCz** is wider for the larger fused aromatic ring system. As a result, compared to E_{HOMO} and E_g of **Cz,** the E_{HOMO} of

BCz is higher and the E_g is narrower. This calculation also indicates that though presence of the 4,5-ethenylene bridge of **Cz,** the **BCz** unit can function as phenanthrene.

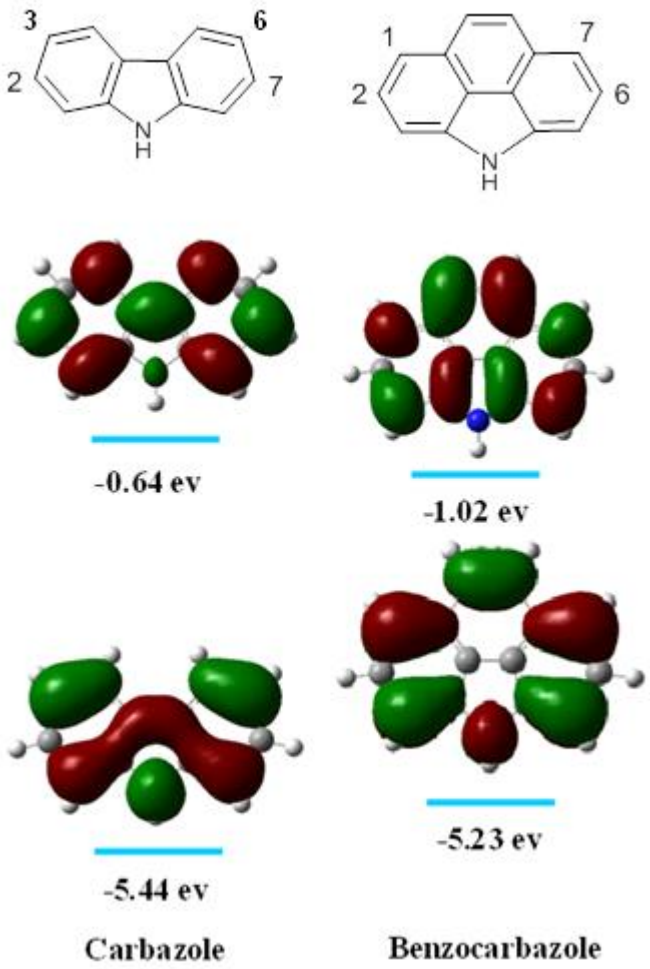

Fig. 2-12 HOMO and LUMO energy levels of carbazole (**Cz**) and benzocarbazole (**BCz**), optimized by DFT calculation with Gaussian 09 program at the B3LYP/6-31G(d) basis set.

The conjugation along the main chain through 2,7-linked **PCz** is thought to be more advantageous than 2,6-linked **PBCz,** because no electron density could be observed in the center of the **BCz** unit according to the electron density maps of HOMO of the **Cz** and **BCz** units. Thus, the wider E_g of **PBCz** can be accounted for the characteristic electron distribution of **BCz**. Similarly, the narrow E_g observed of **1,7-PBCza** can be elucidated by π-conjugation of 1,7-linkage through 8,9-ethenylene of **BCz**.

2.1.2.5. X-ray diffraction analysis

Fig. 2-13 shows the results of π-stacking distance and structural order of the polymers in film state, which were performed by the X-ray diffraction (XRD) analyses. **PECza** and **PECzb** exhibited a broad diffraction hump observed at about 18-19° (d= 4.8, 4.7 Å). On the same time, **PBCza**, **PBCzb** and **1,7-PBCza** showed diffraction humps due to π-stacking in the wider angle at 2θ = 20.50, 21.32, 21.10°, which correspond to distances of 4.33, 4.16, 4.21 Å, respectively. These polymers are considered to be amorphous with loose π-stacking, because all the polymers had no sharp diffraction peaks but only broad humps. Compared with the π-stacking distances of **PECz,** the smaller π-stacking distances observed for **PBCz** suggests that the intermolecular interaction is stronger, which is basically affected by the size of the

conjugated planar unit of the polymers.

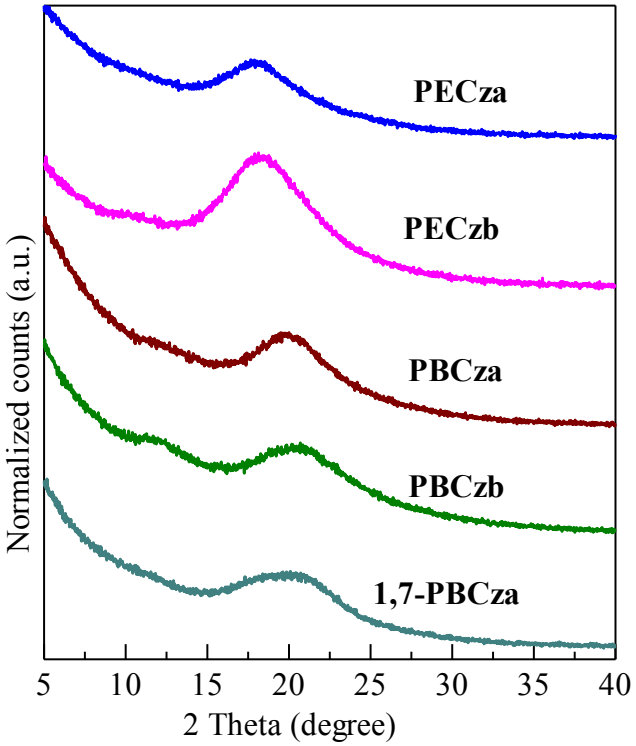

Fig. 2-13 X-ray diffraction patterns of **PECza**, **PECzb**, **PBCza**, **PBCzb** and **1,7-PBCza**.

2.1.3 Summary

In this section, the syntheses and characterizations of a new series of carbazole-based homopolymers, 4,5-ethylene bridged poly(carbazole)s (**PECza**, **PECzb**) and poly(4*H*-benzo[*def*]carbazole)s (**PBCza**, **PBCzb** and **1,7-PBCza**), have been presented. They showed good solubility in common organic solvents, enough high molecular weights, good thermal stability for making thin films and amorphous nature in the film state. The electronic properties of absorption and emission of **PECz** were similar to those of **PCz**, but the Φ_{fl} were somewhat lower than those of **PCz**. On the other hand, compared with **PECz** and **PCz,** poly(2,6-benzocarbazole)s (**PBCza** and **PBCzb**) showed unexpectedly blue-shifted absorption bands, the shallower E_{HOMO}, and the wider E_g, although they have the larger π-conjugation in the monomer unit. These results suggested that the dominant characteristics of poly(2,7-phenanthrene) strained by the N-bridge in **PBCz**.

The PL emission colors can be evaluated by color coordinates in the CIE chromaticity diagram. In $CHCl_3$, the CIE(*x*, *y*) values of **PECza, PECzb, PBCza** and **PBCzb** were almost identical to (0.15, 0.05) in the region of deep blue. In film state, PL emission color of **PECz** (0.16, 0.15) were in the region of blue, while the CIE values for **PBCz** were shifted to greenish blue but kept in the region of blue (0.19, 0.21). The shift of the PL emission color due to the stronger intermolecular interaction between the larger planar units of **PBCz** as suggested in the XRD results, although they have larger E_g than **PECz.** It is considered that **PECz** and **PBCz** have potential to be applied in PLED as blue-light emitting materials, because of the appropriate E_{HOMO} around −5.5 eV for hole injection and appropriate E_g for blue emission. On the same time, **1,7-PBCz** is presented to have unique properties, i.e., the absorption and emission bands were observed in considerable longer region in wavelength with moderate Φ_{fl}, which were quite different compared to those of poly(3,6-carbazole)s. **1,7-PBCza** showed the shallowest E_{HOMO} and narrowest E_g of all the homopolymers synthesized in this work，according to the dominant character of poly(1,8-phenanthrene) strained by the

8,9-ethenylene bridge. Consequently, it fluoresced in blue green (CIE (0.20, 0.33)) in the film state. Therefore, the **1,7-BCz** group has potential to applied in a donor component of donor-acceptor type narrow band gap polymers for organic solar cells.

2.1.4 Experimental

2.1.4.1 General method and instrumentation

All synthetic manipulations were performed by a standard technique using a Schlenk tube. Column chromatography was performed using a silica gel (Kanto Chem., 60 N, 63-120 mm). Photoabsorption in the range of ultraviolet-visible (UV-vis) and photoluminescence (PL) measurements of the polymer samples in $CHCl_3$ and in a form of a thin film coating on a quartz glass were performed using a Shimadzu UV-1800 spectrophotometer and an F-4500 fluorescence spectrophotometer (Hitachi) at room temperature. The fluorescence quantum yield (Φ_{fl}) in $CHCl_3$ were relative to 9,10-diphenylanthracene in cyclohexane (Φ_{fl} = 0.90) as a standard. The number-average molecular weight (M_n) and the weight-average molecular weight (M_w) of the polymers were estimated by a gel permeation chromatography (GPC) system (Shimadzu, LC solution) using polystyrene standards with $CHCl_3$ as an eluent. Nuclear magnetic resonance (NMR) spectra were recorded on a JEOL JNM-ECS 400 spectrometer. The ^1H and ^{13}C chemical shifts are given in units of δ (ppm) relative to δ (TMS) = 0.00 and δ($CDCl_3$) = 77.0 ppm, respectively. Elemental analyses were carried out with a Perkin-Elmer type 2400 apparatus. Thermal gravimetric analysis (TGA) and differential thermal analysis (DTA) were carried out by an Extar 7000 TG/DTA (Seiko) analyzer at a heating rate of 10 °C min^{-1} in an argon atmosphere. Cyclic voltammetry (CV) of polymers in thin film on a Pt disk was performed at a scan rate of 50 mV/s in acetonitrile containing 0.1 M Et_4NBF_4 at room temperature under Ar using a saturated calomel electrode (SCE) as the reference and platinum wire as the counter electrode. The electrochemical data (vs SCE) obtained by cyclic voltammetry was made a correction with the redox potential (4.8 eV) of ferrocene/ferricinium [47, 48].

2.1.4.2 Materials

Reagents and solvents were purchased from Kanto Chemical, Nacalai Tesque Inc, Aldrich and Tokyo Chemical Industry. 1-(1-decylundecyloxy)-4-iodobenzene and 1-Decylundecyl-4-methylbenzenesulfonate were synthesized according to the procedures reported previously [49, 50]. 2,6-Dibrominated **ECz** (**3**) was synthesized by reductive ring closure of **2** that was prepared by nitration of **1** according to the procedures reported previously (Scheme 2-1) [51]. Tetrahydrofuran (THF) distilled after drying with sodium was stored under an argon atmosphere. Dimethylformamide (DMF) and benzene distilled after drying with CaH_2 were stored under an argon atmosphere. The other solvents and all commercially available reagents were used without further purification.

2.1.4.3 Synthesis of monomers and polymers

Synthesis of 2,7-dibromo-9,10-dihydrophenanthrene (1). A mixture of 9,10-dihydrophenanthrene (3 g, 16.6 mmol) and $FeC1_3{\cdot}H_2O$ (55 mg, 0.30 mmol) in H_2O (330 mL) was added dropwise a solution of Br_2 (1.7 mL, 34 mmol) in water (180 mL) over 4 h at room temperature, which was stirred for whole night. The precipitate was collected by filtration as white solid and recrystallized from benzene to gave a white solid (2.8 g, 56 %). ^1H NMR (400 MHz, $CDCl_3$) δ [ppm]: 7.55 (d, J= 8.2 Hz 2H), 7.42 (d, J= 8.2 Hz 2H), 7.38 (s, 2H), 2.83 (s, 4H); ^{13}C NMR (100 MHz, $CDCl_3$) δ [ppm]: 139.1, 132.5, 131.1, 130.2, 125.2, 121.5, 28.5.

Synthesis of 2,7-dibromo-4-nitro-9,10-dihydrophenanthrene (2). To a suspension of **1** (2.8 g, 8.3

mmol), copper(ii) nitrate hydrate (2.0 g, 8.7 mmol), dichloromethane (80 mL) and acetic anhydrous (20 mL), trifluoroacetic acid(3.1 ml, 41.4 mmol) was slowly added, which was reacted with stirring for whole night. After extraction with CH_2Cl_2 from water, drying over $MgSO_4$ and the solvent evaporation, the crude product was purified by column chromatography using ethyl acetate /hexane (1:1) as the eluent to yield product as a pale yellow solid (2.4 g, 76%). ^{1}H NMR (400 MHz, $CDCl_3$) δ [ppm]: 7.69 (s, 1H), 7.59 (s, 1H), 7.46 (s, 1H), 7.36 (d, J= 8.7 Hz 1H), 7.11 (d, J= 8.7 Hz 1H), 2.82 (s, 4H); ^{13}C NMR (100 MHz, $CDCl_3$) δ [ppm]: 157.3, 142.9, 140.3, (134.1 131.2, 130.3, 127.5, 126.3, 125.7, 123.3, 120.6) for 9C, 29.1, 28.4.

Synthesis of 2,6-dibromo-8,9-dihydrobenzo[*def*] carbazole (3). A suspension of triphenylphosphine (3.93 g, 15 mmol) and **2** (2.4 g, 6.2 mmol) in N-methyl-2-pyrrolidone (30 mL) under argon was stirred at 190 °C for 21 h. After cooling to ambient temperature, extraction with CH_2Cl_2 from water, drying over $MgSO_4$ and the solvent evaporation, the crude product was purified by column chromatography using CH_2Cl_2/hexane (2:1) as an eluent to yield **3** as a white solid (1.38 g, 63%). ^{1}H NMR (400 MHz, $CDCl_3$) δ [ppm]: 7.81 (s, 1H), 7.37 (s, 2H), 7.15 (s, 2H), 3.29 (s, 4H); ^{13}C NMR (100 MHz, $CDCl_3$) δ [ppm]: 137.5, 131.3, 121.3, 121.0, 120.3, 111.8, 26.1.

Synthesis of 2,6-dibromo-N-(1-decylundecyl)-8,9-dihydrobenzo[*def*]carbazole (**4a**). A mixture of potassium hydroxide (1.46 g, 26 mmol) and **3** (2 g, 5.7 mmol) in dimethyl sulfoxide (DMSO) (25 mL) was added dropwise solution of 1-decylundecyl-4-methylbenzenesulfonate (2.65 g, 5.7 mmol) in DMSO (14 mL) under argon. The mixture was stirred for 6 h at ambient temperature. After extraction with CH_2Cl_2 from water, drying over $MgSO_4$ and evaporation of the solvent, the crude product was purified by column chromatography using CH_2Cl_2/hexane (1:1) as an eluent giving yellow oil (2.27 g, 62%). ^{1}H NMR (400 MHz, $CDCl_3$) δ [ppm]: 7.34 (s, 2H), 7.11 (s, 2H), 4.26-4.23 (m, 1H), 3.29 (s, 4H), 2.13-2.08 (m, 2H), 1.89-1.83 (m, 2H), 1.29-1.15 (m, 32H), 0.88-0.84 (m, 6H); ^{13}C NMR (100 MHz, $CDCl_3$) δ [ppm]: 138.6, 131.4, 120.8, 119.9, 120.0, 111.4, 57.6, 34.0, 31.8, 29.6, 29.5, 29.4, 29.3, 29.2, 26.1, 22.6, 14.1. Calcd for $C_{35}H_{51}Br_2N$ (645.61): C, 65.11; H, 7.96; N, 2.17. Found: C, 65.42; H, 8.21; N, 2.20.

Synthesis of 2,6-dibromo-N-(p-(1-decylundecyloxy)phenyl)-8,9-dihydrobenzo-[*def*]carbazole (**4b**). A mixture of trans-1,2-cyclohexanediamine (0.011 mL, 0.094 mmol), CuI (3.6 mg, 1.9 mmol), **3** (0.66 g, 1.9 mmol), 1-(1-decylundecyloxy)-4-iodobenzene (4.37 g, 8.5 mmol) and potassium phosphate (0.8 g, 3.7 mmol) in THF (3 mL) was stirred at 65 °C for 72 h. After cooling to ambient temperature, the mixture was mixed with water. After extraction with CH_2Cl_2, drying over $MgSO_4$ and evaporation of the solvent, the crude product was purified by column chromatography using hexane as an eluent to give a white solid (1.1 g, 60%). ^{1}H NMR (400 MHz, $CDCl_3$) δ [ppm]: 7.43 (d, J= 6.8 Hz 2H), 7.39 (s, 2H), 7.18 (s, 2H), 7.06 (d, J= 8.0 Hz 2H), 4.28 (br, 1H), 3.32 (s, 4H), 1.73-1.67 (m, 4H), 1.43-1.27 (m, 32H), 0.90-0.86 (m, 6H); ^{13}C NMR (100 MHz, $CDCl_3$) δ [ppm]: 157.7, 139.0, 131.3, 130.0, 126.1, 126.0, 121.2, 120.5, 116.9, 111.2, 78.5, 33.9, 31.9, 31.5, 29.7, 29.6, 29.3, 26.1, 25.4, 22.7, 22.6, 14.1. Calcd for $C_{41}H_{55}Br_2NO$ (737.71): C, 66.65; H, 7.52; N, 1.90. Found: C, 66.31; H, 7.68; N, 1.97.

Synthesis of 2,6-dibromo-4-(1-decylundecyl)-4*H*-benzo[*def*]carbazole (**5a**). A suspension of **4a** (0.5 g, 0.78 mmol) and 2,3-dichloro-5,6-dicyano-1,4-benzoquinone (DDQ) (0.42 g, 1.8 mmol) in benzene (77 mL) was refluxed under a N_2 atmosphere for 8 h. After cooling to ambient temperature, the mixture was mixed with water. After extraction with CH_2Cl_2, drying over $MgSO_4$ and evaporation of the solvent, the crude product was purified by column chromatography using hexane as an eluent to give a white solid (0.42 g, 85%). ^{1}H NMR (400 MHz, $CDCl_3$) δ [ppm]: 7.90 (s, 2H), 7.83 (s, 2H), 7.59 (s, 2H), 4.46-4.43 (m, 1H),

2.21-2.18 (m, 2H), 1.94-1.88 (m, 2H), 1.18-0.96 (m, 32H), 0.82-0.77 (m, 6H). ^{13}C NMR (100 MHz, $CDCl_3$) δ [ppm]: 138.1, 127.7, 126.0, 120.7, 118.3, 118.2, 110.0, 58.1, 34.3, 31.9, 29.7, 29.6, 29.5, 29.4, 29.2, 25.3, 22.6, 14.1. Calcd for $C_{35}H_{49}Br_2N$ (643.59): C, 65.32; H, 7.67; N, 2.18. Found: C, 65.57; H, 8.02; N, 2.05.

Synthesis of 2,6-dibromo-4-(p-(1-decylundecyloxy)phenyl)-4*H*-benzo[*def*]carbazole (**5b**). According to the procedure for **5a,** dibromobenzocarbazole **5b** was similarly synthesized**,** giving yellow oil (0.48 g, 96%). ^{1}H NMR (400 MHz, $CDCl_3$) δ [ppm]: 7.99 (s, 2H), 7.96 (s, 2H), 7.75 (s, 2H), 7.61 (d, J= 9.1 Hz 2H), 7.13 (d, J= 9.1 Hz 2H), 4.34-4.30 (m, 1H), 1.77-1.69 (m, 4H), 1.48-1.27 (m, 32H), 0.90-0.85 (m, 6H). ^{13}C NMR (100 MHz, $CDCl_3$) δ [ppm]: 157.8, 140.8, 130.3, 127.8, 126.2, 126.0, 121.2, 120.1, 119.3, 117.0, 109.9, 78.6, 33.9, 31.9, 31.5, 29.7, 29.6, 29.3, 25.4, 22.7, 22.6, 14.1. Calcd for $C_{41}H_{53}Br_2NO$ (735.69): C, 66.84; H, 7.26; N, 1.90. Found: C, 66.47; H, 7.50; N, 1.75.

Synthesis of 4-(1-decylundecyl)-4*H*-benzo[*def*]carbazole (**6a**). Dibromobenzocarbazole **5a** (0.8 g, 1.24 mmol) was dissolved in anhydrous THF (12.5 mL) and cooled to –78 °C under N_2 atmosphere, in which n-BuLi solution (1.6 M in hexane, 1.63 mL, 2.6 mmol) was added dropwise with stirring. The mixture was stirred at –78 °C for 20 min and then methanol (0.4 mL) was added. The reaction mixture was stirred for 1 h at ambient temperature, quenched with water (40 mL), and extracted with CH_2Cl_2. After drying over $MgSO_4$ and the solvent evaporation, the crude product was purified by column chromatography using hexane as an eluent to give a white solid (0.428g, 72%). ^{1}H NMR (400 MHz, $CDCl_3$) δ [ppm]: 8.05 (s, 2H), 7.81(t, J= 7.8 Hz 2H), 7.73 (d, J= 7.8 Hz 2H), 7.53 (d, J= 7.8 Hz 2H), 4.66 (br, 1H), 2.38-2.35 (m, 2H), 2.02-1.99 (m, 2H), 1.24-1.09 (m, 32H), 0.90-0.82 (m, 6H). ^{13}C NMR (100 MHz, $CDCl_3$) δ [ppm]: 129.4, 127.4, 126.5, 126.0, 121.6, 115.9, 114.5, 57.6, 34.5, 31.9, 31.8, 29.7, 29.6, 29.4, 29.3, 25.4, 22.6, 14.1.

Synthesis of 1,7-dibromo-4-(1-decylundecyl)-4*H*-benzo[*def*]carbazole (**7a**). A suspension of **6a** (0.35g, 0.72 mmol) and NBS (0.26g, 1.44 mmol) in chloroform (3.5 mL) was stirred under a nitrogen atmosphere at 40 °C for 8 h. After cooling to ambient temperature, the mixture was mixed with water. After extraction with dichloromethane, drying over $MgSO_4$ and evaporation of the solvent, the crude product was purified by column chromatography using hexane as an eluent to give a white solid (0.327g, 70%). ^{1}H NMR (400 MHz, $CDCl_3$) δ [ppm]: 8.18 (s, 2H), 7.97 (d, J= 7.7 Hz 2H), 7.43 (d, J= 7.8 Hz 2H), 4.59 (br, 1H), 2.33-2.29 (m, 2H), 2.0-1.95 (m, 2H), 1.28-0.99 (m, 32H), 0.88-0.82 (m, 6H). ^{13}C NMR (100 MHz, $CDCl_3$) δ [ppm]: 140.1, 133.8, 129.9, 127.6, 126.1, 108.4, 57.9, 34.4, 31.8, 31.6, 29.6, 29.4, 29.3, 29,2, 26.0, 22.6, 14.1.

Synthesis of poly[8,9-dihydro-N-(1-decylundecyl)-4*H*-benzo[*def*]carbazole-2,6-ylene] (PECza). A solution of bis(1,5-cyclooctadiene)nickel(0) ($Ni(cod)_2$) (0.28 g, 1.03 mmol), 1,5-cyclooctadiene (cod) (0.25 g, 2.38 mmol) and 2,2'-bipyridine (bpy) (0.18 g, 1.15mmol) in DMF (2.5 mL) was heated to 80 °C under an argon atmosphere for 30 min. The **4a** (0.301 g, 0.46 mmol) dissolved in 2.5 mL of THF under argon was added to the mixture solution. The mixed solution was heated at 80 °C for 72 h. After the reaction solution was cooled to ambient temperature, the polymer was firstly precipitated from methanol/HCl aq, and then reprecipitated from methanol/NH_3 aq and last from methanol, respectively. The resultant polymer was successively extracted with acetone, hexane and chloroform by Soxhlet extraction. The chloroform extract was again precipitated from methanol. **PECza** was gained as a yellow soild (0.21 g, 92%). ^{1}H NMR (400 MHz, $CDCl_3$) δ [ppm]: 7.48 (br, 2H), 7.32 (br, 2H), 4.56-4.55 (m, 1H), 3.50-3.41 (m, 4H), 2.38-2.36 (m, 2H), 1.99 (br, 2H), 1.31-1.09 (m, 32H), 0.90-0.82 (m, 6H). Calcd for $C_{35}H_{53}N$ (487.82): C, 86.18; H, 10.95; N, 2.87. Found: C, 86.25; H, 10.24; N, 2.95.

Synthesis of poly[8,9-dihydro-N-(p-(1-decylundecyloxy)phenyl)-4*H*-benzo[*def*] carbazole-2,6-ylene] (**PECzb**). According to the procedure for **PECza,** polymerization of **4b** abtained **PECzb** as a yellow solid (0.22 g, 94%). ^{1}H NMR (400 MHz, $CDCl_3$) δ [ppm]: 7.62 (d, J= 8.4 Hz 2H), 7.51 (s, 2H), 7.31 (br, 2H), 7.07 (d, J= 8.4 Hz 2H), 4.29-4.26 (m, 1H), 3.47 (br, 4H), 1.73-1.70 (m, 4H), 1.50-1.25 (m, 32H), 0.90-0.83 (m, 6H). Calcd for $C_{41}H_{57}NO$ (645.61): C, 84.92; H, 9.91; N 2.42. Found: C, 84.95; H, 9.32; N, 2.56.

Synthesis of poly[4-(1-decylundecyl)-4*H*-benzo[*def*]carbazole-2,6-ylene] (**PBCza**). In a similar way to the synthetic procedure for **PECza**, polymerization of **5a** abtained **PBCza** as a yellow solid (0.16 g, 91%).^{1}H NMR (400 MHz, $CDCl_3$) δ [ppm]: 8.26-8.15 (m, 4H), 8.03-7.99 (m, 2H), 4.92-4.90 (m, 1H), 2.62-2.59 (m, 2H), 2.16-2.14 (m, 2H), 1.42-1.08 (m, 32H), 0.90-0.79 (m, 6H). Calcd for $C_{35}H_{51}N$ (485.80): C, 86.53; H, 10.28; N, 2.88. Found: C, 86.35; H, 10.28; N, 2.81.

Synthesis of poly[4-(p-(1-decylundecyloxy)phenyl)-4*H*-benzo[*def*]carbazole-2,6-ylene] (**PBCzb**). In a similar way to the synthetic procedure for **PECza**, polymerization of **5b** abtained **PBCzb** as a yellow solid (1.1 g, 65%).^{1}H NMR (400 MHz, $CDCl_3$) δ [ppm]: 8.21 (br, 4H), 8.08 (br, 2H), 7.88 (d, J= 7.6 Hz 2H), 7.17 (d, J= 7.6 Hz 2H), 4.32 (br, 1H), 1.85-1.69 (m, 4H), 1.27-1.24 (m, 32H), 0.89-0.82 (m, 6H). Calcd for $C_{41}H_{55}NO$ (577.90): C, 85.21; H, 9.59; N, 2.42. Found: C, 84.62; H, 9.41; N, 2.29.

Synthesis of poly[4-(1-decylundecyl)-4*H*-benzo[*def*]carbazole-1,7-ylene] (**1,7-PBCza**). In a similar way to the synthetic procedure for **PECza**, polymerization of **7a** abtained **1,7-PBCza** as a green solid (0.15g, 72%). ^{1}H NMR (400 MHz, $CDCl_3$) δ [ppm]: 8.07-8.03 (m, 4H), 7.69-7.64 (m, 2H), 4.78-4.77 (m, 1H), 2.51-2.46 (m, 2H), 2.17-2.07 (m, 2H), 1.29-0.94 (m, 32H), 0.80-0.65 (m, 6H). Calcd for $C_{35}H_{51}N$ (485.80): C, 86.53; H, 10.28; N, 2.88. Found: C, 85.95; H, 10.35; N, 2.92.

^{1}H NMR spectra of **4a**

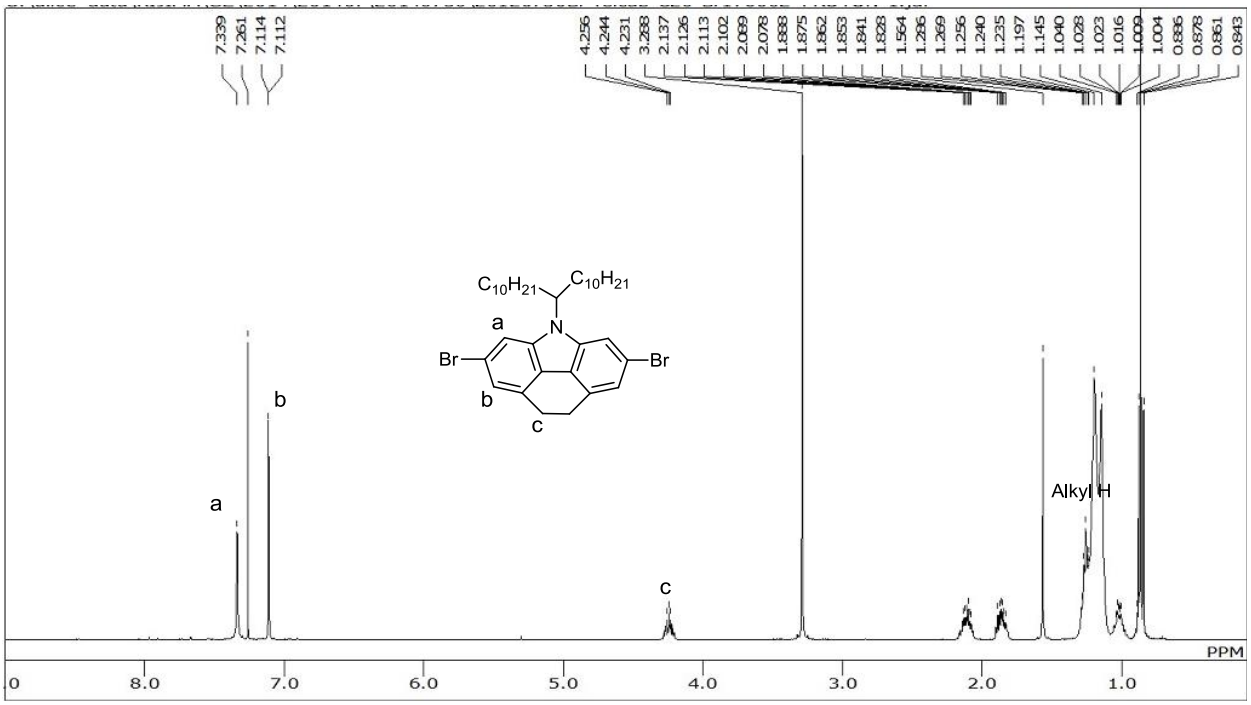

^{1}H NMR spectra of **5a**

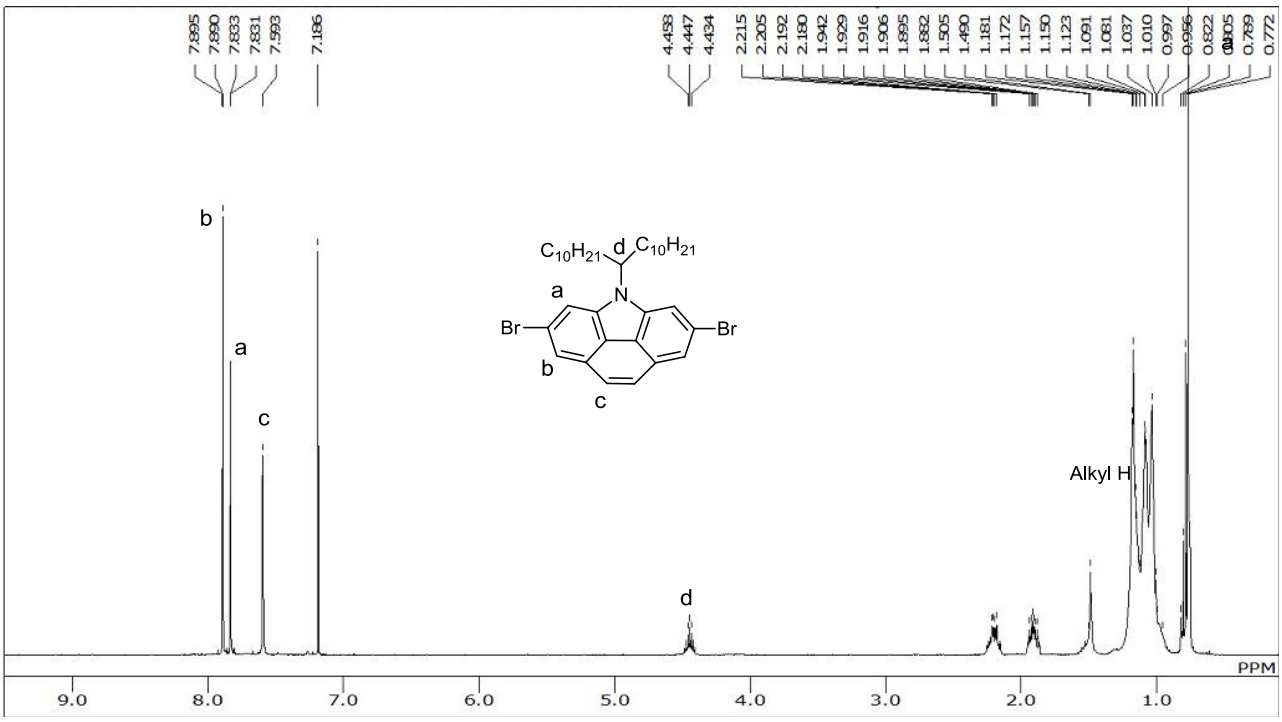

^{13}C NMR spectra of **5a**

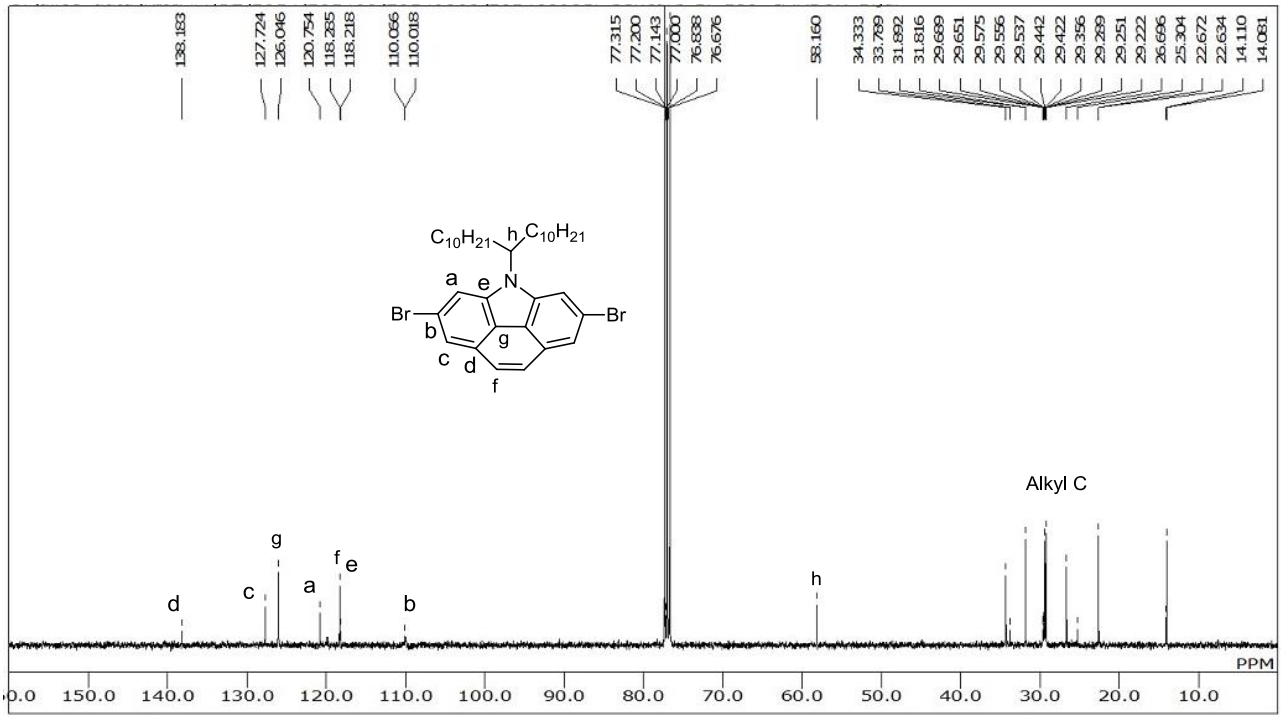

^{1}H NMR spectra of **5b**

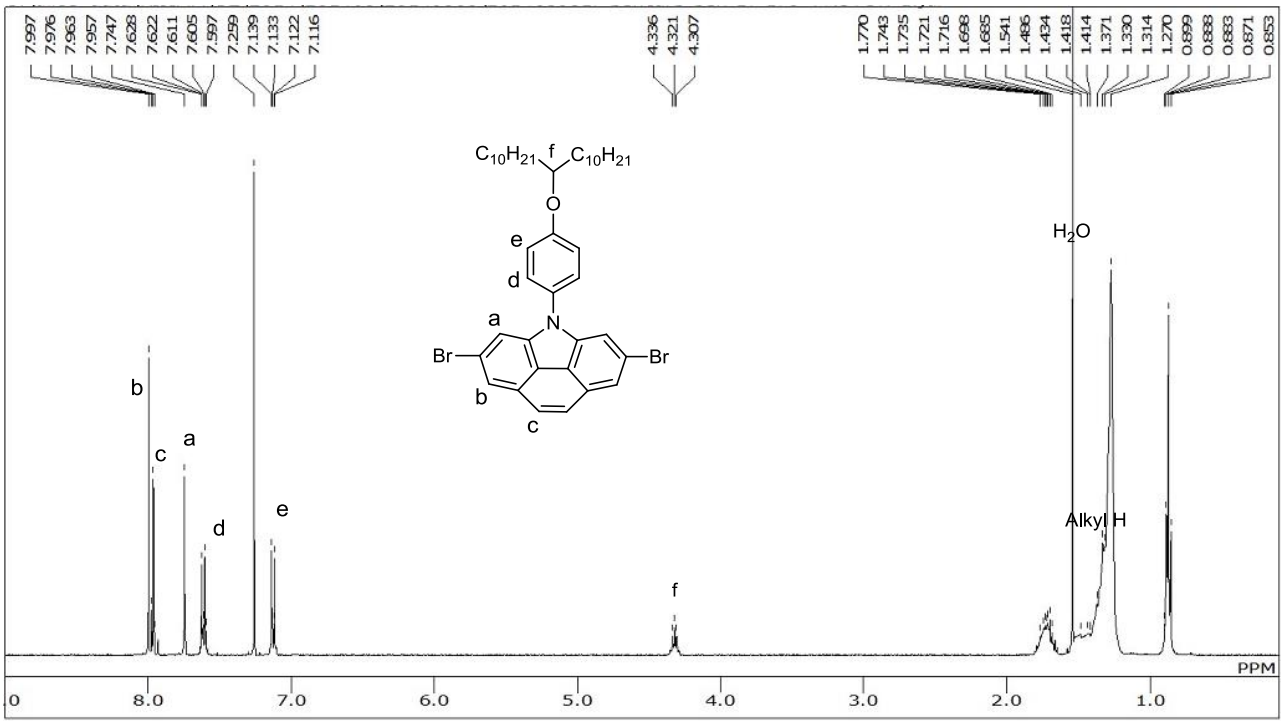

^{13}C NMR spectra of **5b**

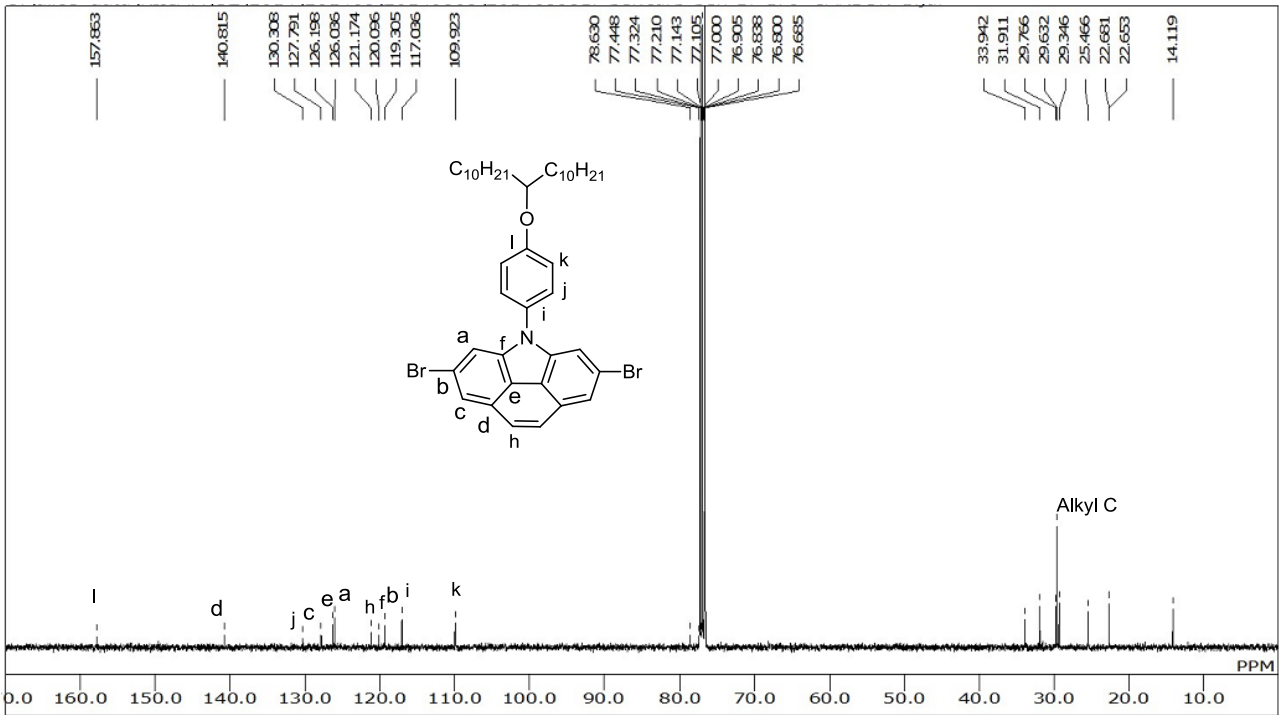

^{1}H NMR spectra of **7a**

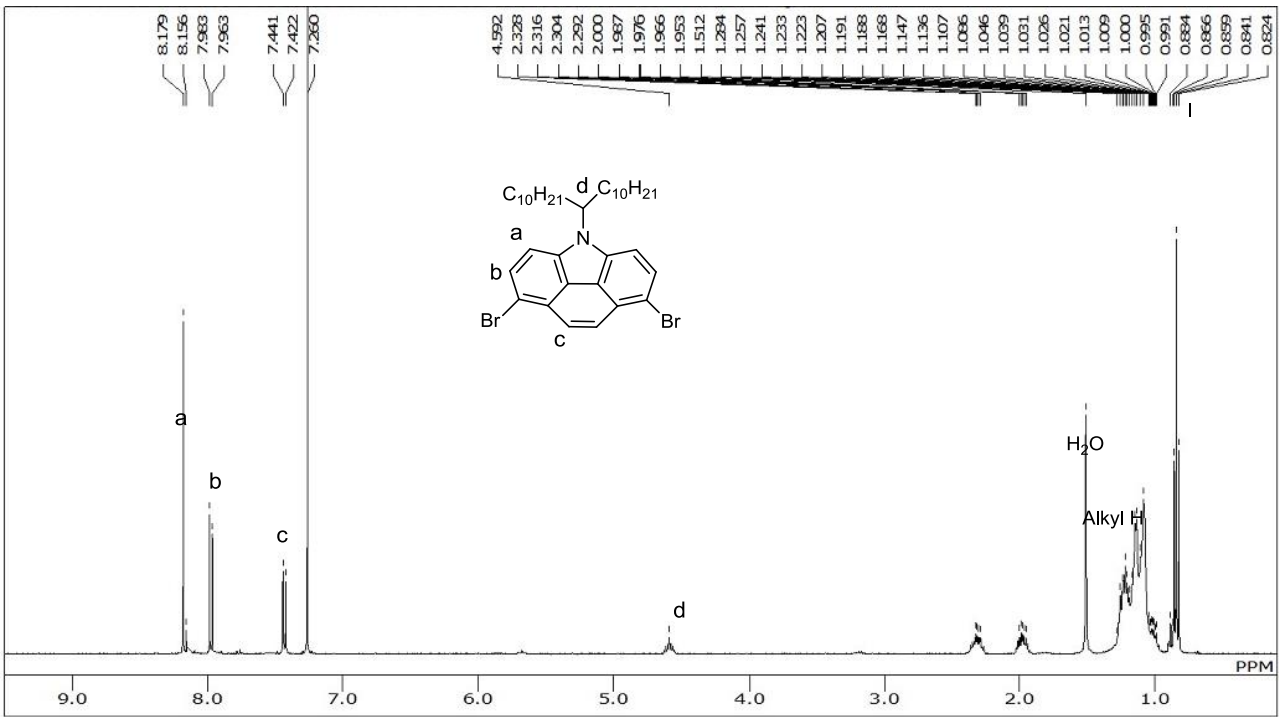

^{1}H NMR spectra of **PECza**

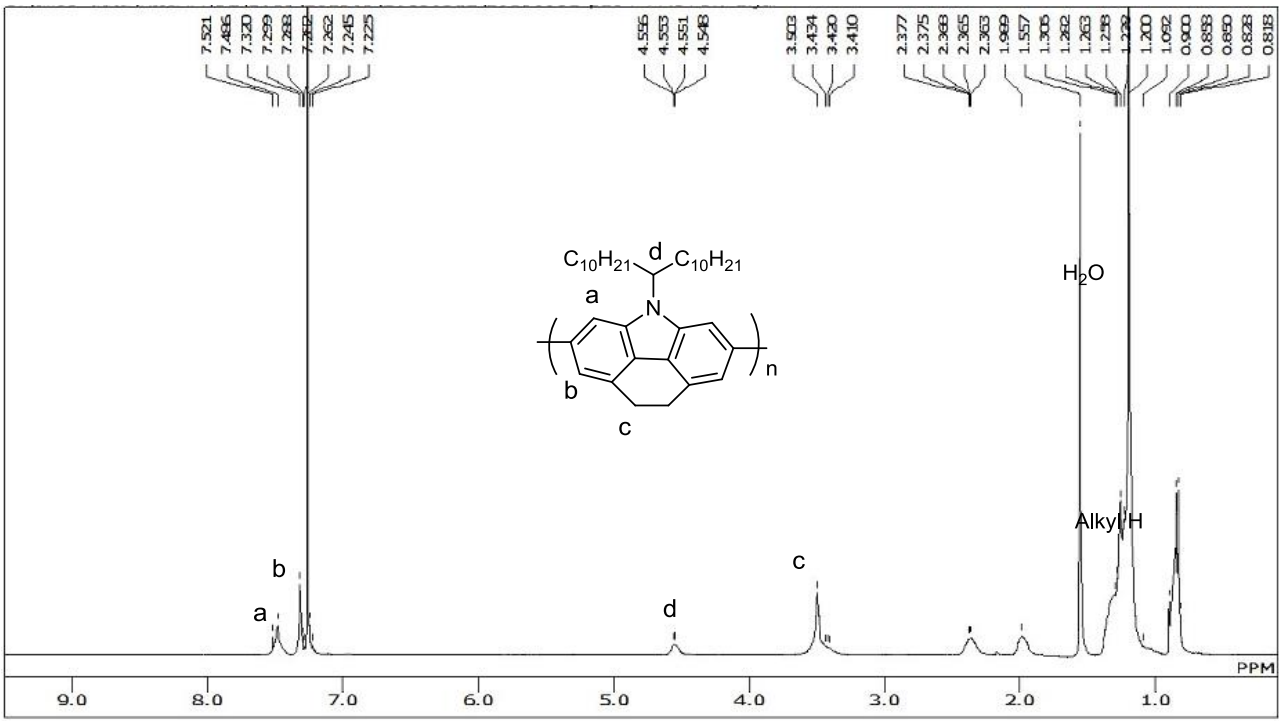

^{1}H NMR spectra of **PBCza**

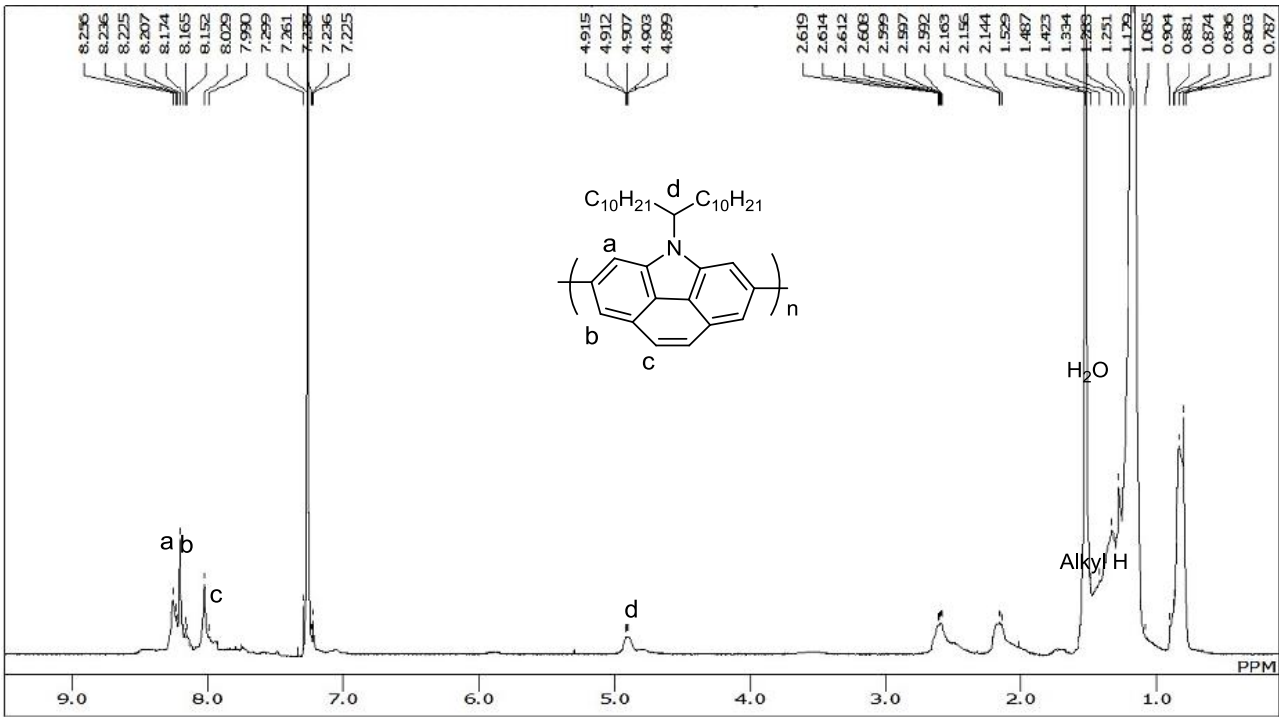

^{1}H NMR spectra of **PECzb**

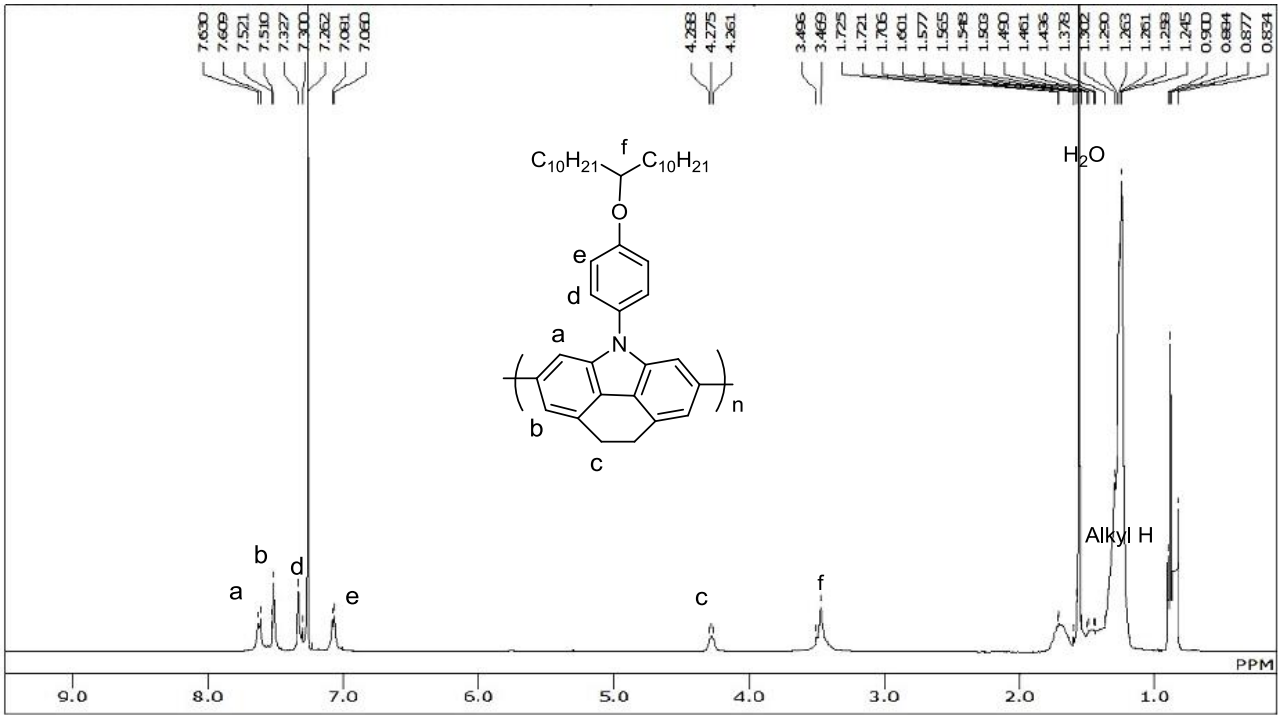

^{1}H NMR spectra of **PBCzb**

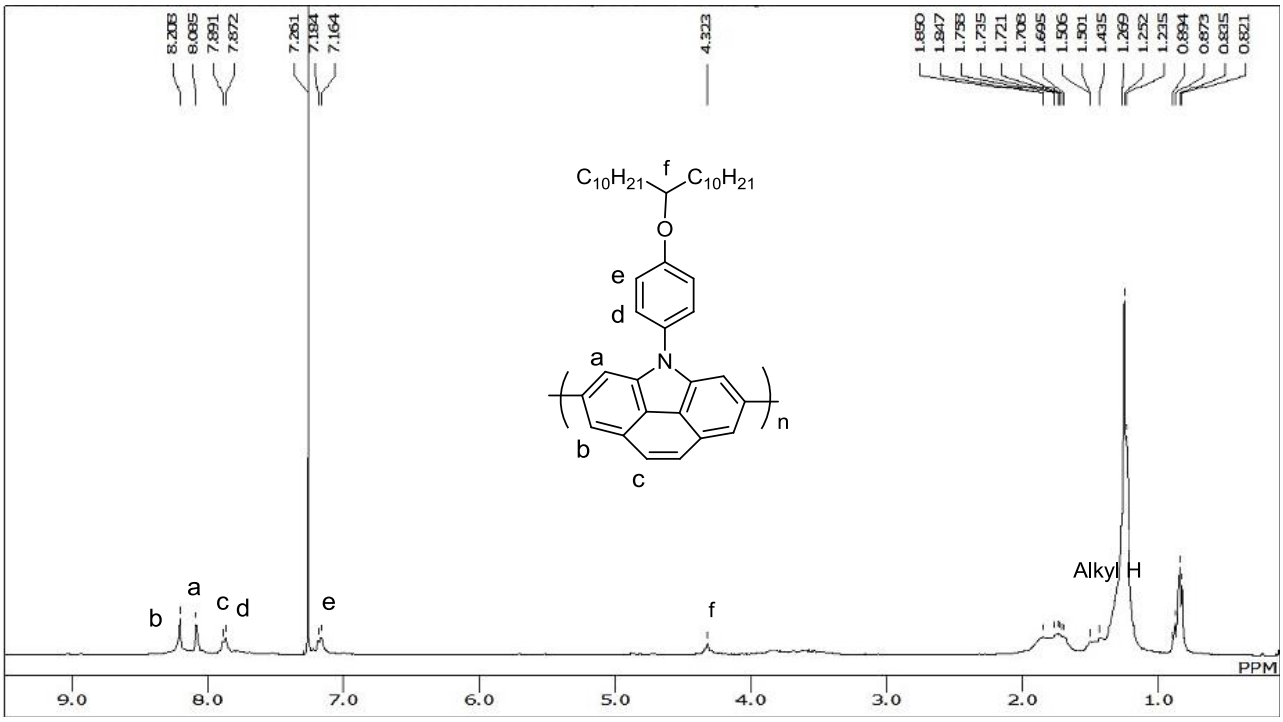

^{1}H NMR spectra of **1,7-PBCza**

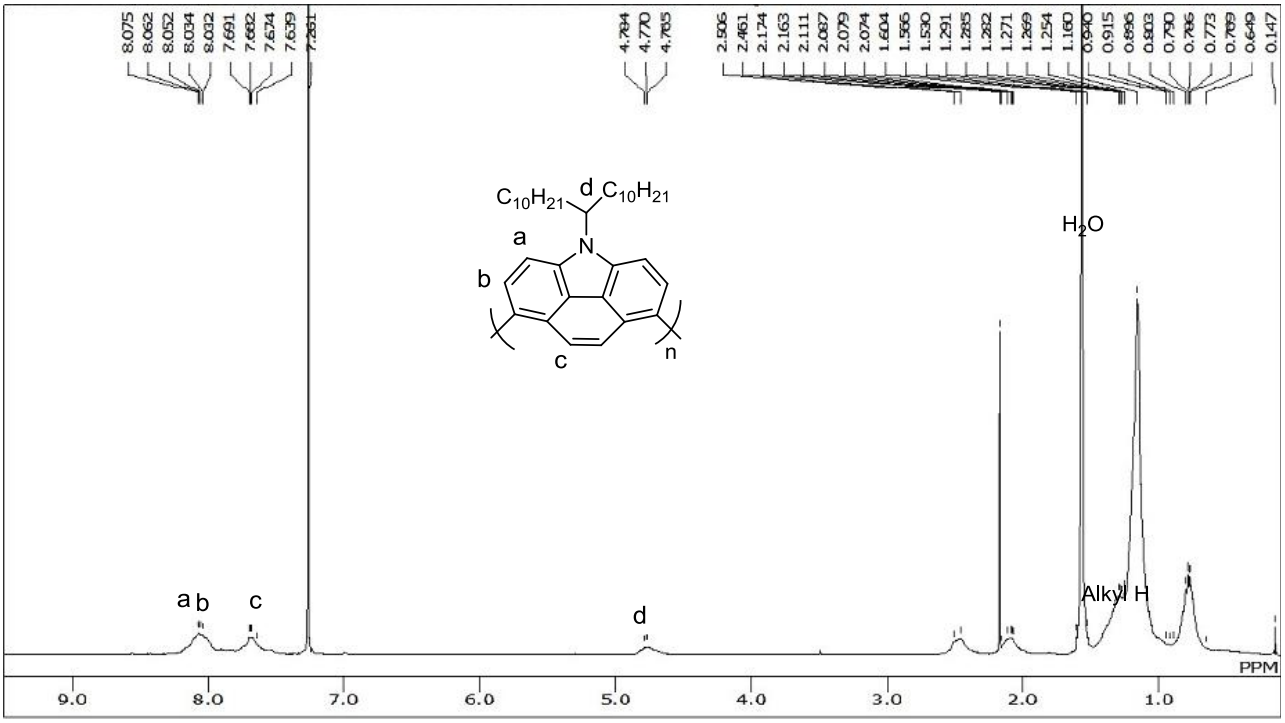

2.2 Synthesis and characterization of D-A polymers having azine unit for blue light emission.

2.2.1 Background

Conjugated polymers have gained great significance for various organic electronic applications. In order to develop high-efficiency blue emitting materials, one effective strategy is to select electron-donating and electron-accepting groups used in the conjugated backbone. This donor-acceptor (D-A) system is expected to highten E_{LUMO}, giving rise to a series of intriguing properties such as improved resistance to oxidation, facilitated electron injection, and ambipolar characteristics.

In this chapter section, the synthesis, characterization and photoluminescence properties of carbazole/fluorene-based polymers, **PCz-triAz**, **PF-tetrAz** and **PF-triAz,** shown in Fig.2-14 were investigated. Herein, the carbazole/fluorene sequences were selected as electron donor for the reason of good thermal and electrochemical stability, high fluorescence yield and facile chemical functionalization [52, 53], while 1,2,4,5-tetrazine (**tetrAz**) and 1,3,5-triazine (**triAz**) were chosen as electron acceptor for their electron deficiency [54].

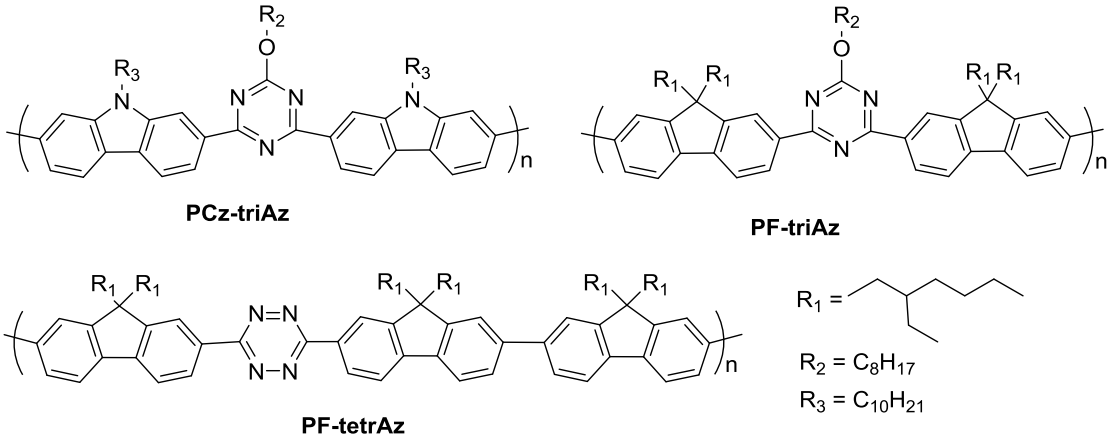

Fig. 2-14 Chemical structures of **PCz-triAz**, **PF-tetrAz** and **PF-triAz**

2.2.2 Results and discussion

2.2.2.1. Synthesis

The general synthetic routes toward the monomers and polymers **PF-tetrAz, PF-triAz** and **PCz-triAz**, are outlined in Scheme 2-4 and Scheme 2-5. The cyclization of **1** was carried out with anhydrous hydrazine by heating to give dihydrotetrazine intermediate **2,** which was oxidized instantly into the fully aromatic tetrazine **3** for its instability. Tetrazine **3** was polymerized by Suzuki coupling reaction with 2, 2'-(9,9-bis(2-ethylhexyl)-9*H*-fluorene-2,7-diyl)bis-1,3,2-dioxaborolane to affort **PF-tetrAz**. 2,7-Dibromo-9,9-bis(2-ethylhexyl)fluorene reacted with **4** to give **5**. The alkyl group was introduced into N-position of 2,7-dibromocarbazole by the procedure reported previously [37], giving **6**. Monomer **7** was similarly synthesized according to the procedure of **5.** Homopolymerization of **5** and **7 b**y the Yamamoto reaction afforded **PCz-triAz** and **PF-triAz**, respectively.

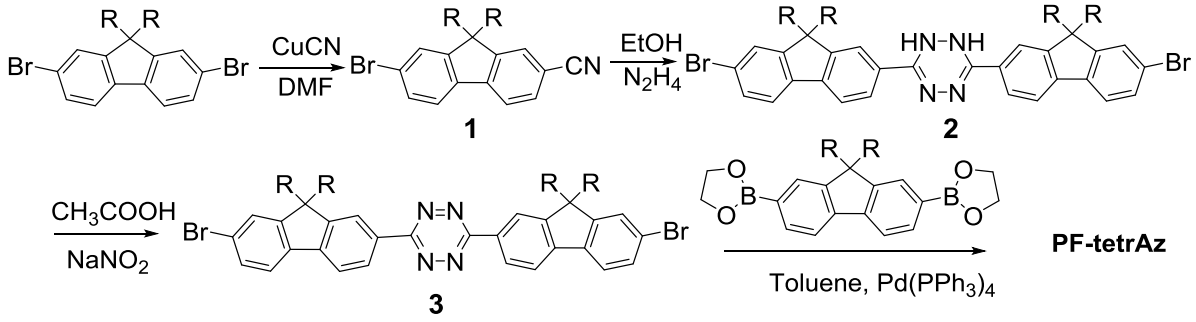

Scheme 2-4. Synthetic routes of **PF-tetrAz**

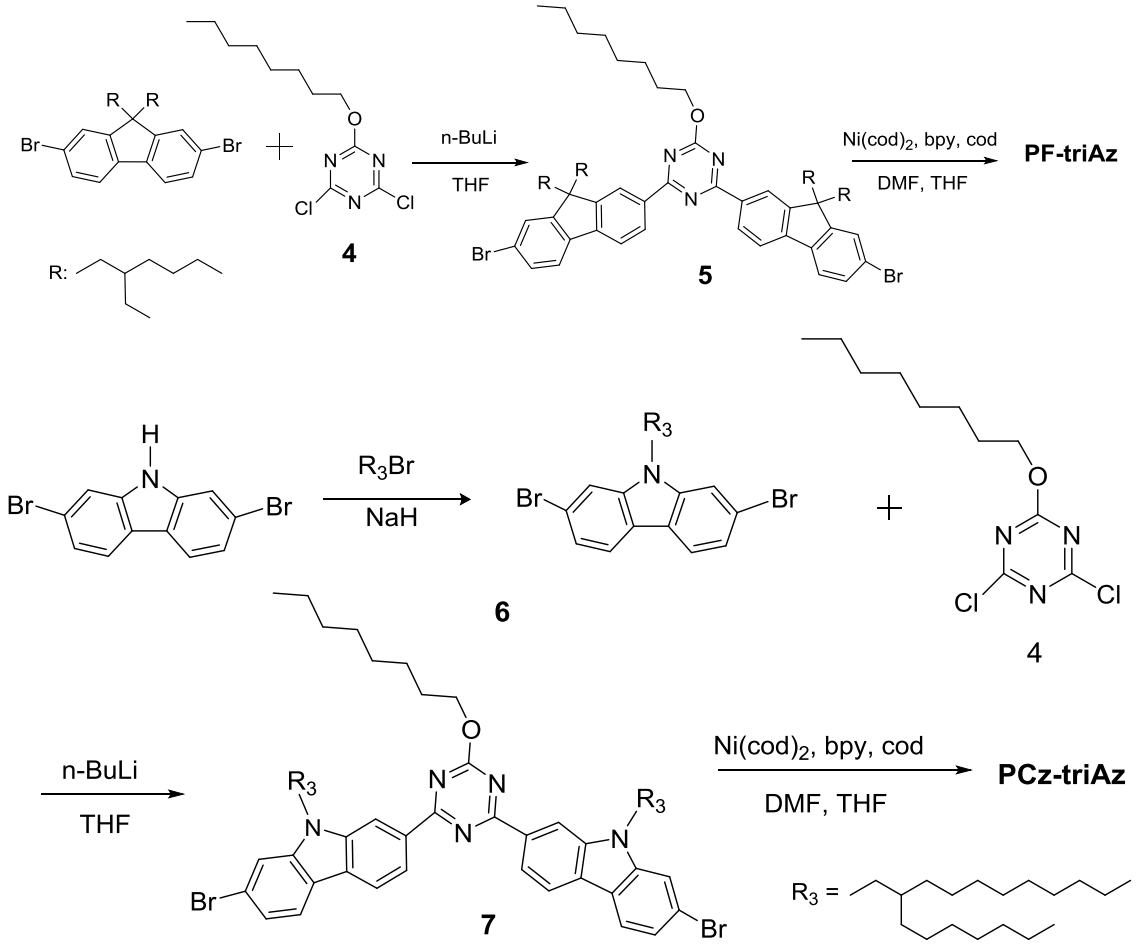

Scheme 2-5. Synthetic routes of **PF-tetrAz** and **PCz-triAz**

2.2.2.2 Solubility and thermal stability

All of the copolymers have a good solubility in usual organic solvents such as $CHCl_3$, chlorobenzene, and *o*-dichlorobenzene. The polymers were identified by NMR and elemental analyses. The GPC results were summarized in Table 2-5. These copolymers showed good processability to make thin cast films. The M_n of **PF-tetrAz, PF-triAz** and **PCz-triAzz** were 7.0, 14.5 and 7.5 kg/mol, respectively, which were not so high but enough to investigate their basic properties and to examine basic characteristics of OLED. The TGA results are shown in Fig. 2-15. These polymers had a good thermal stability, and their temperatures of 5 wt% loss in TGA (T_d) were around 370 °C, respectively, which suggests that all of copolymers have good thermal stability for fabricating OLED devices.

Table 2-5. GPC and TGA results of the polymers.

Polymer	M_n[a] （kg·mol-1）	M_w (kg·mol-1)	M_w/M_n	DP[b]	T_d (ºC)[c]
PF-tetrAz	7.0	7.6	1.08	5	363
PF-triAz	14.5	21.9	1.52	14.5	387
PCz-triAz	7.5	8.2	1.10	8.5	376

[a] GPC analysis was carried out in $CHCl_3$ using polystyrene as the standard.

[b]DP was estimated from M_n.

[c]Temperature of 5 % weight loss determined by TGA under an argon atmosphere.

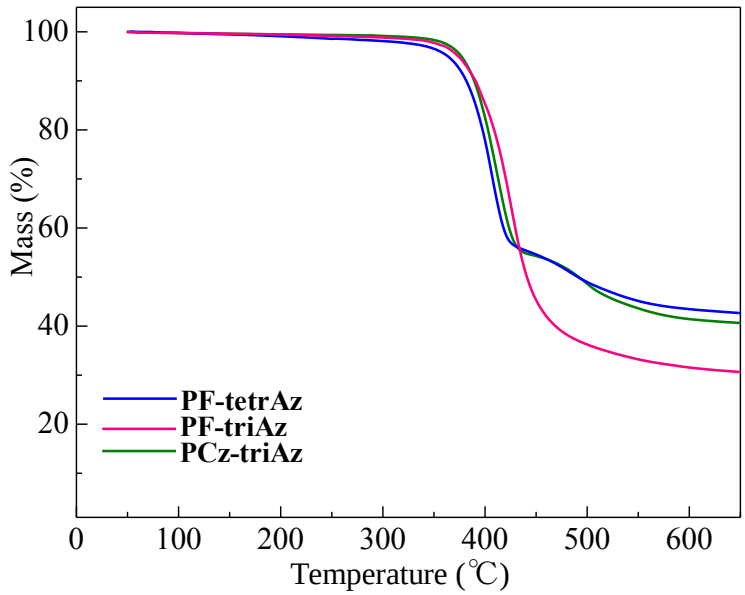

Fig. 2-15 TGA curves of the copolymers.

2.2.2.3 Optical properties.

The photophysical properties of dilute solution and thin films of **PF-tetrAz, PF-triAz** and **PCz-triAz** were investigated with UV-vis and PL, and the results are shown in Fig. 2-16. The UV-vis absorption and the emission spectra data for polymer were summarized in Table 2-6.

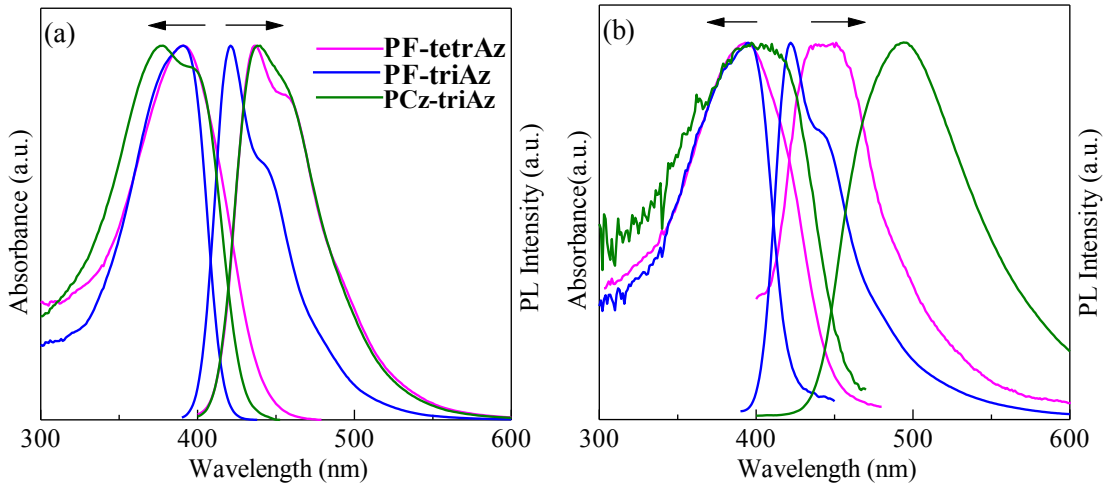

Fig. 2-16 UV-vis absorption spectra and photoluminescence (PL) of the polymers in $CHCl_3$ (a) and film state (b).

Absorption and PL spectra of **PF-tetrAz, PF-triAz** and **PCz-triAz** in $CHCl_3$ are shown in Fig.2-16a. The absorption maxima in wavelength (λ_{max}) at 390 nm for **PF-tetrAz,** 394 nm for **PF-triAz** and 378 nm for **PCz-triAz** are due to π-π* transition of the conjugated main chains. The absorption λ_{max} of **PCz-triAz** is shorter compared with those of **PF-tetrAz** and **PF-triAz** due to the good electron-donating ability of carbazole. The absorption λ_{max} of **PF-triAz** is slightly red-shift compared with that of **PF-tetrAz**, which indicates that π-conjugation of **PF-triAz** is longer than that of **PF-tetrAz**. The emission peaks in solution were observed at 437 nm for **PF-tetrAz,** 421 nm for **PF-triAz** and 438 nm for **PCz-triAz**. Stokes shifts of **PCz-triAz** in the solution was 60 nm, which was much larger than those of **PF-tetrAz** (47 nm) and **PF-triAz** (27 nm). This large Stokes shift is in charge lowering Φ_{fl}.

Table 2-6 Optical properties of the copolymers.

Polymer	$\lambda_{max,\ Abs}$ (nm)		$\lambda_{max,\ Em}$ (nm)		$\Phi_{fl}{}^{a}$	$E_g{}^{opt}$ (eV)
	$CHCl_3$	film	$CHCl_3$	film		
PF-tetrAz	390	393	437	451	0.63	2.80
PF-triAz	394	395	421	422	0.97	2.98
PCz-triAz	378	397	438	495	0.62	2.77

[a]Measured in $CHCl_3$ solution with 9,10-diphenylanthracene in cyclohexane as the standard (Φ_{fl}= 0.90)

Fig.2-16b shows absorption and PL spectra of **PF-tetrAz, PF-triAz** and **PCz-triAz** in thin solid film state. Compared with absorption spectra in solution, the absorption of **PCz-triAz** showed broad and red shift compared with the absorption in film, while those of **PF-tetrAz** and **PF-triAz** are slightly red shift compared with their absorption in film. The broadening and red shift of absorption spectra in the film state indicated that there were some aggregations or interactions of the polymer chains in the solid state. The $E_g{}^{opt}$ estimated from the onset of the absorption spectrum in the film state were 2.80 eV for **PF-tetrAz** and 2.65 eV for **PCz-triAz**, which were smaller than that of **PF-triAz** (2.98 eV). Compared with PL spectra of **PF-tetrAz, PF-triAz** and **PCz-triAz** in solution, the red shifts were observed in their film.The PL maxmum of **PF-triAz** in the film state was shorter in wavelength than that of **PF-tetrAz**. This can be attributed to the restrained intermolecular aggregation and the higher polarizability of the **tetrAz** group with the larger dipole moment

than **triAz** unit [55]. **PF-tetrAz, PF-triAz** and **PCz-triAz** showed intense blue PL emission with CIE coordinates (x, y = 0.16, 0.12; 0.16, 0.07; 0.20, 0.32, respectively) in the film state and good relative Φ_{fl} of 0.63, 0.97 and 0.62, respectively, in $CHCl_3$, which suggests that **PF-tetrAz** and **PF-triAz** are considered to be good polymeric blue emitters compare to a series of polyfluorene derivatives [56].

2.2.2.4. Electrochemical properties

Electrochemical analysis of thin-film samples of the polymers was employed to estimate E_{HOMO} and E_{LUMO}. The CV results of **PF-tetrAz, PF-triAz** and **PCz-triAz** are shown in Fig. 2-17, and the estimated values are summarized in Table 2-7.

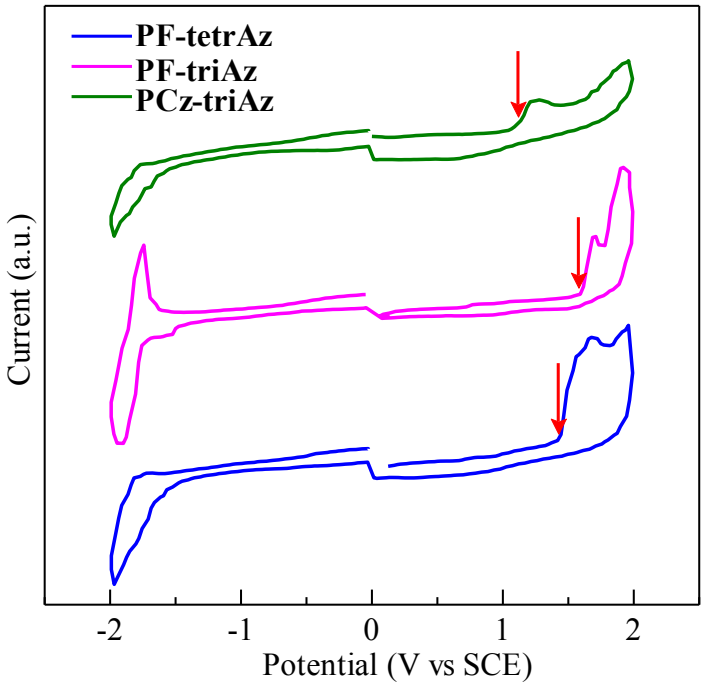

Fig. 2-17 Cyclic voltammograms of **PF-tetrAz, PF-triAz** and **PCz-triAz**

According to the anodic scan, all of the copolymers showed irreversible oxidation peak, which were assigned to the fluorene/carbazole units with rich eletrons easy to oxidate. The E_{HOMO} estimated from the onset potential of an oxidation peak of **PCz-triAz** was −5.47 eV, which was shallower than those of **PF-tetrAz** (–5.83 eV) and **PF-triAz** (–6.0 eV). This could be caused by the stronger electron-donating ability of the carbazole unit. The E_{HOMO} of **PF-tetrAz** was higher about 0.17 eV than that of **PF-triAz,** which could be caused by the delocalization of the HOMO because of good planarity between the fluorene and **tetrAz** segments. Upon the cathodic sweep, **PF-triAz** exhibited quasireversible reduction waves, whereas **PF-tetrAz** and **PCz-triAz** showed weak irreversible reduction waves. The E_{LUMO} of **PF-tetrAz** (–2.85 eV) is slightly higher than that of **PF-triAz** (–2.88 eV), on account of higher electron-deficiency of **tetrAz** compared to **triAz**. The above results suggest that higher electronegativity of the azine unit is responsible for lowering of both E_{HOMO} and E_{LUMO} of the polymers.

Table 2-7 HOMO-LUMO energy gaps and the energy levels of the polymers.

Polymer	E_g^{opt} (eV)	E_{HOMO} (eV)	E_{LUMO} (eV)	E_g^{ec} (eV)
PF-tetrAz	2.80	–5.83	–2.85	2.98
PF-triAz	2.98	–6.0	–2.88	3.12
PCz-triAz	2.65	−5.47	−2.7	2.77

From the E_{HOMO} and E_{LUMO}, the E_g^{ec} values of 2.98, 3.12 and 2.77 eV are obtained for **PF-tetrAz**, **PF-triAz** and **PCz-triAz,** respectively, which are similar to E_g^{opt}. These energy gaps with suitable E_{HOMO} and E_{LUMO} are good for lessening driving voltage and augmenting efficiency of OLEDs [57].

2.2.2.5. Electroluminescence properties

The EL properties of the copolycondensates are investigated by constructing OLEDs devices that have configuration of indium tin oxide (ITO)/ poly(3,4-ethylenedioxythiophene):poly(styrenesulfonate) (PEDOT:PSS)/ copolymer/ LiF/ Al, and the results are summarized in Table 2-8. Due to **PF-tetrAz** based devices quickly died. Figure 2-18 shows OLEDs structure, luminance vs. operating voltages and current density vs. operating voltages characteristics of the OLEDs.

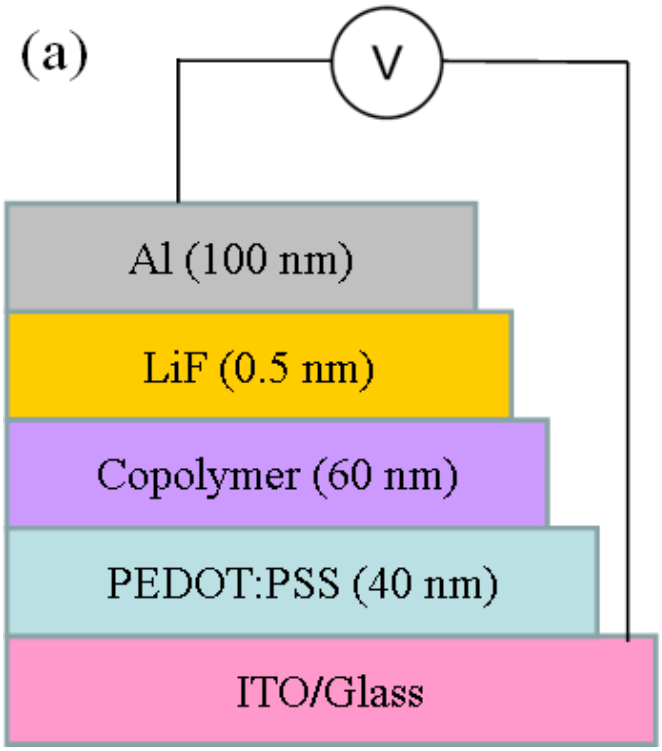

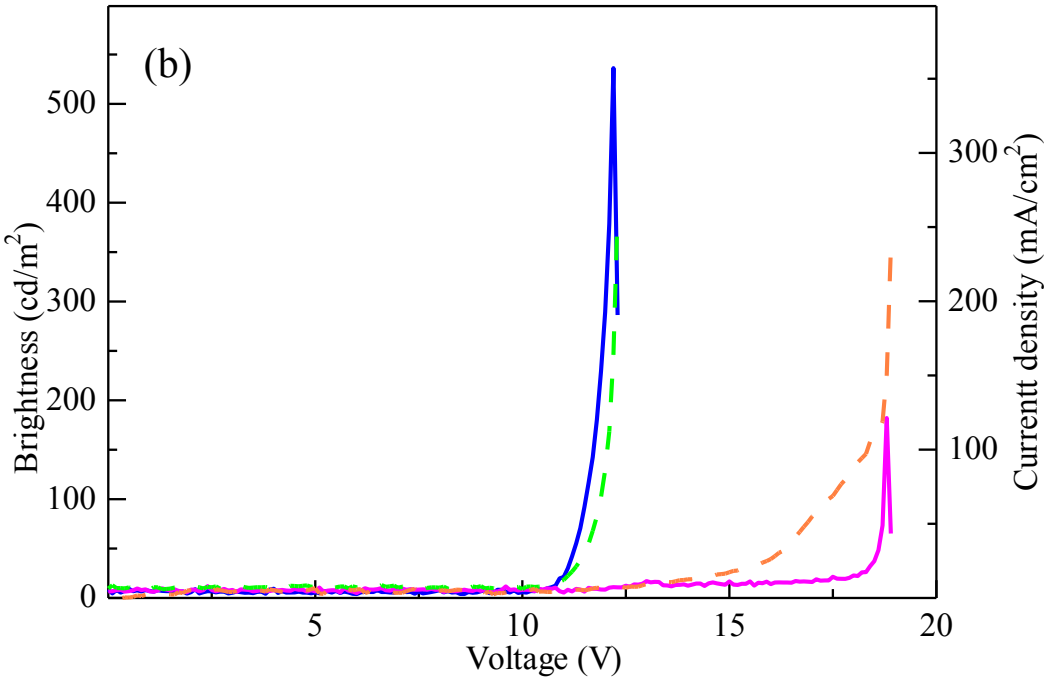

Fig. 2-18 The structure (a), luminance-voltage (*L*-*V*) curves and current density-voltage (*J*-*V*) curves (b) of the OLEDs devices, solid line is luminace of **PF-triAz** (blue) and **PCz-triAz** (pink); dsahed line is current density of **PF-triAz** (green) and **PCz-triAz** (orange).

Table 2-8. EL properties of the polymers.

Polymer	L_{max} (voltage)	Current density at L_{max}	Max. efficiency (voltage)	Remark
	cd m^{-2} (V)	mA cm^{-2}	cd A^{-1} (V)	
PCz-triAz	182 (18.8)	225	0.21 (5.1)	greenish blue
PF-tetrAz	–	–	–	quickly die
PF-triAz	536 (12.2)	163	0.35 (11.9)	blue

The turn-on voltages of the **PF-triAz** and **PCz-triAz** copolymer-based devices were about 10 V and 12 V, respectively, which suggest that interfacial barriers of carrier injection are different from each other. Their emission colors were viewed as blue emission for **PF-triAz** and greenish blue for **PCz-triAz**-based ones. The maximum brightness of the **PF-triAz**-based devices and **PCz-triAz** copolymer-based devices were about 536 and 182 cd/m^2, while the current density were 163 and 225 mA/cm^2, respectively, and the maximum current efficiencies were about 0.35 and 0.21 cd/A, respectively. Clearly, the **PF-triAz** copolymer-based devices showed the better EL performances than the **PCz-triAz**-based devices. This might be attributed to the low molecular weight of **PCz-triAz**. Low molecular weight led to the poor thin film quality and low brightness and small current efficiency of the **PCz-triAz**-based device. Consequently, the azine unit increased the current efficiency of the OLED devices compared polyfluorene and polycarbazole based devices, which showed the current efficiency 0.25 and 0.20 cd/A [58, 59].

2.2.3 Summary

In summary, three blue luminescence polymers **PF-tetrAz**, **PF-triAz** and **PCz-triAz**, have been developed by combination of the fluorene/carbazole sequences as an electron-donor and the **tetrAz** or **triAz** core as an electron-acceptor. All of the copolymers were obtained in high yields, and they showed a good solubility in common organic solvents and good thermal stability. They showed similar electronic properties of absorption and emission in $CHCl_3$ solution, the values of λ_{max}(abs) and λ_{max}(em) of each polymer were about 380 and 430 nm, respectively. In the thin film states, **PF-triAz** showed deep blue fluorescence with the values of λ_{max}(em) at 422 nm with CIE coordinates (0.16, 0.07). **PF-tetrAz**, **PF-triAz** and **PCz-triAz** showed acceptable E_{HOMO} (–5.83, –6.0 and –5.47 eV) for hole transport and proper E_g (2.98, 3.12 and 2.77 eV) for blue emission. We fabricated the OLEDs devices that have a configuration of ITO/ PEDOT:PSS/ copolymer/ LiF/ Al using these polymers as the emitting layer materials, and investigated their EL performances for the first time. **PF-triAz** based OLEDs devices showed maximum brightness and the maximum current efficiencies were 536 cd/m^2 and 0.35 cd/A, respectively. According to these results, these D-A copolymers have a great potential to be applied in OLED as the blue-light emitting materials.

2.2.4 Experimental

2.2.4.1 Fabrication and Measurement of OLED Devices

The OLED devices were fabricated in the configuration of ITO/ PEDOT:PSS/ copolymers/LiF/ Al. The patterned ITO (conductivity: 10 Ω/square) glass was precleaned by ultrasonication in 2-propanol and successively in acetone. The precleaned ITO glass was treated in an ultraviolet-ozone chamber. A thin layer (40 nm) of PEDOT:PSS was spin-coated on the ITO at 3000 rpm in 3 min and air-dried at 110 °C for 10 min on a hot plate. The substrate was transferred to a glovebox under N_2 atmosphere. Solutions of the copolymers at various blending ratios in toluene were subsequently spin-coated on the PEDOT:PSS layer. LiF (0.5 nm) and Al (100 nm) were deposited on the emitting layer with conventional thermal evaporation at the chamber pressure lower than 5×10^{-4} Pa, which provided the devices with an active area of 2×2 mm^2. The thickness of emitting layers and PEDOT:PSS layers were measured using a stylus-type film thickness meter (ULVAC E. S., Inc., Tokyo, Japan, Dektak). The luminance-current density-voltage (*L*-*J*-*V*) curves were measured using Keithley 2612A and TOPCON BM-9M with measurement angle at 0.2 Å.

2.2.4.2 Materials

Three polymers (**PF-tetrAz**, **PF-triAz** and **PCz-triAz**) were synthesized according to the Scheme 2-4 and Scheme 2-5. Reagents and solvents were purchased from Kanto Chemical, Tokyo Chemical Industry, Aldrich and Nacalai Tesque Inc. 2,7-dibromocarbazole, 7-bromo-9,9-bis(2-ethylhexyl)-9*H*-fluorene-2-carbonitrile (**1**)**,** 2,4-dichloro-6-(octyloxy)-1,3,5-triazine (**4**) and 2,2'-(9,9-bis(2-ethylhexyl)-9*H*-fluorene-2,7-diyl)bis-1,3,2-dioxaborolane were synthesized according to the procedures reported previously [60-63]. Tetrahydrofuran (THF) distilled after drying with sodium was stored under an argon atmosphere. Dimethylformamide (DMF) distilled after drying with CaH_2 was stored under an argon atmosphere. The other solvents and all commercially available reagents were used without further purification.

2.2.4.3 Synthesis of monomers and polymers

Synthesis of 7-bromo-9,9-bis(2-ethylhexyl)-9*H*-fluorene-2-carbonitrile (1). A suspension of Cu(I)CN (0.16 g, 1.82 mmol) and 2,7-dibromo-9,9-bis(2-ethylhexyl)fluorine (1 g, 1.82 mmol) in 8 mL of DMF was refluxed for 24 h. After cooling to ambient temperature, the mixture was mixed with water. After

extraction with dichloromethane, drying over $MgSO_4$ and the solvent evaporation, the crude product was purified by column chromatography using hexane/CH_2Cl_2 (9:1) as an eluent to give a light yellow oil (0.46 g, 51.2%). ^{1}H NMR (400 MHz, $CDCl_3$) δ [ppm]: 7.75 (d, J= 7.8 Hz 1H), 7.65-7.63 (m, 3H), 7.55-7.50 (m, 2H), 1.98 (d, J= 4.1 Hz 4H), 0.90-0.49 (m, 30H). ^{13}C NMR (100 MHz, $CDCl_3$) δ [ppm]: 153.3, 144.7, 138.2, 131.3, 130.5, 127.7, 127.5, 122.0, 120.3, 119.6, 109.7, 55.5, 44.3, 34.6, 28.0, 27.1, 22.6, 14.0, 10.8, 10.3.

Synthesis of 3,6-bis(7-bromo-9,9-bis(2-ethylhexyl)-9H-fluorene-2-yl)-1,2-dihydro [1,2,4,5]tetrazine (**2**). To mixture of **1** (0.2 g, 0.41 mmol) in ethanol (1 mL) was added hydrazine (0.019 mL, 0.615 mmol) and sulfur (0.008 g, 0.25 mmol) quickly. The suspension was heated reflux for 3h with stirring and then put into an ice bath for further solidification. The precipitate was collected by filtration and washed with 2 x 10 mL of cold ethanol to give a crude orange dihydrotetrazine, which was reacted in the next step without further purification.

Synthesis of 3,6-bis(7-bromo-9,9-bis(2-ethylhexyl)-9H-fluorene-2-yl)-[1,2,4,5]tetrazine (**3**). The orange solid of **2** was dissolved in 1 mL of acetic acid at ambient temperature with stirring. $NaNO_2$ (0.028 g, 0.41 mmol) was added to the solution at 0 °C. After complete of the reaction, the purple precipitate was collected by filtration and washed with 2 × 5 mL of methanol to give a dark purple solid (0.176 g, 84.6%). ^{1}H NMR (400 MHz, $CDCl_3$) δ [ppm]: 8.08 (s, 2H), 8.01 (d, J= 8.25 Hz 2H), 7.78 (d, J= 8.25 Hz 2H), 7.62 (d, J= 8.25 Hz 2H), 7.56 (s, 2H), 7.50 (d, J= 8.25 Hz 2H), 2.12-2.03 (m, 8H), 1.28-1.25 (m, 4H), 0.91-0.77 (m, 32H), 0.56-0.50 (m, 24H). ^{13}C NMR (100 MHz, $CDCl_3$) δ [ppm]: 177.3, 157.7, 153.3, 144.7, 138.2, 130.5, 130.4, 128.4, 127.6, 127.5, 122.0, 120.3, 55.5, 44.2, 34.7, 33.6, 28.0, 27.1, 22.6, 14.1, 10.3.

Synthesis of 2,4-dichloro-6-(octyloxy)-1,3,5-triazine (4). A suspension of 1-decanol (1.72g, 11 mmol), cyanuric chloride (1.5g, 8.13 mmol), and collidine (1.1 mL) in acetone (10 mL) was stirred in an ice-bath for another one hour. After warming to ambient temperature, the mixture was mixed with water. After extraction with dichloromethane, drying over $MgSO_4$ and the solvent evaporation, the crude product was purified by column chromatography using hexane/dichloromethane (1:1) as an eluent to give a white oil (1.90g, 88%).^{1}H NMR (400 MHz, $CDCl_3$) δ [ppm]: 4.47 (t, J= 6.9 Hz 2H),1.82-1.76 (m, 2H), 1.45-1.26 (m, 10H), 0.89-0.85 (m, 3H). ^{13}C NMR (100 MHz, $CDCl_3$) δ [ppm]: 172.4, 171.0, 70.7, 31.7, 29.1, 28.4, 28.2, 25.7, 22.6, 14.0.

Synthesis of 2-octyloxy-4,6-bis(7-bromo-9,9-bis(2-ethylhexyl)-9*H*-fluorene-2-yl)-1,3,5-triazine (**5**). 9,9-Bis(2-ethylhexyl)-2,7-dibromofluorene (0.44 g, 0.80mmol) was dissolved in 4 mL of dry THF and cooled to –78 °C under N_2 atmosphere, in which n-BuLi solution (1.6 M in hexane, 0.56 mL, 0.9 mmol) was added dropwise with stirring. The mixture was stirred at –78 °C for one hour and **4** (0.11 g, 0.4 mmol) was added slowly. The reaction solution was stirred for another 15 min at –78 °C. Afterward, the solution was allowed to warm up to ambient temperature and stirred for one day, and quenched with addition of water. After extraction with dichloromethane, drying over $MgSO_4$ and the solvent evaporation, the crude product was purified by column chromatography using dichloromethane/hexane (1:2) as eluent to afford a yellow oil (0.088g, 51%). ^{1}H NMR (400 MHz, $CDCl_3$) δ [ppm]: 8.68-8.65 (m, 4H), 7.82 (d, J= 7.78 Hz 2H), 7.65 (d, J= 7,78 Hz 2H), 7.58 (d, J= 7.78 Hz 2H), 7.51 (d, J= 7.78 Hz 2H), 4.66 (br, 2H), 2.14-1.94 (m, 10H), 1.32-1.24 (m, 6H), 0.92-0.71 (m, 36H), 0.58-0.50 (m, 27H). ^{13}C NMR (100 MHz, $CDCl_3$) δ [ppm]: 173.5, 170.3, 153.9, 150.4, 144..5, 139.4, 134.5, 130.1, 128.4, 127.5, 124.6, 121.7, 121.6, 119.6, 68.1, 55.3, 44.3, 34.7, 33.5, 31.8, 29.4, 29.1, 28.8, 28.1, 27.1, 26.0, 22.7, 22.6, 14.1, 14.0, 10.4.

Synthesis of 2,7-dibromo-9-(2-heptylundecyl)-9*H*-carbazole (**6**). A mixture of 2,7-dibromocarbazole (1.26g, 3.89mmol) and NaH (0.25 g,) was stirred 30 min at 0 ºC, and then 8-(bromomethyl)heptadecane (1.3g, 3.9 mmol) was added. The reaction mixture was allowed to stirr for 24 h at room temperature. The mixture was poured into water. After extraction with CH_2Cl_2, drying over $MgSO_4$ and the solvent evaporation, the crude product was purified by column chromatography (silica gel, hexane/CH_2Cl_2, 1:1, as an eluent) to give oil (1.99 g, 89%).^{1}H NMR (400 MHz, $CDCl_3$) δ [ppm]: 7.89 (d, J= 8.24 Hz 2H), 7.50 (s, 2H), 7.34 (d, J= 8.24 Hz 2H), 4.06 (d, J= 7.33 Hz 2H), 2.08 (m, 1H), 1.34-1.22 (m, 28H), 0.90-0.84 (m, 6H). ^{13}C NMR (100 MHz, $CDCl_3$) δ [ppm]: 141.8, 122.5, 121.4, 121.2, 119.6, 112.3, 47.8, 37.6, 36.1, 31.9, 31.8, 31.6, 29.9, 29.8, 29.6, 29.5, 29.3, 29.2, 27.8, 26.4, 22.7, 22.6, 14.1, 14.0.

Synthesis of 2-octyloxy-4,6-bis(7-bromo-9-(2-heptylhendecyl)-9*H*-carbazole-2-yl)- 1,3,5-triazine (**7**). **6** (0.36 g, 0.80mmol) was dissolved in dry THF (4 mL) and cooled to –78 °C under nitrogen atmosphere, in which 1.6 M n-BuLi/hexane solution (0.56 mL, 0.9 mmol) was added dropwise with stirring. The mixture was kept at –78 °C for 1 h and **4** (0.11 g, 0.4 mmol) was slowly added. The reaction mixture was stirred for another 15 min at –78 °C. Afterward, the solution was allowed to warm up to room temperature and stirred for 24 h, and quenched with addition of water. After extraction with CH_2Cl_2, drying over $MgSO_4$ and the solvent evaporation, the crude product was purified by column chromatography (silica gel, CH_2Cl_2/hexane, 1:2, as eluent) to afford a light yellow solid (0.113 g, 55%).^{1}H NMR (400 MHz, $CDCl_3$) δ [ppm]: 8.74 (s, 2H), 8.59 (d, J= 8.24 Hz 2H), 8.17 (d, J= 8.24 Hz 2H), 7.99 (d, J= 8.24 Hz 2H), 7.58 (s, 2H), 7.37 (d, J= 8.24 Hz 2H), 4.70 (d, J= 6.4 Hz 2H), 4.40-4.37 (m, 4H), 1.97-1.91 (m, 2H), 1.42-1.20 (m, 68H), 0.89-0.80 (m, 15H). ^{13}C NMR (100 MHz, $CDCl_3$) δ [ppm]: 175.2, 172.5, 142.9, 140.8, 132.8, 125.9, 122.4, 122.1, 121.2, 120.6, 120.3, 120.0, 112.4, 110.2, 68.4, 68.0, 47.8, 37.7, 31.9, 31.8, 31.7, 31.6, 30.8, 30.0, 29.9, 29.6, 29.5, 29.4, 29.3, 29.2, 29.1, 28.8, 26.5, 25.9, 22.7, 22.6, 19.2, 14.1, 14.0, 13.8.

Synthesis of poly[(9,9,9',9',9",9"-hexaxis(2-ethylhexyl)[2,2':7',2''-ter-9H-fluorene]-7,7"-diyl)-([1,2,4,5]tetrazine-3,6-diyl)] (**PF-tetrAz**). A mixture solution of 2,2'-(9,9-bis(2-ethylhexyl)-9*H*-fluorene-2,7-diyl)bis-1,3,2-dioxaborolane (0.037 g, 0.07 mmol), aqueous K_2CO_3 (2M, 0.7 mL), tetrakis(triphenylphosphine) palladium ($Pd(PPh_3)_4$, 4.1 mg) and **3** (0.071 g, 0.07 mmol) in 1.0 mL of toluene was heated reflux with vigorous stirring for 72 h under argon atmosphere. After the reaction solution was cooled to ambient temperature, the resultant precipitate was firtly precipitated from methanol/HCl aq, and reprecipitated from methanol/NH_3 aq and from methanol, respectively. The polymer was successively extracted with acetone, hexane and chloroform by Soxhlet extraction. The chloroform extract was again precipitated from methanol. **PF-tetrAz** was given as an orange solid (0.077g, 80%). ^{1}H NMR (400 MHz, $CDCl_3$) δ [ppm]: 8.12-8.02 (m, 4H), 7.90-7.83 (m, 4H), 7.78-7.59 (m, 8H), 7.49 (br, 1H), 7.35-7.30 (m, 1H), 2.17-2.0 (m, 12H), 1.31-1.11 (m, 6H), 0.89-0.80 (m, 48H), 0.63-0.57 (m, 36H). $C_{89}H_{122}N_4$ (1246.89): Calcd. C 85.66, H 9.85, N 4.49; Found. C 83.48, H 9.33, N 4.38.

Synthesis of poly[(9,9,9',9'-tetrakis(2-ethylhexyl)-9H-fluorene-7,7'-diyl)-2-octyloxy-1,3,5-triazine-4,6-diyl)] (**PF-triAz**). A mixture solution of bis(1,5-cyclooctadiene)nickel(0) ($Ni(cod)_2$) (0.110 g, 0.40 mmol), 2,2'-bipyridine (bpy) (0.070 g, 0.448mmol) and 1,5-cyclooctadiene (cod) (0.10 g, 0.92 mmol) in 1 mL of DMF was heated under an argon atmosphere for 30 min at 80 °C. To the mixture was added **5** (0.083 g, 0.184 mmol) dissolved in1 mL of THF under argon. The mixture solution was heated for 72 h at 80 °C. After the reaction solution was cooled to ambient temperature, the resultant polymer was firstly precipitated from methanol/HCl aq, and reprecipitated from methanol/NH_3 aq and from methanol, respectively. The precipitate was successively extracted with acetone, hexane and chloroform by Soxhlet

extraction. The chloroform extract was again precipitated from methanol. **PF-triAz** was obtained as a white solid (0.060g, 83%). ^{1}H NMR (400 MHz, $CDCl_3$) δ [ppm]: 8.73 (br, 4H), 7.92-7.89 (m, 4H), 7.70-7.67 (m, 4H), 4.68 (d, J= 5.6 Hz 2H), 2.17 (br, 8H), 2.01-1.97 (m, 2H), 1.47-1.25 (m, 6H), 0.93-0.87 (m, 36H), 0.73-0.53 (m, 27H). $C_{71}H_{103}N_3O$ (1013.70): Calcd. C 84.05, H 10.23, N 4.14; Found. C 82.23, H 9.66, N 3.84.

Synthesis of poly[(9,9'-bi(2-heptylhendecyl)-9*H*-carbazole-7,7'-diyl)-2-octyloxy-1,3,5-triazine-4,6-diyl)] (**PCz-triAz**). Similarly, polymerization of **7** gave **PCz-triAz** as a light yellow solid (0.13 g, 90%). ^{1}H NMR (400 MHz, $CDCl_3$) δ [ppm]: 8.82-8.67 (m, 3H), 8.31-8.28 (m, 5H), 7.77-7.67 (m, 4H), 4.75 (br, 2H), 4.57 (br, 4H), 2.05 (br, 6H), 1.43-1.23 (m, 64H), 0.91-0.82 (m, 15H). $C_{57}H_{77}N_7O$ (817.70): Calcd. C 80.71, H 9.15, N 8.26; Found. C 78.50, H 8.57, N 8.09.

^{1}H NMR spectra of **5**

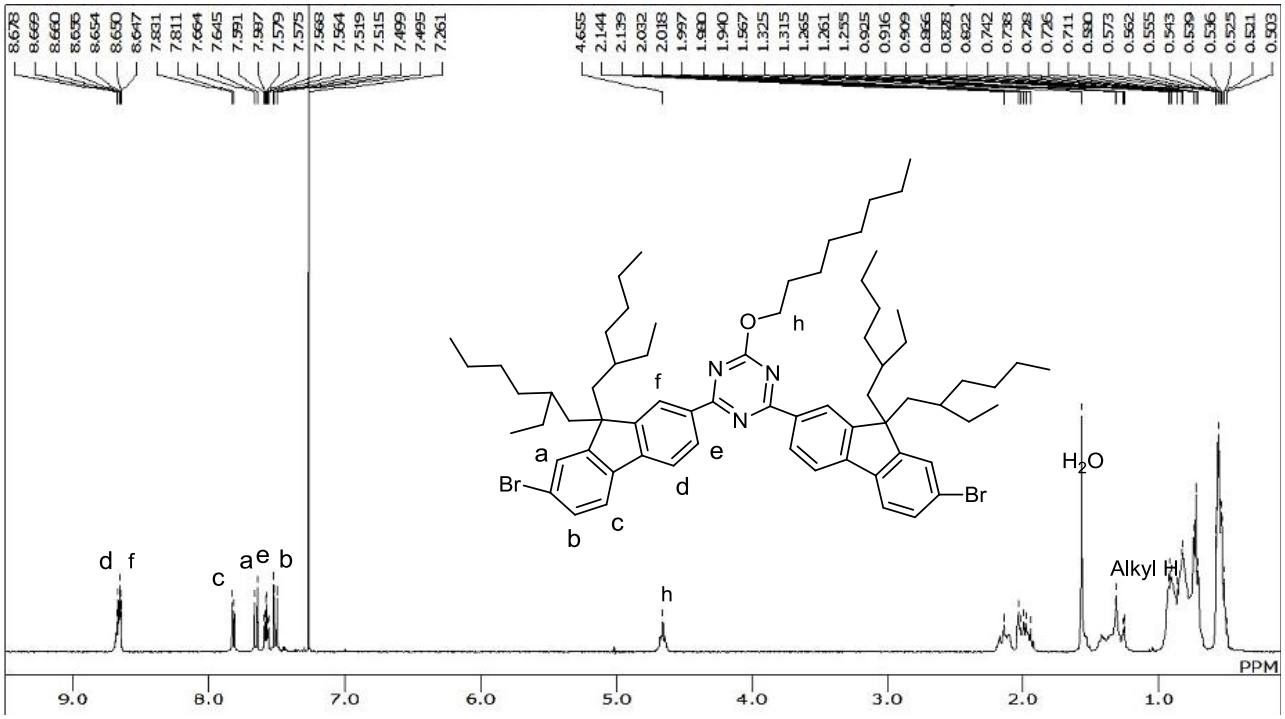

^{13}C NMR spectra of **5**

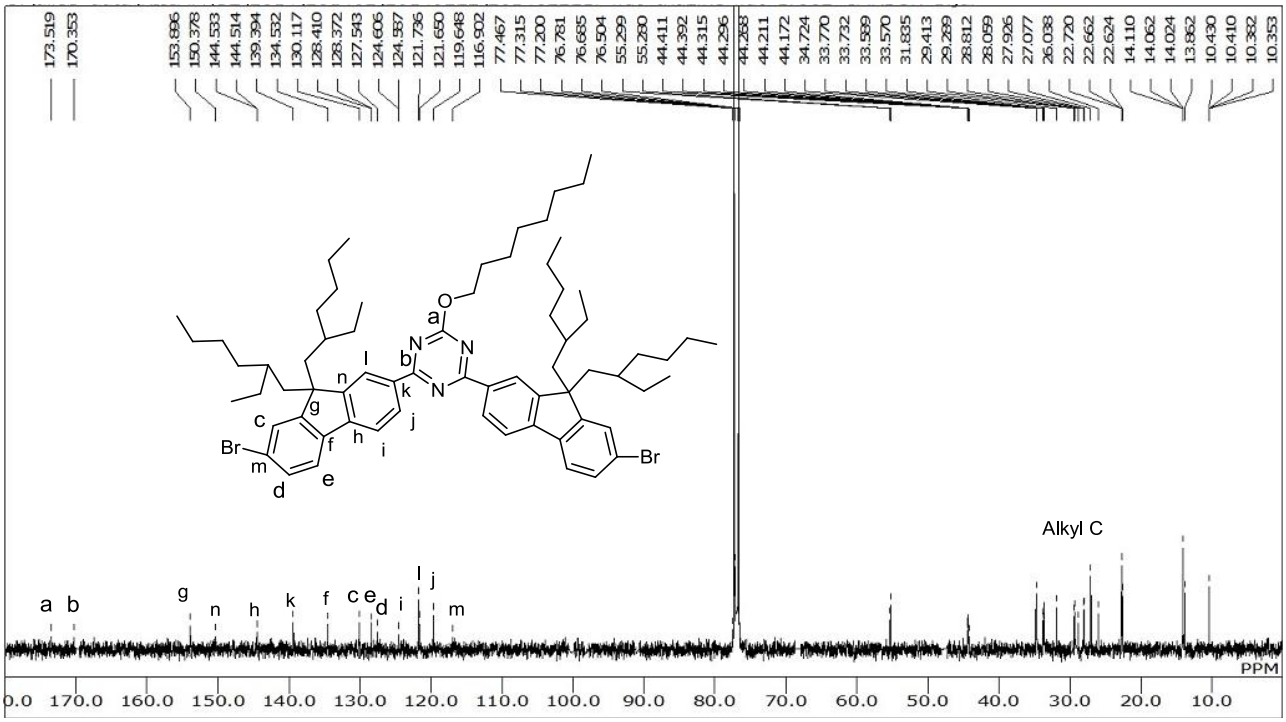

^{1}H NMR spectra of **4**

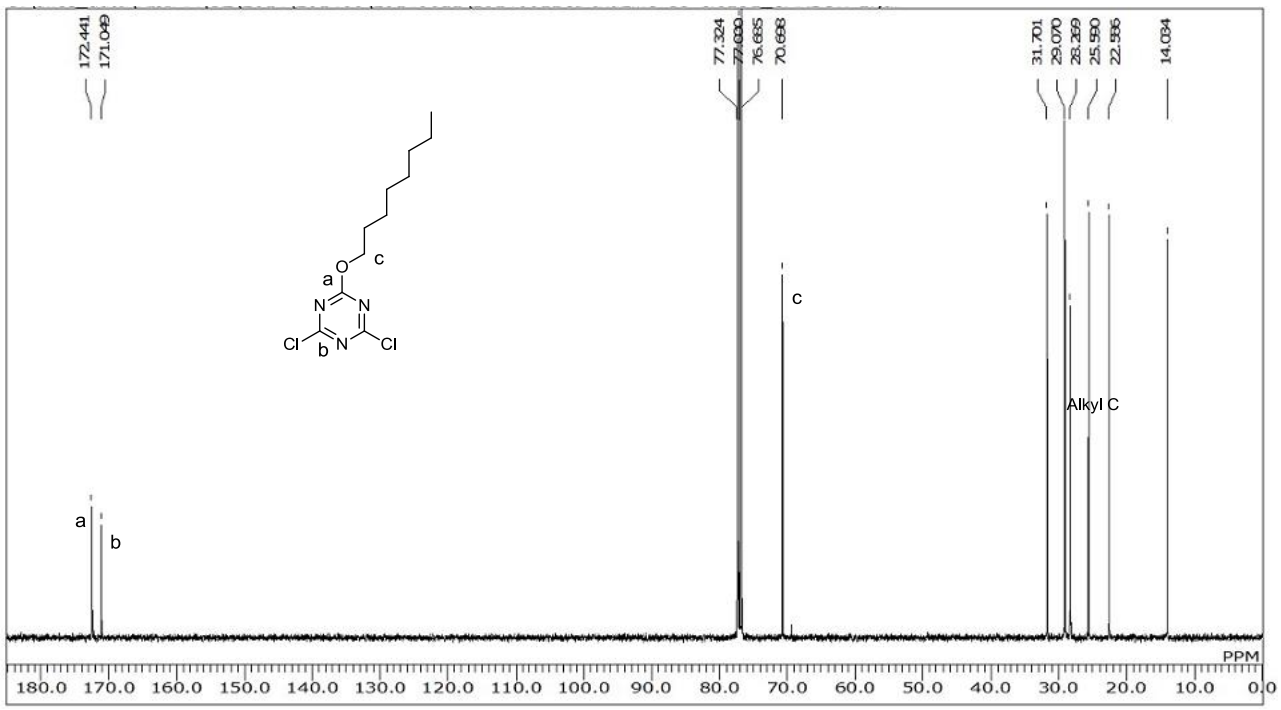

^{1}H NMR spectra of 7

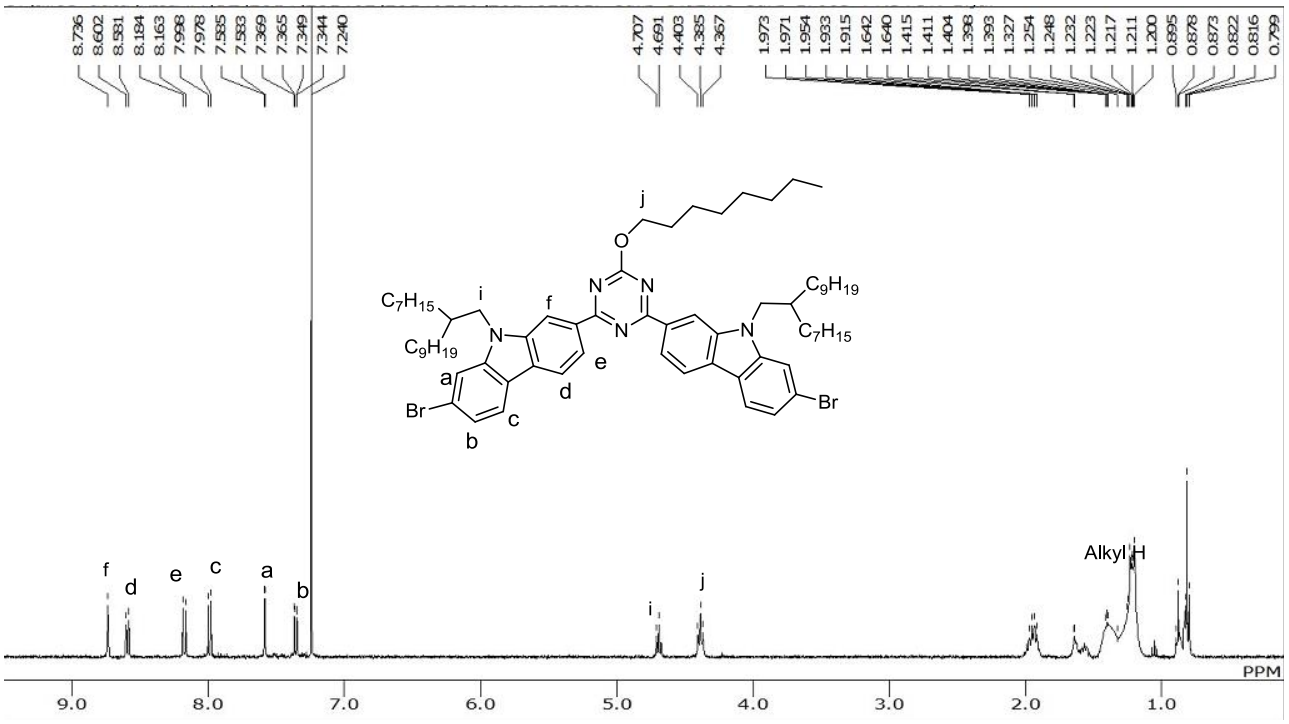

^{1}H NMR spectra of **PF-triAz**

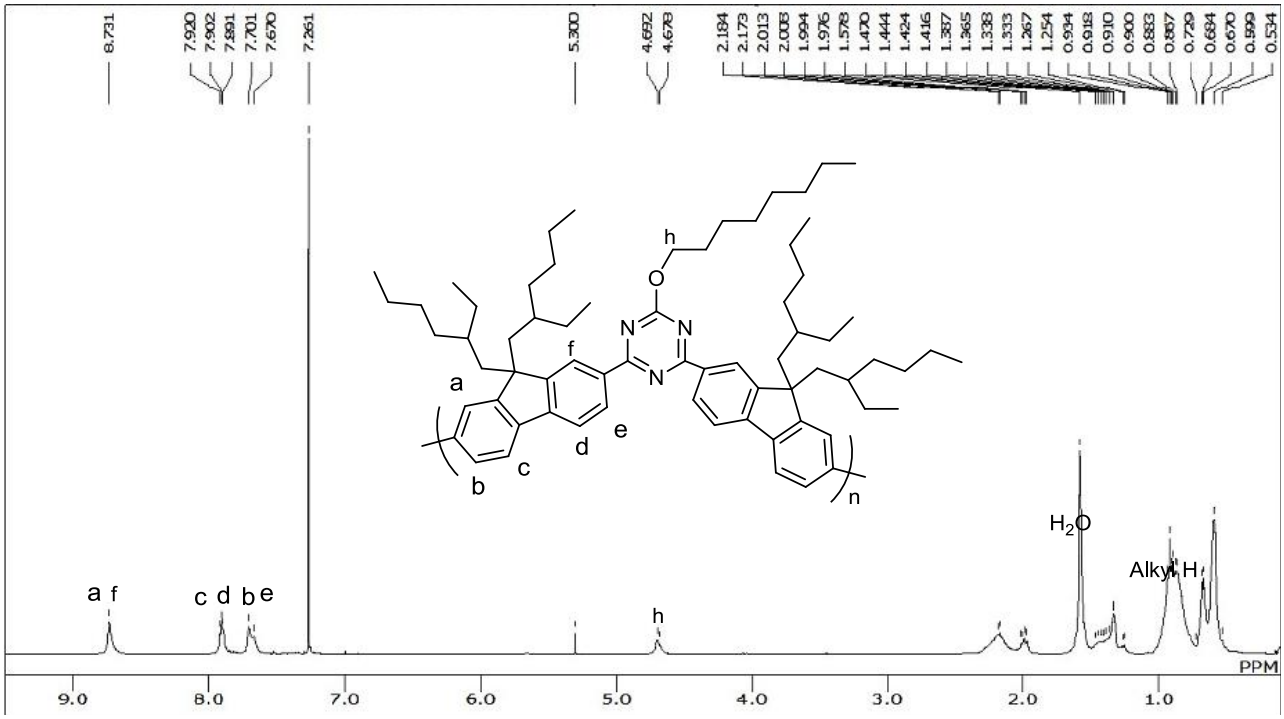

^{1}H NMR spectra of **PF-tetrAz**

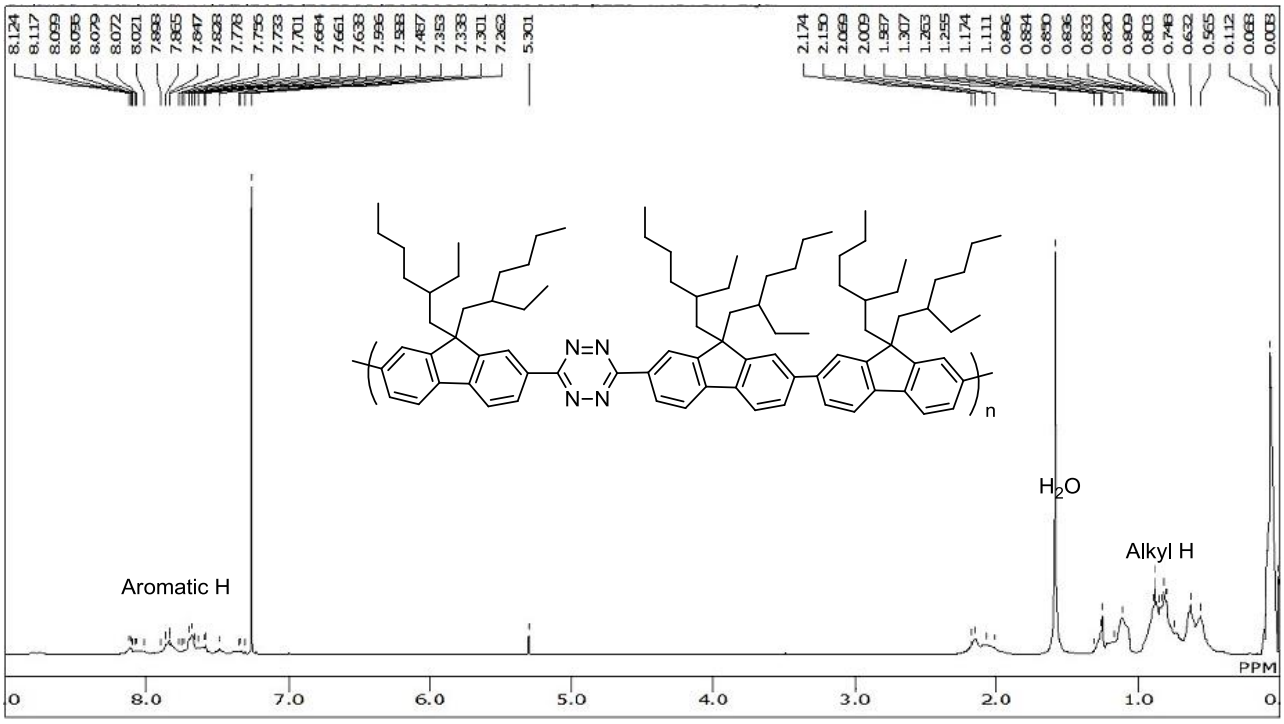

^{1}H NMR spectra of **PCz-triAz**

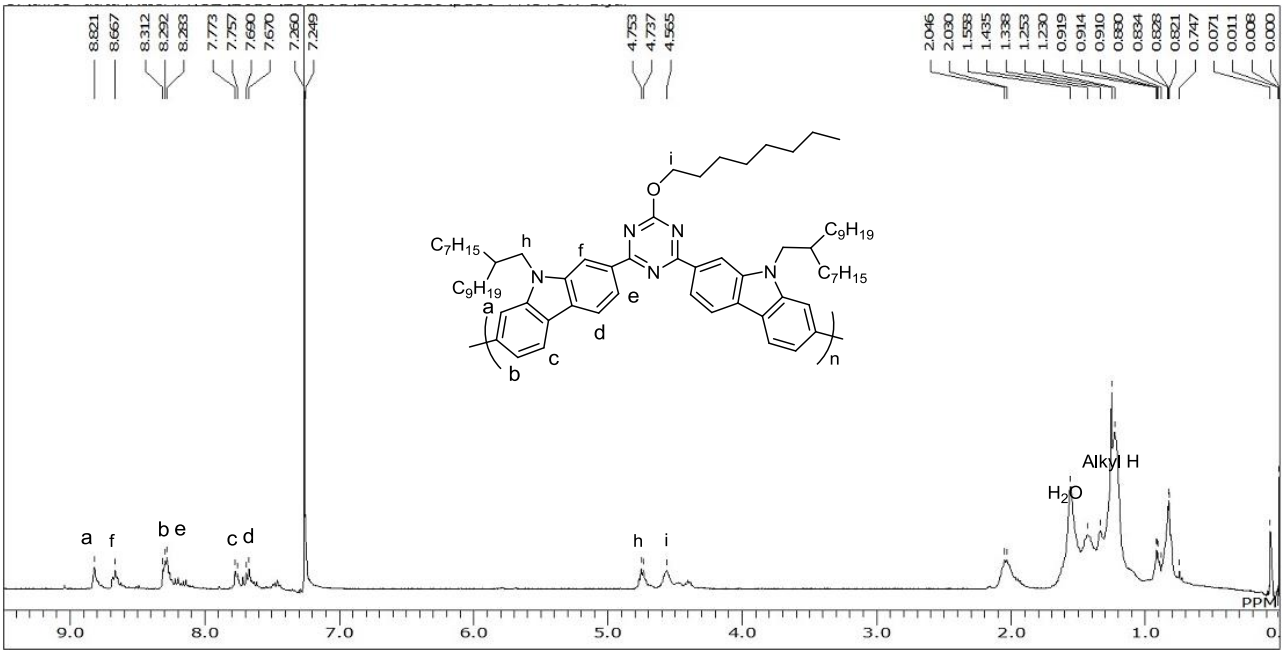

2.3 Efficient blue luminescence D-π-A type copolymers having sulfone/phosphine oxide unit

2.3.1 Background

During the last few decades, electrical devices based on organic materials have emerged as an interesting and promising alternative to their inorganic counterparts. Organic materials could offer critical advantages such as being more environmentally friendly and less expensive in many electrical applications. One application, a light-emitting device, has used in the form of polymer light-emitting diodes (PLEDs). The PLEDs technology has been applied in consumer-market but some shortcomings are still existence. The efficiency of PLEDs depends crucially on the work functions of the charge carrier injectors, leading to limitations in the choice of electrode materials and allowed active material thickness [64].

Another type of electroluminescent device, the polymer light emitting electrochemical cells (LECs), were invented in 1995 by Qibing Pei and Alan Heeger's group at Santa Barbara [65]. Polymer LECs are fundamentally different from PLEDs since their incorporation of about a single emitting layer of luminescent polymers blended with electrolytes or ionic liquids between electrodes (Fig. 2-19). Owing to the addition of an electrolyte, the active layer of LECs allows to be ionic conductors as well as electronic conductors.

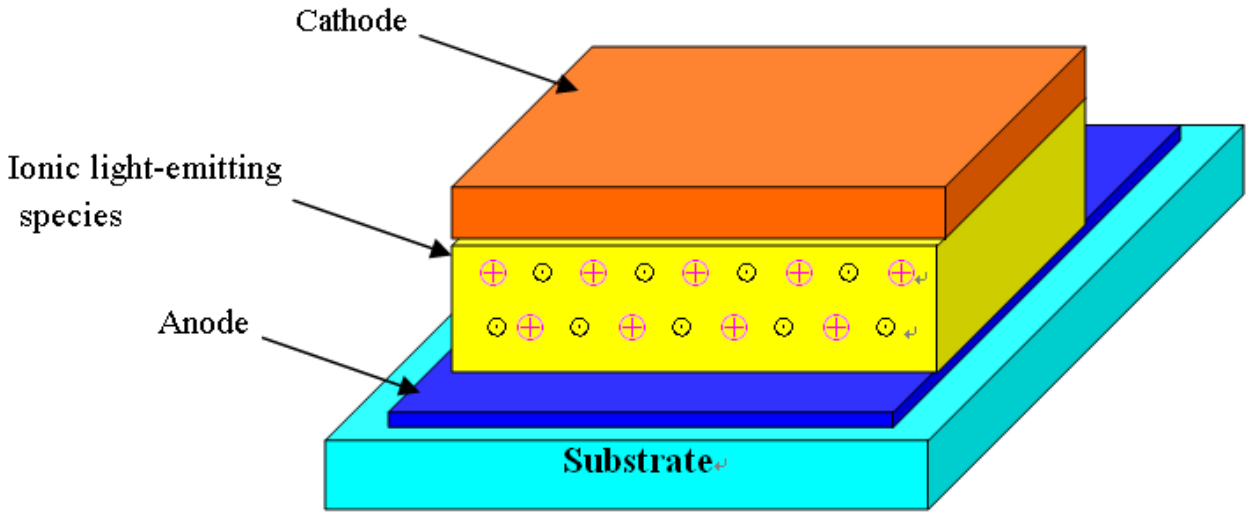

Fig. 2-19 The Structure of LECs

In order to explain the showed characteristics of LECs, the operating mechanism were investigated. In simplest form of the polymer LECs, itsconsists of a single emitting layer of luminescent polymers mixed with solvated ions. When a bias voltage is firstly applied, ionic charge will be built up on the surface of the polymer film. At same time, an equal electronic charge was built uo on the electrode surface [66]. A very strong electric field was exsited at the interface enabling the electronic charges to move through into the polymer. Once a voltage greater than the energy gap of the polymer is applied, the charge injection occurs with electrons injecting from the cathode and holes injected from the anode. As a result, the luminescent polymer near the cathode/ anode is reduced/ oxidized by gaining electrons/ losing electrons, respectively. The mobile ions from the polymer electrolyte redistribute until they are conducted between the reduced/oxidized polymer segments to compensate the electronic charges. When the expanding p and n doping regions eventually meet within the electric field between the electrodes, the light emitting junction is eventually formed and the injected electrons and holes recombine and emit light. [67].

Due to the good conductive and tends to form ohmic contact with electrodes and polymer, the LECs show more balanced and efficient charge carrier injection. Consequently, the LECs typically exhibits low turn on voltage which approximately equal to the energy band gap E_g (E_g is the polymer energy band gap) and high external quantum efficiency. As the same reason, the LECs performance is relatively insensitive to the thickness of the active layer polymer film and to kinds of electrode materials [67].

Table 2-9. The comparision of polymer LEDs and LECs [68]

	Polymer LEDs	**Polymer LECs**
Active layer	Conjugated polymer material	Blend of conjugated polymer and electrolyte
Thickness of active layer	Thin	Insensitive
Anode	High work-function	Insensitive
Cathode	Low work-function	Insensitive
Operating voltage	Depending on kinds of electrodes, contacting conditions and Energy bandgap	Depending on Energy bandgap
Response speed	High	Low
Fabrication	Simpler	Simpler

Some potential advantages of LECs such as low operating voltage, high efficiency and insensitivity to the electrode materials etc as listed in Table 2-9. As the presence of ions, the external quantum efficiency of LECs is not dependent on the injection balance, because charges are easily injected. Although the LECs have possessed many attractive device characteristics, but some drawbacks existed due to the electrochemical doping process itself. For example, the operational lifetime of LECs is typically very short, because of the irreversible degradation of the luminescent polymers leading to lower external qunatum efficiency, when they are doped during continuous operation [67]. Furthermore, due to the limitation of the electrochemical doping process and the formation of a emitting junction by the slow ionic motion, the response time of LECs is normally slow, ranging from seconds to hours [67, 69, 70]. In order to make LECs suitable for lighting, more effective ways have been studied.

Although LECs have these advantages, the pure blue LECs are still rare. Chen et al. have developed efficient sky-blue LECs with luminance, CIE index and current efficiency of 5.3 cd m^{-2}, 2.6 cd A^{-1} and (0.21, 0.33), respectively [71]. He et al. have presented pure blue LECs with performances of 39 cd m^{-2}, 0.65 cd A^{-1} and CIE (0.20, 0.28), respectively [72]. However, the blue emitting LECs using polymers as the active layer have no report.

One type of compound that typically consist of an electron-donating and an electron-accepting group connected through a π-conjugated linker, has attracted much technological research interest because of their unique optical and electrical properties. In order to obtain pure blue emitting materials, donor-π-acceptor (D-π-A) type copolymers have aroused intensive interest because they not only possess high fluorescent quantum yields owing to the effective radiative decay of their excited intramolecular charge-transfer state but also show good bipolar charge-transporting properties for their constituting of hole- and electron-transporting moieties [73]. Because D-π-A type fluorophores were used, the device configurations

were effectively simplify and the electroluminescence efficiencies were tremendously enhanced [74, 75]. However, the D-π-A structure in main chain of copolymer enlarged π-conjugation and the intramolecular charge-transfer lead to remarkable fluorescence red shifts [76]. One easy strategy for preserving well blue emission is to control the length of π-conjugation and the intramolecular charge-transfer inside main chain.

Herein, in order to develop pure blue emitting conjugated polymers, sulfone/phosphine oxide units were as chosen electron-acceptor (A) due to its good electron injection properties. More importantly, the sulfone/phosphine oxide unit can segment the local π conjugation and limit the intramolecular charge-transfer. Moreover, in this work, two benzene rings were linked to the sulfone/phosphine oxide unit, which also served for controlling local π-conjugation because of its tetrahedral/trigonal-pyramidal structure. This conformation could effectively hinder close molecular packings in the solid state, and prevent excimer formation and fluorescence quenching [77]. Furthermore, the confinement of the intramolecular charge-transfer by sulfone/phosphine oxide unit was beneficial to conductivity in LECs device. Fluorene/carbazole units were selected as as the emissive and electron-donor (D) unit for hole injection and transport functions.

Seven D-π-A type copolymers, poly[4,4'-diphenylsulfone-*alt*-9,9-bis(2-ethylhexyl)-9*H*-fluorene-2,7-diyl] (**PFDSO**), poly[4,4'-diphenylsulfone-*alt*-(9,9,9',9'-tetrakis(2-ethylhexyl)-9*H*-fluorene-7,7'-diyl)] (**PDFDSO**), poly[4,4'-diphenylsulfone-*alt*-(9-(2-heptylundecyl)-9*H*-carbazole-2,7-diyl)] (**PCDSO**), poly[4,4'-diphenylsulfone-*alt*-(4-(1-decylundecyl)-4*H*-benzo[*def*]carbazole-2,6-diyl)] (**PBCDSO**), poly[4,4'-diphenyl(phenylphosphinylidene)-*alt*-9,9-bis(2-ethylhexyl)- 9*H*-fluorene-2,7-diyl] (**PFTPO**), poly[4,4'-diphenyl(phenylphosphinylidene)-*alt*-(9- (1-decylundecyl)-9*H*-carbazole-2,7-diyl)] (**PCTPO**) and poly[4,4'-diphenyl(phenylphosphinylidene)-*alt*-(4-(1-decylundecyl)-4*H*-benzo[*def*]carbazole-2,6-diyl)] (**PBCTPO**), shown in Fig.2-20 and Fig. 2-21, were synthesized and characterized. An organic ionic liquid, methyltrioctylammonium trifluoromethanesulfonate (MATS) (Fig. 2-21), was used to introduce mobile ions into the emitting layer of copolymers. The MATS shows the easy processing and good free-standing film quality [78]. Finally, the optical and electronic properties of these copolymers were investigated, and the PLEDs and LECs devices embedded with the mixture of copolymers and ionic liquid as the emitting layer were evaluated.

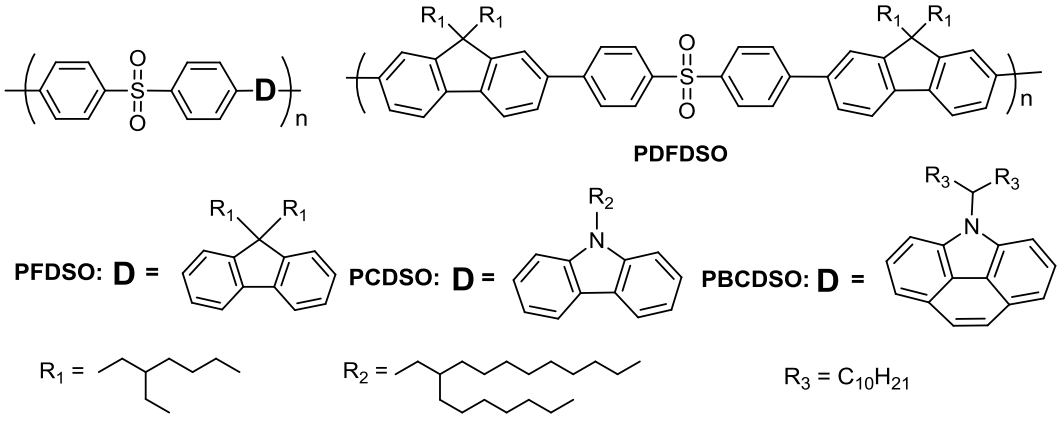

Fig.2-20 The chemical structures of **PFDSO**, **PDFDSO**, **PCDSO** and **PBCDSO**

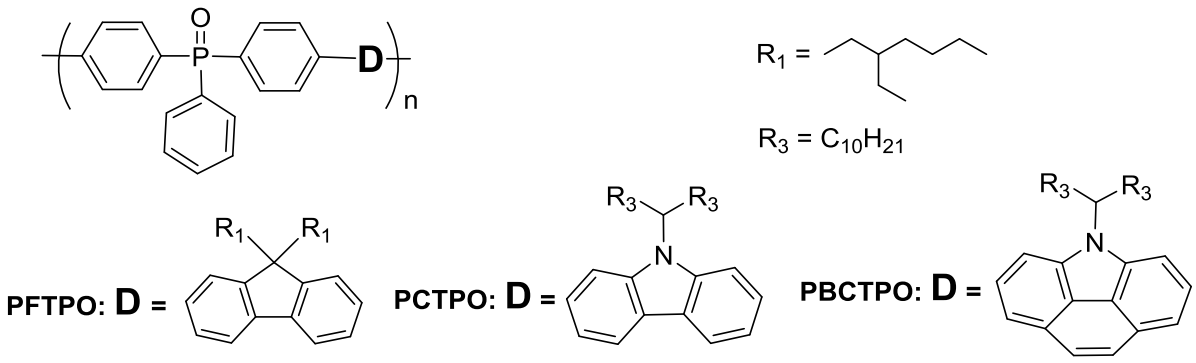

Fig. 2-21 The chemical structures of **PFTPO**, **PCTPO**, **PBCTPO** and MATS.

2.3.2 Results and discussion

2.3.2.1. Synthesis

The general synthetic routes toward the monomers and polymers are depicted in Scheme 2-6 and Scheme 2-7. 2,7-dibromo-9-(2-heptylundecyl)-9*H*-carbazole (**4**) was carried out according to the procedure in our last section. The sulfone intermediate **2** was prepared from 1-bromo-4-iodobenzene, sequentially, a coupling reaction was carried out with sulfur powder, copper (I) iodide and lithium hydroxide monohydrate as the catalyst to give **1.** The oxidation of **1** was performed to give **2** by using $KMnO_4$ and $MnSO_4$. The diboronic esters **3, 5** and **6** were synthesized by coupling of 2,7-dibromo-9,9-bis(2-ethylhexyl)fluorene, **4,** 2,6-dibromo-4-(1-decylundecyl)-4*H*-benzo[*def*]carbazole, and bis(pinacolato)diboron with $PdCl_2$(dppf) as the catalyst, respectively. Lithiation of 2,7-dibromo-9,9-bis(2-ethylhexyl)fluorene with n-butyllithium (n-BuLi) followed by treatment with 2-isopropoxy-4,4,5,5-tetramethyl-1,3,2-dioxaborolane gave **7**. The coupling reaction of **7** and **2** gave **8**. The phosphine oxide intermediate **9** was prepared from 1,4-dibromobenzene by sequential lithium-halogen exchange with *n*BuLi, coupling with dichlorophenylphosphine, and oxidation with hydrogen peroxide. Homopolymerization of **8** by the Yamamoto reaction afforded **PDFDSO** as a light yellow solid. The copolymers, **PFDSO**, **PCDSO**, **PBCDSO**, **PFTPO, PCTPO** and **PBCTPO** were synthesized by Suzuki coupling polymerizations of **3**, **5** and **6** with **2** and **9**, respectively.

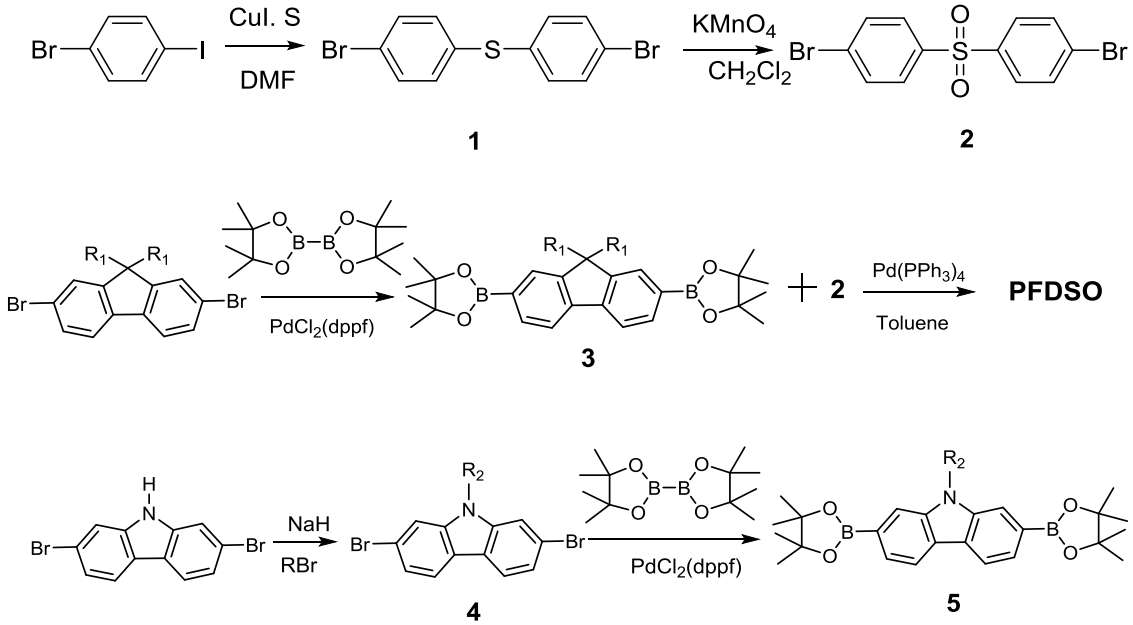

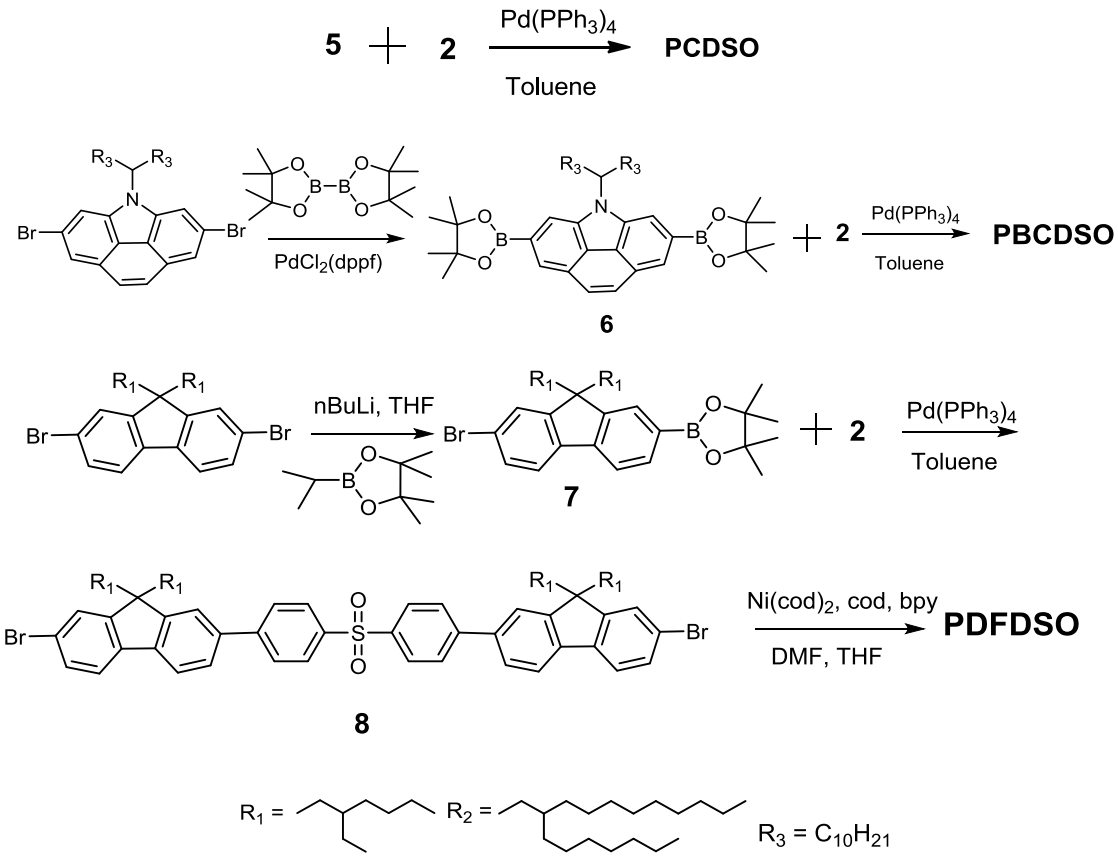

Scheme 2-6. Synthetic routes of **PFDSO**, **PDFDSO**, **PCDSO** and **PBCDSO**

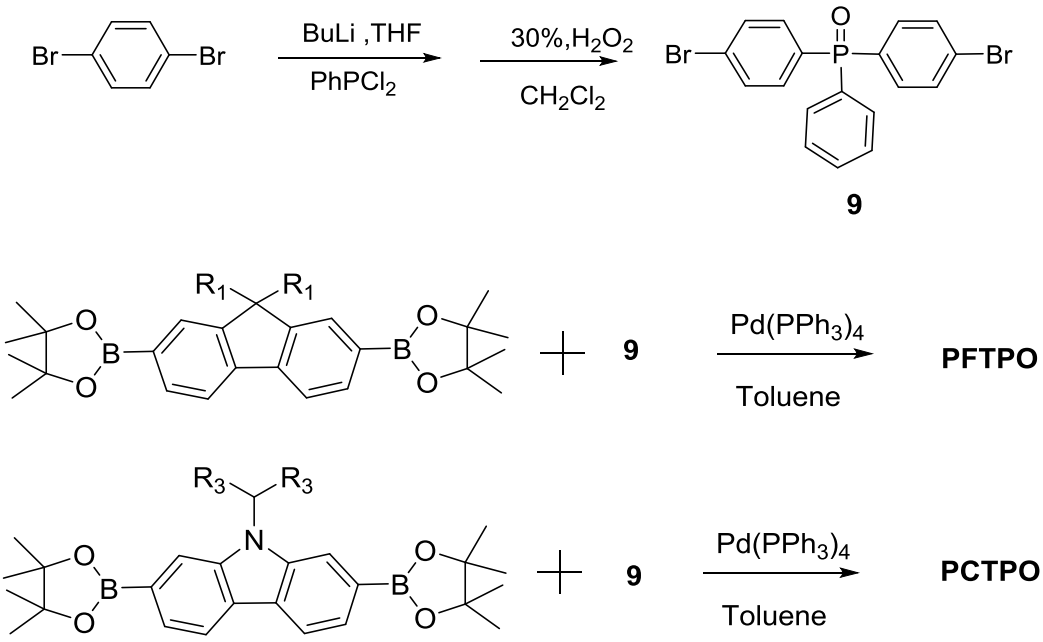

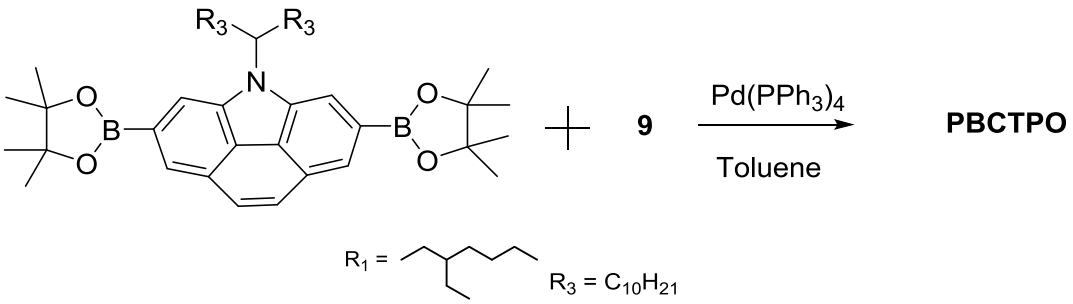

Scheme 2-7. Synthetic routes of **PFTPO**, **PCTPO** and **PBCTPO**

2.3.2.2. Solubility and thermal stability

All of the copolymers have a good solubility in usual organic solvents such as $CHCl_3$, chlorobenzene, and *o*-dichlorobenzene. These polymers were identified by NMR and elemental analyses. The results of GPC were summarized in Table 2-10. All of the copolymers showed good processability to make thin cast films. The M_n of **PFDSO**, **PDFDSO**, **PCDSO**, **PBCDSO**, **PFTPO**, **PCTPO** and **PBCTPO** were more than 10 kg/mol, which were not so high but enough to investigate their basic electronic properties and to examine characteristics of LECs. These polymers had a good thermal stability, and their temperatures of 5 wt % loss in TGA (T_d) were around 370 °C, respectively, which suggests that all of copolymers have good thermal stability for fabricating LECs devices.

Table 2-10 the GPC and TGA results of the copolymers.

Polymer	M_n （kg·mol^{-1}）	M_w (kg·mol^{-1})	M_w/M_n	DP^a	T_d (°C)[b]
PFDSO	18.3	32.9	1.8	30.3	386
PDFDSO	11.0	13.5	1.26	11.1	375
PCDSO	11.6	13.7	1.18	20.2	374
PBCDSO	25.6	31.8	1.24	36.6	403-
PFTPO	11.5	16.2	1.4	16.6	366
PCTPO	10.9	13.7	1.2	16.2	351
PBCTPO	14.0	21.8	1.5	18.4	400

[a]DP was estimated from M_n.

[b]Temperature of 5 % weight loss determined by TGA under an argon atmosphere.

2.3.2.3. Optical properties.

The photophysical properties of dilute solution and thin films of **PFDSO**, **PDFDSO**, **PCDSO**, **PBCDSO**, **PFTPO**, **PCTPO** and **PBCTPO** were investigated with UV-vis and PL, and the results are shown in Fig. 2-22, Fig. 2-23 and Fig. 2-24. The UV-vis absorption and the emission spectra data for polymers were summarized in Table 2-11 and Table 2-12.

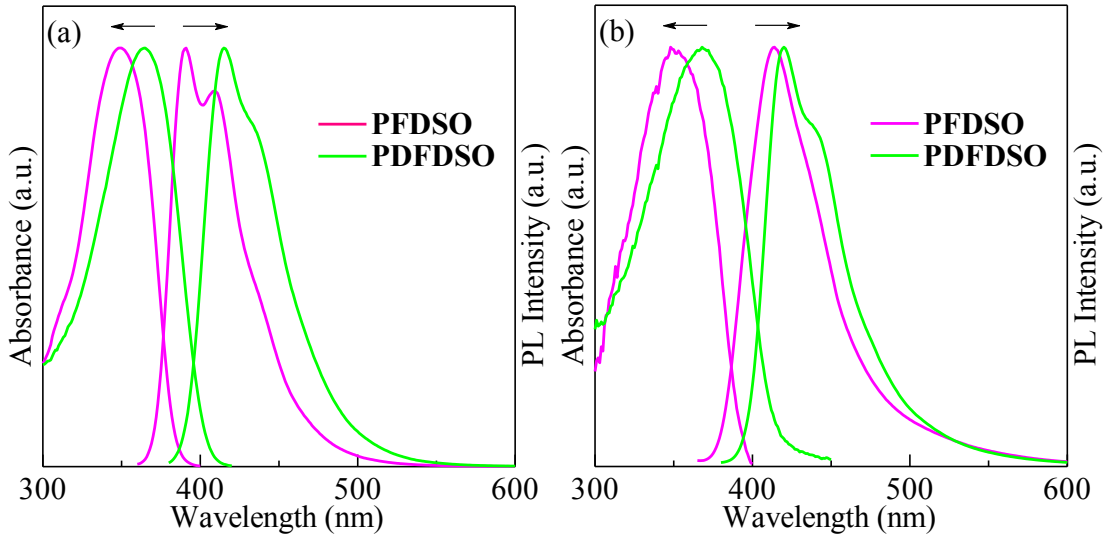

Fig. 2-22 UV-vis and PL spectra of **PFDSO** and **PDFDSO** in $CHCl_3$ (a) and film state (b).

The absorption and PL spectra of **PFDSO** and **PDFDSO** in $CHCl_3$ are shown in Fig. 2-22a. The absorption λ_{max} in wavelength at 349 nm for **PFDSO** and 365 nm for **PDFDSO** are due to π-π* transition of the conjugated backbone. Compared with **PFDSO**, the absorption λ_{max} of **PDFDSO** is longer in wavelengths, which indicates that π-conjugation of **PDFDSO** is longer than that of **PFDSO.** The emission peaks were observed at 409 nm for **PFDSO** and 415 nm for **PDFDSO** in solution. Stokes shifts (Δλ) of **PFDSO** in the solution was 60 nm, which was slightly larger than that of **PDFDSO** (50 nm). The larger Δλ is due to the lager structural change between ground and excited states, which might affect lowering Φ_{fl}.

Table 2-11 Optical properties, HOMO-LUMO energy gaps, and the energy levels of the polymers.

Polymer	$\lambda_{max,\ Abs}$ (nm)		$\lambda_{max,\ Em}$ (nm)		Φ_{fl}	E_g^{opt} (eV)	E_{HOMO} (eV)	E_{LOMO} (eV)	E_g^{ec} (eV)
	in $CHCl_3$	film	in $CHCl_3$	film					
PFDSO	349	350	409	414	0.60	3.20	–6.05	–2.68	3.37
PDFDSO	365	368	415	420	0.68	3.05	–5.79	–2.63	3.16
PCDSO	348	351	434	446	0.63	3.04	−5.66	−2.65	3.01
PBCDSO	325	325	447	449	0.50	3.23	−5.62	−2.31	3.31

Fig. 2-22b shows the absorption and PL spectra of **PFDSO** and **PDFDSO** in the thin film state. The absorption of **PFDSO** and **PDFDSO** are slightly broadened and red-shifted in the film state compared with absorption spectra in solution, which indicated that there were some aggregations or interactions of the polymer chains in the solid state. The E_g^{opt} between HOMO and LUMO of the **PFDSO** and **PDFDSO** estimated from the onset of the absorption spectrum in the film state was 3.20 eV for **PFDSO**, which was larger than that of **PDFDSO** (3.05 eV). The slight red shifts were observed in film state compared with PL spectra of **PFDSO** and **PDFDSO** in solution. The reason might attribute to the existence of the diphenylsulfone unit, which has effectively prevented close packing of constituent molecules and suppressed intermolecular aggregation because of the noncoplanar configuration.

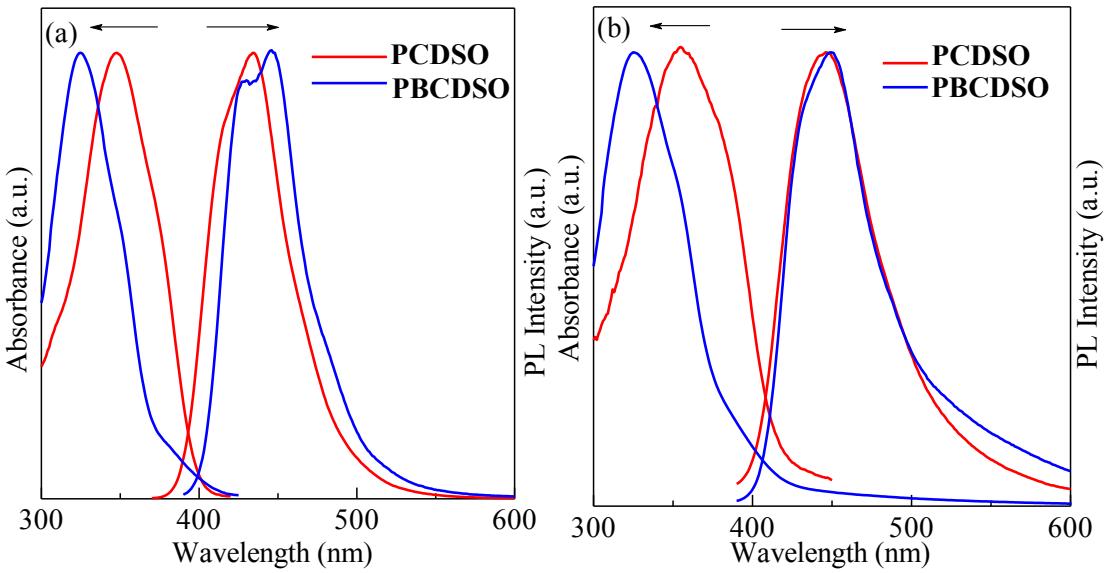

Fig. 2-23 UV-vis and PL spectra of **PCDSO** and **PBCDSO** in $CHCl_3$ (a) and film state (b).

Fig. 2-23a shows the absorption and PL spectra of **PCDSO** and **PBCDSO** in $CHCl_3$. The absorption λ_{max} at 348 nm for **PCDSO** and 325 nm for **PBCDSO** are due to π-π* transition of the conjugated main chain. Although **PBCDSO** includes an extended π-conjugated structure of phenanthrene in the unit, the absorption λ_{max} of **PBCDSO** shows unexpectedly blue-shifted in comparison to that of **PCDSO**. The emission peaks were observed at 434 nm for **PCDSO** and 447 nm for **PBCDSO** in solution. The Δλ of **PCDSO** in the solution was 86 nm, which was slightly smaller than that of **PBCDSO** (122 nm). The larger Δλ of **PBCDSO** might be responsible for the lower Φ_{fl} than that of **PCDSO**.

The absorption and PL spectra of **PCDSO** and **PBCDSO** in the thin film are shown in Fig. 2-23b. In the film state, the absorption of **PCDSO** and **PBCDSO** were slightly broadened and red-shifted compared with absorption spectra in solution, which indicated that there were some aggregations or interactions of the polymer chains in the film state. The E_g^{opt} between HOMO and LUMO of the **PCDSO** and **PBCDSO** estimated from the onset of the absorption spectrum in the film state was 3.04 eV for **PCDSO**, which was smaller than that of **PBCDSO** (3.23 eV). The large E_g values of **PBCDSO** were responsible for the blue shifts of $\lambda_{max, Abs}$ in solution.

Table 2-12 Optical properties, HOMO-LUMO energy gaps, and the energy levels of the polymers.

Polymer	$\lambda_{max, Abs}$ (nm)		$\lambda_{max, Em}$ (nm)		Φ_{fl}	E_g^{opt} (eV)	E_{HOMO} (eV)	E_{LOMO} (eV)
	in $CHCl_3$	film	in $CHCl_3$	film				
PFTPO	339	344	380	404	1.00	3.30	−6.04	−2.74
PCTPO	339	340	423	425	0.66	3.18	−5.75	−2.75
PBCTPO	318	320	437	439	0.55	3.37	−5.58	−2.21

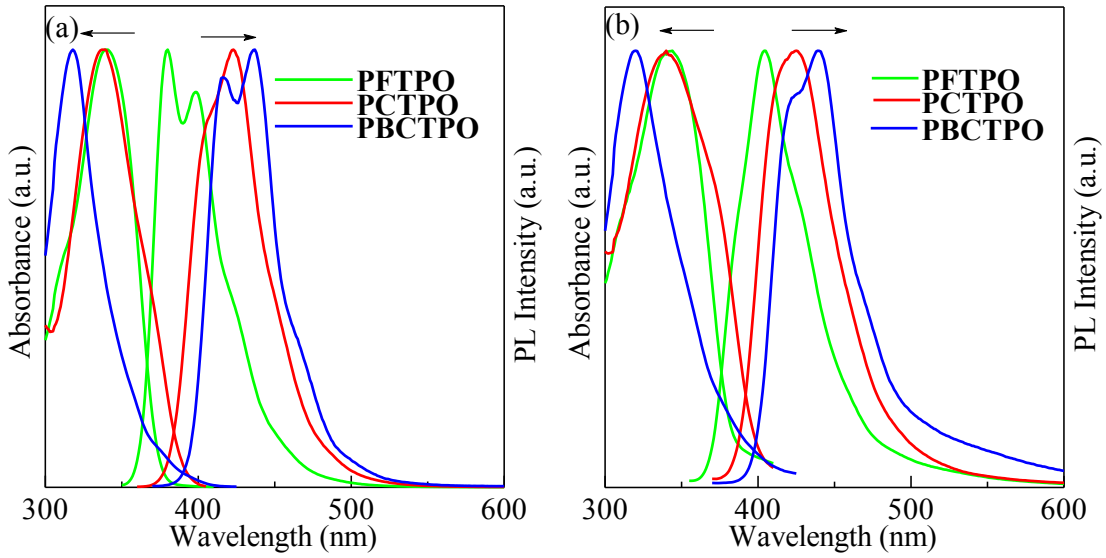

Fig. 2-24 UV-vis and PL spectra of **PFTPO**, **PCTPO** and **PBCTPO** in $CHCl_3$ (a) and film state (b)

The absorption and PL spectra of **PFTPO**, **PCTPO** and **PBCTPO** in $CHCl_3$ are shown in Fig. 2-24a. The absorption λ_{max} in wavelength at 339 nm for **PFTPO,** 339 nm for **PCTPO** and 318 nm for **PBCTPO** are due to π-π^* transition of the conjugated main chain. The absorption λ_{max} of **PBCTPO** was unexpectedly blue-shifted in comparison to those of **PFTPO** and **PCTPO,** although it includes an extended π-conjugated structure of phenanthrene in the unit. Consequently, they fluoresced deep-blue in $CHCl_3$. The emission peaks were observed at 380 nm for **PFTPO,** 423 nm for **PCTPO** and 437 nm for **PBCTPO** in solution. The $\Delta\lambda$ of **PBCTPO** in the solution was 119 nm, which was larger than those of **PFTPO** (41 nm) and **PCTPO** (84 nm). The larger $\Delta\lambda$ of **PBCTPO** might be responsible for the lower Φ_{fl} than those of **PFTPO** and **PCTPO**.

The absorption and PL spectra of **PFTPO**, **PCTPO** and **PBCTPO** in the thin film are shown in Fig. 2-24b. The absorption of **PFTPO**, **PCTPO** and **PBCTPO** in the film state were slightly broadened and red-shifted compared with absorption spectra in solution, which indicated that there were some aggregations or interactions of the polymer chains in the film state. The E_g^{opt} between HOMO and LUMO of the **PFTPO**, **PCTPO** and **PBCTPO** estimated from the onset of the absorption spectrum in the film state was 3.37 eV for **PBCTPO**, which was larger than that of **PFTPO** (3.30 eV) and **PCTPO** (3.18 eV). The large E_g values of **PBCTPO** are responsible for the blue shifts of $\lambda_{max,\ Abs}$ in solution.

2.3.2.4 Electrochemical properties

Electrochemical analysis of the thin-film sample of the polymers was employed to estimate E_{HOMO} and E_{LUMO}. The CV results of **PFDSO**, **PDFDSO**, **PCDSO**, **PBCDSO**, **PFTPO**, **PCTPO** and **PBCTPO** are shown in Fig. 2-25 and Fig. 2-26, and the estimated values are summarized in Table 2-11 and Table 2-12.

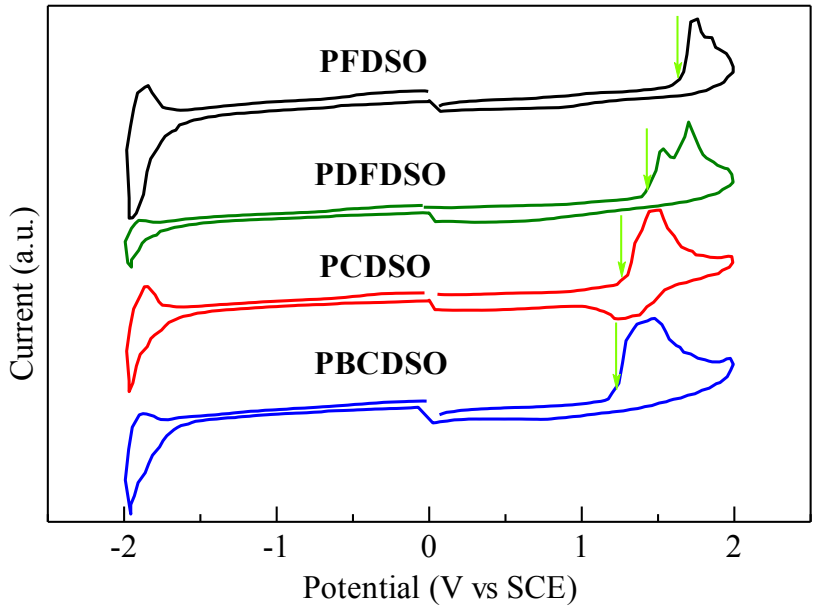

Fig. 2-25 Cyclic voltammograms of **PFDSO**, **PDFDSO**, **PCDSO** and **PBCDSO**

As show in Fig. 2-25, **PFDSO**, **PDFDSO** and **PBCDSO** had irreversible oxidation peaks during the anodic scan, which were assigned to the oxidation of the fluorene/benzo[*def*]carbazole units, while **PCDSO** had weak irreversible oxidation waves. The E_{HOMO} estimated from the onset potential of an oxidation peak of **PDFDSO** was –5.79 eV, which was higher about 0.26 eV than that of **PFDSO** (–6.05 eV). This result could be attributed to the longer π-conjugation of **PDFDSO** than that of **PFDSO.** The E_{HOMO} of **PBCTPO** (–5.62 eV) was shallower than that of **PCTPO**. During the cathodic scan, **PFDSO** exhibited quasireversible reduction waves, whereas **PDFDSO**, **PCDSO** and **PBCDSO** showed weak irreversible reduction waves. The E_{LUMO} of **PFDSO**, **PDFDSO**, **PCDSO** and **PBCDSO** were –2.68, –2.63, –2.65, –2.31 eV, respectively, estimated from the onset potentials of reduction. The E_g^{ec} of **PFDSO**, **PDFDSO**, **PCDSO** and **PBCDSO** were determined as 3.37, 3.16, 3.01 and 3.31 eV by calculating from E_{HOMO} and E_{LUMO}, respectively. The differences between the band gap values directly measured by CV (E_g^{ec} : 3.37, 3.16, 3.01 and 3.31 eV) and the optical band gap values obtained from UV-vis spectra (E_g^{opt} : 3.20, 3.05, 3.04, 3.23 eV) are approximately consistent. These energy gaps with suitable E_{HOMO} and E_{LUMO} should contribute to augmenting efficiency of blue emitting polymer devices.

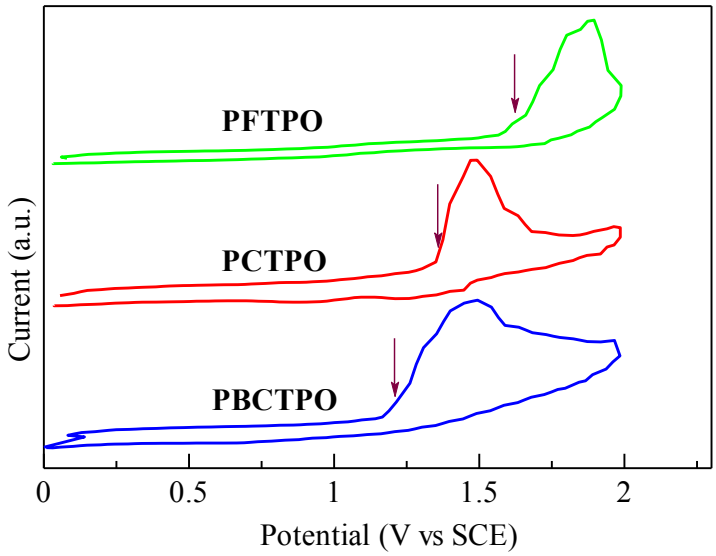

Fig. 2-26 Cyclic voltammograms of **PFTPO**, **PCTPO** and **PBCTPO**

In Fig. 2-26, **PFTPO**, **PCTPO** and **PBCTPO** showed irreversible oxidation peaks during the anodic scans, which are assigned to the oxidation of the donor units. The E_{HOMO} estimated from the onset potential of an oxidation peak of **PBCTPO** was –5.58 eV, which was shallower than those of **PFTPO** (–6.04 eV) and **PCTPO**, which might be attributed to an extended π-conjugated structure of phenanthrene in the **PBCTPO.** Because it was difficult to recognize the position of onset potentials in the reduction waves of these copolymers in the film state, the energy levels of LUMO (E_{LUMO}) were estimated from the E_{HOMO} and optical band gap (E_g) using the equation, $E_{LUMO} = E_{HOMO} + E_g$. The E_{LUMO} of **PFTPO**, **PCTPO** and **PBCTPO** were determined to be –2.74, –2.75 and –2.21 eV, respectively. The above results suggest that electronegativity of the phosphine oxide unit is responsible for lowering of both E_{HOMO} and E_{LUMO} of the polymers.

2.3.2.5 Electroluminescence properties

For the sake of investgate the application pontential of **PFDSO** and **PDFDSO,** firstly they were used as an emitting layer materials for PLEDs with a device structure of ITO/ PEDOT:PSS (40 nm)/copolymer/LiF (0.5 nm)/Al (100 nm). Unfortunately, **PFDSO** and **PDFDSO** based devices showed very weak light due to the large band gap. The LEC devices based on **PFDSO** and **PDFDSO** were fabricated with a device configuration: ITO/PEDOT:PSS/copolymer:MATS/Al (Fig. 2-27a) to explore their application potentials. The active layer using copolymers and ionic liquid MATS with mass ratio of 50:1 was coated with a spin coater of the mixture solution from toluene at speed of 1000 rpm, yielding a layer thickness of approximately 65 nm. Fig. 2-27b shows the EL spectra of the LECs devices based on **PFDSO** and **PDFDSO**, which exhibit EL peaks at 449 and 434 nm, respectively. All of the results are summarized in Table 2-13. The electroluminescence with CIE coordinates were (0.18, 0.15) and (0.17, 0.10) (as shown in Fig. 2-28) for blue emtting polymer LECs, respectively. Compared to the corresponding PL spectra in film state, the EL spectra are slightly red shifted about 21 and 14 nm, respectively, which different from polyfluorene derivatives with unwanted long wavelength emission [79]. This attributed to the existence of the diphenylsulfone unit with the tetrahedral electronic conformation, which has prevented intermolecular aggregation

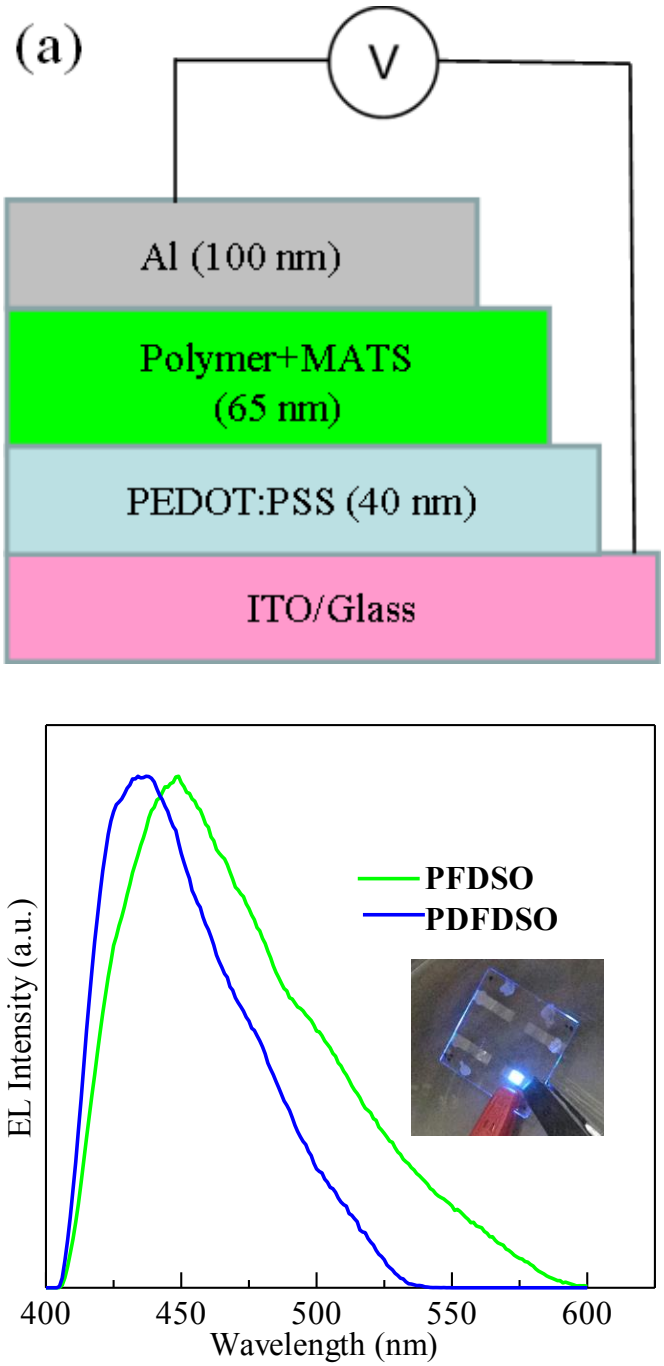

Fig. 2-27 LECs structure (a) and EL spectra of **PFDSO** and **PDFDSO**-based LECs (b).

Table 2-13 Characteristics of **PFDSO** and **PDFDSO**-based LECs[a]

Polymer	Maximum luminance (cd m^{-2})	Maximum current density (mA cm^{-2})	Maximum current efficiency (cd A^{-1})	$\lambda_{max, EL}$ (nm)	CIE coordinates
PFDSO	139 [8.5]	50 [8.5]	0.28 [8.5]	449	0.18, 0.15
PDFDSO	890 [6.8]	56 [6.8]	1.60 [6.8]	434	0.17, 0.10

[a]The device structure: ITO/ PEDOT:PSS (40 nm)/ polymer:MATS/ Al (100 nm)

The current luminescence-voltage (*L*-*V*) and density-voltage (*J*-*V*) curves of the **PFDSO** and **PDFDSO** based LECs devices operated with a sweep rate of 0.01 V/s are shown in Fig. 2-29. The luminance and current density of two copolymer based devices increased slowly with the increase of voltage, which reveals the characteristics of LECs devices. The luminance of **PFDSO** and **PDFDSO** based LECs devices increased rapidly and reached a luminance of 139 and 890 cd m^{-2}, respectively, with current density 50 and 56 mA cm^{-2}, respectively. The current efficiency of **PDFDSO** based LECs device was 1.60 cd A^{-1}, which was higher than that of **PFDSO** based LECs device. The **PDFDSO** based device exhibited higher EL properties than **PFDSO** based one**,** which suggests that there was a longer π-conjugation controlled by the sulfone unit in **PDFDSO**. It is noted that compared with reported LECs with CIE coordinates of (0.20, 0.28), brightness (39 cd m^{-2}) and current efficiency (0.65 cd A^{-1}) [72], and CIE coordinates of (0.20, 0.34), brightness (24 cd m^{-2}) and current efficiency (0.89 cd A^{-1}) [71], this is the first time to report a high efficiency and pure blue emission polymer LECs.

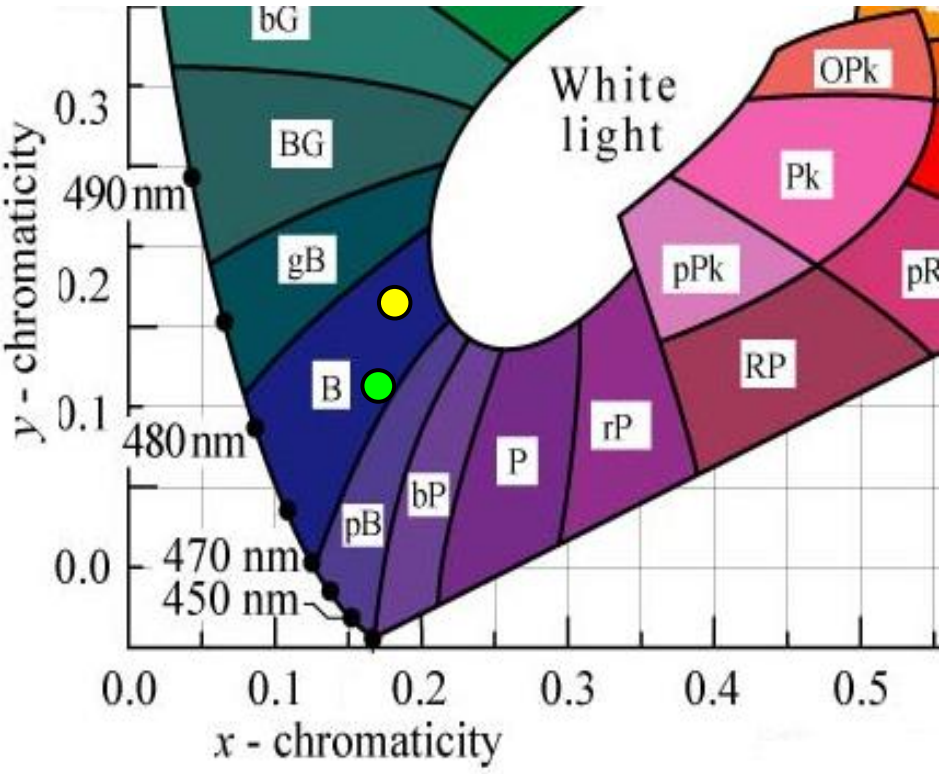

Fig. 2-28 The EL colour of **PFDSO** (yellow) and **PDFDSO** (green) -based LECs in CIE program.

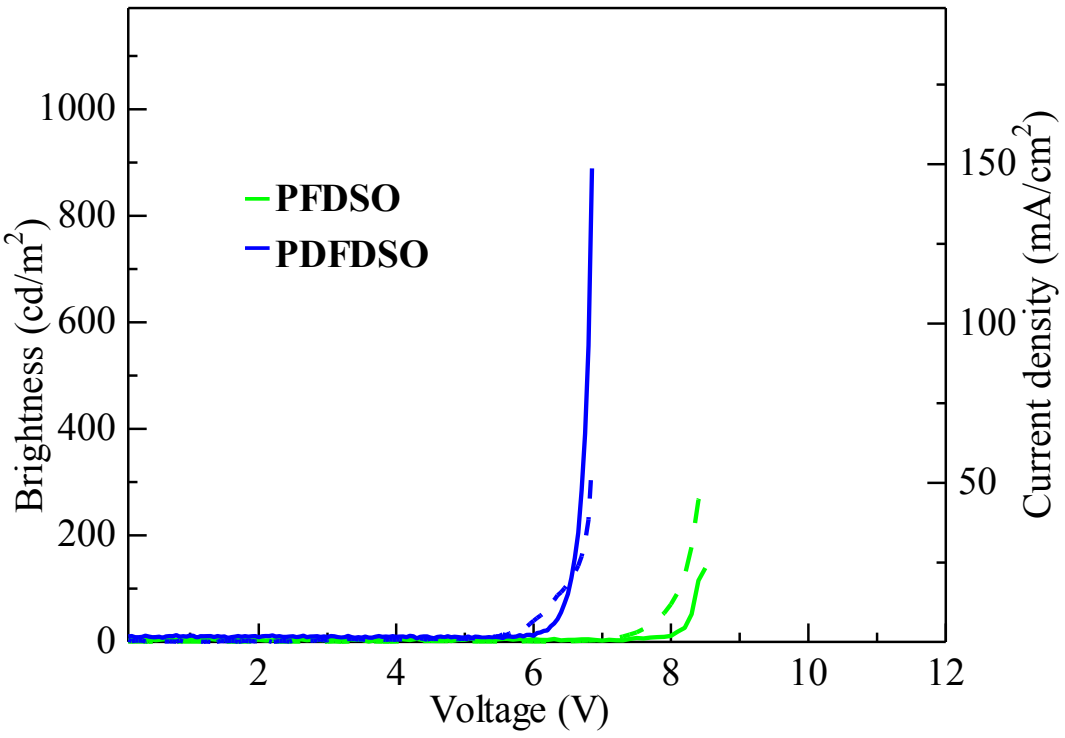

Fig. 2-29 Luminance (solid line) and current density (dashed line) versus voltage curves of **PFDSO** and **PDFDSO**-based LECs.

2.3.3 Summary

A new series of D-π-A type copolymers, which have controlled π-conjugation through introducing sulfone/phosphine oxide unit for preserve blue emission have been designed and synthesized. These copolymers showed good solubility in common organic solvents, enough high molecular weights to make thin films, and good thermal stability showing about 380 °C of temperature at 5 wt% loss in TGA. Basic properties of these polymers were investigated for the applications in LECs with a configuration of ITO/ PEDOT:PSS/ copolymer:MATS/ Al. The devices based on **PFDSO** and **PDFDSO** exhibit EL peaks at 449 and 434 nm with CIE coordinates of (0.18, 0.15) and (0.17, 0.10), respectively. Moreover, the **PDFDSO** based device showed a high luminance of 890 cd m^{-2} with current efficiency of 1.60 cd A^{-1}. These results suggest that it is an effective way for blue emission polymers by controlling the length of π-conjugation.

2.3.4 Experimental

2.3.4.1 Fabrication and Measurement of LECs Devices

The LEC devices were fabricated in the configuration of ITO/ PEDOT:PSS/ polymers:MATS/Al. The patterned ITO (conductivity: 10 Ω/square) glass was precleaned by ultrasonication in 2-propanol and successively in acetone. The precleaned ITO glass was treated in an ultraviolet-ozone chamber. A thin layer (40 nm) of PEDOT:PSS was spin-coated on the ITO at 3000 rpm in 3 min and air-dried at 110 °C for 10 min on a hot plate. The substrate was transferred to a glovebox under N_2 atmosphere. Solutions of the copolymers and MATS at various blending ratios in toluene were subsequently spin-coated on the PEDOT:PSS layer. Al (100 nm) were deposited on the emitting layer with conventional thermal evaporation at the chamber pressure lower than 5×10^{-4} Pa, which provided the devices with an active area of 2×2 mm^2. The thickness of emitting layers and PEDOT:PSS layers were measured using a stylus-type film thickness meter (ULVAC

E. S., Inc., Tokyo, Japan, Dektak). The luminance-current density-voltage (*L-J-V*) curves were measured using Keithley 2612A and TOPCON BM-9M with measurement angle at 0.2 Å.

2.3.4.2 Materials and Synthesis of monomers and polymers

Reagents and solvents were purchased from Kanto Chemical, Tokyo Chemical Industry, Aldrich and Nacalai Tesque Inc. Dimethylformamide (DMF) and CH_2Cl_2 distilled after drying with CaH_2 were stored under an argon atmosphere. Tetrahydrofuran (THF) distilled after drying with sodium was stored under an argon atmosphere. The other solvents and all commercially available reagents were used without further purification.

Synthesis of di(4-bromophenyl)sulfide (**1**). A mixture of 1-bromo-4-iodobenzene (7.14 g, 0.025 mol), CuI (0.33 g, 1.68 mmol) ,sulfur powder (0.81 g, 0.025 mol), and $LiOH{\cdot}H_2O$ (2.13 g, 0.05 mol) in 45 mL of DMF were stirred at 100 °C for 12 h. After cooling to ambient temperature, the mixture was mixed with water. After extraction with dichloromethane, drying over $MgSO_4$ and the solvent evaporation, the crude product was purified by column chromatography using hexane/dichloromethane (1:1) as an eluent to give a pure yellow solid (3.58 g, 83%). ^{1}H NMR (400 MHz, $CDCl_3$) δ [ppm]: 7.43 (d, J= 8.8 Hz 4H), 7.19 (d, J= 8.8 Hz 4H). ^{13}C NMR (100 MHz, CDCl3) δ [ppm]: 134.4, 132.5, 132.2 121.4.

Synthesis of di(4-bromophenyl)sulfone (**2**). A suspension of **1** (0.5 g, 1.45 mmol), Manganese(II) sulfate monohydrate (0.73 g, 4.3 mmol), and potassium permanganate ($KMnO_4$) (0.73 g, 4.6 mmol) in 11 mL of dichloromethane were stirred continuously for 10 h. After extraction with dichloromethane from water, drying over $MgSO_4$ and the solvent evaporation, the crude product was purified by column chromatography (silica gel, dichloromethane/hexane 1:1, as eluent) to afford a yellow solid (0.46 g, 85%). ^{1}H NMR (400 MHz, $CDCl_3$) δ [ppm]: 7.78 (d, J= 8.4 Hz 4H), 7.65 (d, J= 8.4 Hz 4H). ^{13}C NMR (100 MHz, $CDCl_3$) δ [ppm]: 140.2, 132.7, 129.1, 128.8.

Synthesis of 2,7-bis(4,4,5,5-tetramethyl-1,3,2-dioxaborolan-2-yl)-9,9- bis(2-ethylhexyl)-fluorene (**3**). A mixture of 2,7-dibromo-9,9-bis(2-ethylhexyl)fluorene (1.22 g, 2.22 mmol), bis(pinacolato)diboron (2.03 g, 7.97 mmol), 1,1'-bis(diphenylphosphino)ferrocene]dichloropalladium(II) ($PdCl_2$(dppf)) (0.113 g, 0.133 mmol), and potassium acetate (1.30 g, 13.28 mmol) in DMF (20 mL) was stirred under argon atmosphere at 60 °C for one day. After cooling to ambient temperature, the solution was mixed with water. After extraction with dichloromethane, drying over $MgSO_4$ and the solvent evaporation, the crude product was purified by column chromatography using hexane/dichloromethane (1:1, v/v) as an eluent to give a pure white solid (1.32g, 92%). ^{1}H NMR (400 MHz, $CDCl_3$) δ [ppm]: 7.83 (d, J= 8.0 Hz 2H), 7.75 (s, 2H), 7.70 (d, J= 8.0 Hz 2H), 2.0 (d, J= 7.7 Hz 4H), 1.38-1.19 (m, 24H), 0.85-0.46 (m, 30H). ^{13}C NMR (100 MHz, $CDCl_3$) δ [ppm]: 150.0, 143.8, 133.4, 130.3, 119.2, 83.5, 54.7, 43.9, 34.6, 33.4, 27.8, 27.1, 24.7, 22.6, 14.0, 10.2.

Synthesis of 2,7-bis(4,4,5,5-tetramethyl-1,3,2-dioxaborolan-2-yl)- 9-(2-heptylundecyl)-9*H*-carbazole (5). According to the procedure for **3,** the diboronic ester **5** was similarly synthesized giving light yellow oil (0.56 g, 71%). ^{1}H NMR (400 MHz, $CDCl_3$) δ [ppm]: 8.11 (d, J= 7.79 Hz 2H), 7.87 (s, 2H), 7.66 (d, J= 7.79 Hz 2H), 4.25 (d, J= 7.33 Hz 2H), 2.19 (br, 1H), 1.43-1.39 (m, 24H), 1.35-1.21 (m, 28H), 0.90-0.83 (m, 6H). ^{13}C NMR (100 MHz, $CDCl_3$) δ [ppm]: 140.9, 139.9, 125.0, 124.7, 119.9, 115.6, 83.7, 47.4, 37.6, 31.9, 31.8, 31.7, 29.9, 29.8, 29.6, 29.3, 29.2, 26.4, 26.2, 24.9, 24.8, 22.7, 22.6, 14.1, 14.0.

Synthesis of 2,7-bis(4,4,5,5-tetramethyl-1,3,2-dioxaborolan-2-yl)-4-(1-decylundecyl)-4*H*-

benzo[*def*]carbazole (6). According to the procedure for **3,** the diboronic ester **6** was similarly synthesized giving white solid (0.59 g, 60%).^{1}H NMR (400 MHz, $CDCl_3$) δ [ppm]: 8.26 (s, 2H), 8.02 (s, 2H), 7.97(s, 2H), 4.75 (br, 1H), 2.42-2.38 (m, 2H), 2.05-2.01 (m, 2H), 1.45 (m, 24H), 1.26-1.11 (m, 31H), 0.89-0.82 (m, 6H). ^{13}C NMR (100 MHz, $CDCl_3$) δ [ppm]: 132.3, 127.5, 126.2, 123.7, 121.8, 111.4, 111.1, 83.8, 57.7, 34.6, 31.8, 29.5, 29.4, 29.3, 26.9, 26.8, 25.0, 22.6, 14.1.

Synthesis of 2-(7-bromo-9,9-bis(2-ethylhexyl)fluoren-2-yl)-4,4,5,5-tetramethyl- 1,3,2-dioxaborolane (**7**). 2,7-Dibromo-9,9-bis(2-ethylhexyl)fluorene (0.80 g, 1.46 mmol) was dissolved in 6 mL of dry THF and cooled to –78 °C under N_2 atmosphere, in which n-BuLi solution (1.6 M in hexane, 1.08 mL, 1.7 mmol) was added dropwise with stirring. The mixture was stirred at –78 °C for 1 h and 2-isopropoxy-4,4,5,5-tetramethyl-1,3,2-dioxaborolane (0.35 mL, 1.7 mmol) was added slowly. The reaction solution was stirred for another 15 min at –78 °C. Afterward, the mixture was allowed to warm up to ambient temperature and stirred for one day, and quenched with addition of water. After extraction with dichloromethane, drying over $MgSO_4$ and the solvent evaporation, the crude product was purified by column chromatography using ethyl acetate/hexane (1:5, v/v) as an eluent to afford white solid (0.62 g, 72%). ^{1}H NMR (400 MHz, $CDCl_3$) δ [ppm]: 7.94 (br, 2H), 7.65 (d, J= 7.3 Hz 1H), 7.57 (d, J= 8.2 Hz 1H), 7.51 (d, J= 8. Hz 1H), 7.44 (d, J= 8.2 Hz 1H), 2.0-1.93 (m, 4H), 1.36 (s, 12H), 0.88-0.46 (m, 30H). ^{13}C NMR (100 MHz, $CDCl_3$) δ [ppm]: 153.4, 149.2, 143.0, 140.4, 133.7, 130.4, 130.3, 129.8, 127.4, 121.3, 120.9, 118.9, 83.6, 55.1, 44.2, 43,9, 34.6,34.5, 33.5, 33.4, 28.0, 27.7, 27.2, 27.0, 24.9, 24.7, 22.7, 22.6, 14.0, 10.4, 10.2.

Synthesis of 4,4'-bis(7-bromo-9,9-bis(2-ethylhexyl)-9H-fluorene-2-yl)diphenylsulfone (**8**). A mixture of **7** (0.52 g, 0.87 mmol), tetrakis(triphenylphosphine) palladium ($Pd(PPh_3)_4$, 50 mg), aqueous K_2CO_3 (2 M, 1.5 mL) and **2** (0.14 g, 0.35 mmol) in 2.5 mL of toluene was heated reflux with vigorous stirring for 72 h under an argon atmosphere. After the reaction mixture was cooled to ambient temperature, the solution was mixed with water. After extraction with dichloromethane, drying over $MgSO_4$ and the solvent evaporation, the crude product was purified by column chromatography using hexane/dichloromethane (1:1, v/v) as an eluent to give a light yellow solid (0.32 g, 80%). ^{1}H NMR (400 MHz, $CDCl_3$) δ [ppm]: 8.07 (d, J= 8.2 Hz 4H), 7.76-7.74 (m, 6H), 7.58 (d, J= 7.8 Hz 2H), 7.57-7.51 (m, 6H), 7.47 (d, J= 7.8 Hz 2H), 2.01-1.97 (m, 8H), 0.90-0.69 (m, 36H), 0.58-0.47 (m, 24H). ^{13}C NMR (100 MHz, $CDCl_3$) δ [ppm]: 153.0, 151.3, 140.8, 140.1, 139.4, 130.1, 130.0, 128.2, 127.8, 127.5, 127.4, 126.5, 122.9, 121.3, 121.1, 120.2, 55.3, 44.3, 34.7, 33.7, 28.1, 27.0, 22.7, 14.0, 10.3.

Synthesis of bis(4-bromophenyl)(phenyl)phosphine oxide (9). 1,4-Dibromobenzene (3.54 g, 15 mmol) was dissolved in 120 mL of dry THF and cooled to –78 °C under nitrogen atmosphere, in which n-BuLi solution (1.6 M in hexane 9 mL, 15 mmol) was added slowly with stirring. The reaction solution was strred at this temperature for 3 h, and then dichlorophenylphosphine (1 mL, 7.4 mmol) was added. The resulting solution was stirred for a further 3 h at –78 ^{o}C before quenching with methano(l5 mL). Afterward, the solution was allowed to warm up to ambient temperature and quenched with addition of water. After extraction with dichloromethane, drying over $MgSO_4$, the solvent had been completely removed, 30% hydrogen peroxide (22 mL) and dichloromethane (45 mL) were added to the obtained residue and the mixture stirred overnight at ambient temperature. After extraction with dichloromethane, drying over $MgSO_4$ and the solvent evaporation, the crude product was purified by column chromatography using ethyl acetate /hexane (1:5, v/v) as an eluent to afford white solid (2.5 g, 77%). ^{1}H NMR (400 MHz, $CDCl_3$) δ [ppm]: 7.64-7.60 (m, 6H), 7.57-7.48 (m, 7H). ^{13}C NMR (100 MHz, $CDCl_3$) δ [ppm]: 133.5, 133.4, 132.4, 132.3, 132.0, 131.9, 131.8, 131.5, 130.8, 130.4, 128.8, 128.7, 127.5, 127.4.

Synthesis of poly[2,7-(9,9-bis(2-ethylhexyl)fluorene)-alt-4,4'-diphenylsulfone] (**PFDSO**). Suspension of **3** (0.42 g, 0.8 mmol), aqueous K_2CO_3 (2 M, 1.88 mL), **2** (0.30 g, 0.8 mmol), and $Pd(PPh_3)_4$ (46.2 mg) in 6.5 mL of toluene was heated reflux with vigorous stirring under an argon atmosphere for 72 h. After the reaction mixture was cooled to ambient temperature, the resultant precipitate was firstly precipitated from methanol/HCl aq, and reprecipitated from methanol/NH_3 aq and from methanol, respectively. The polymer was successively washed and extracted with acetone, hexane and chloroform by Soxhlet extraction. The chloroform extract was again precipitated from methanol. The final product was dried under vacuum for whole night, affording a light yellow solid (0.396g, 82%). ^{1}H NMR (400 MHz, $CDCl_3$) δ [ppm]: 8.07 (d, J= 8.4 Hz 4H), 7.80-7.74 (m, 6H), 7.56 (d, J= 8.4 Hz 4H), 2.05 (d, J= 5.2 Hz 4H), 0.88-0.70 (m, 18H), 0.57-0.47 (m, 12H). ^{13}C NMR (100 MHz, $CDCl_3$) δ [ppm]: 151.6, 141.1, 137.8, 137.7, 128.2, 127.8, 126.5, 122.9, 120.5, 55.2, 44.3, 34.6, 33.7, 28.1, 27.0, 22.6, 14.0, 10.3. $C_{41}H_{50}O_2S$ (606.91): Calcd. C 81.14, H 8.30; Found. C 80.14, H 7.86.

Synthesis of poly[2,7'-(9,9,9'9'-tetrakis(2-ethylhexyl)fluorene)-alt-4,4'-diphenylsulfone] (**PDFDSO**). A mixture of bis(1,5-cyclooctadiene)nickel(0) (Ni(cod)2) (0.17 g, 0.62 mmol), 1,5-cyclooctadiene (cod) (0.15 g, 1.38 mmol) and 2,2'-bipyridine (bpy) (0.11 g, 0.71 mmol) in 2 mL of DMF was heated for 30 min at 80 °C under an argon atmosphere. To the mixture solution was added **5** (0.31 g, 0.27 mmol) dissolved in 2 mL of THF under argon. The reaction mixture was heated for 72 h at 80 °C. After the reaction mixture was cooled to ambient temperature, the resultant precipitate was firstly precipitated from methanol/HCl aq, and reprecipitated from methanol/NH_3 aq and from methanol, respectively. The polymer was successively extracted with acetone, hexane and chloroform by Soxhlet extraction. The chloroform extract was again precipitated from methanol. The final product was dried under vacuum for whole night, affording a light yellow solid (0.23 g, 84%). ^{1}H NMR (400 MHz, $CDCl_3$) δ [ppm]: 8.08 (d, J= 7.6 Hz 4H), 7.78-7.76 (m, 8H), 7.61-7.56 (m, 8H), 2.08-2.07 (m, 8H), 0.90-0.51 (m, 60H). ^{13}C NMR (100 MHz, $CDCl_3$) δ [ppm]: 153.9, 153.8, 145.0, 144.6, 141.8, 137.4, 137.2, 134.4, 133.9, 130.9, 128.2, 127.8, 120.2, 55.2, 44.3, 34.7, 33.6, 28.2, 27.1, 22.7, 14.0, 10.4. $C_{68}H_{86}O_2S$ (967.49): Calcd. C 84.42, H 8.96. Found. C 83.81, H 9.43.

Synthesis of poly[2,7-(9-(2-heptylundecyl)-9*H*-carbazole)-alt-4,4'-diphenylsulfone] (**PCDSO**). According to the synthetic procedure for **PFDSO,** polymerization of **5** with **2** abtained **PCDSO** as a light yellow solid (0.228g, 70%). ^{1}H NMR (400 MHz, $CDCl_3$) δ [ppm]: 8.16 (d, J= 8.0 Hz 2H), 8.11 (d, J =8.0 Hz 4H), 7.87-7.81 (m, 4H), 7.55 (d, J =8.0 Hz 2H), 7.46 (d, J =8 Hz 2H), 4.23 (d, J =6.8 Hz 2H), 2.17 (s, 1H), 1.39-1.16 (m, 28H), 0.90-0.81 (m, 6H); ^{13}C NMR (100 MHz, $CDCl_3$) δ [ppm]: 156.5, 142.0, 140.1, 137.3, 137.2, 135.5, 133.6, 132.6, 131.7, 128.3, 128.2, 122.6, 122.5, 121.1, 118.8, 108.0, 51.3, 46.9, 38.6, 35.0, 31.8, 31,7, 31.5, 29.9, 29.8, 29.5, 29.2, 29.1, 26.5, 22.6, 22.5, 14.1, 14.0. $C_{42}H_{53}NO_2S$ (635.95): Calcd. C 79.18, H 8.27, N 2.25; Found. C 76.59, H 7.89, N 1.98.

Synthesis of poly[2,7-(4-(1-decylundecyl)-4*H*-benzo[*def*]carbazole)-alt-4,4'-diphenylsulfone] (**PBCDSO**). According to the synthetic procedure for **PFDSO,** polymerization of **6** with **2** abtained **PBCDSO** as a light yellow solid (0.148 g, 78.3%). ^{1}H NMR (400 MHz, $CDCl_3$) δ [ppm]: 8.18-8.11 (m, 6H), 7.95-7.91 (m, 6H), 7.68-7.66 (m, 2H), 4.71 (br, 1H), 2.37 (br, 2H), 2.05 (br, 2H), 1.25-1.08 (m, 31H), 0.81-0.77 (m, 6H). ^{13}C NMR (100 MHz, $CDCl_3$) δ [ppm]: 157.5, 142.4, 139.4, 135.8, 135.7, 129.5, 128.2, 128.1, 127.6, 127.3, 126.9, 116.2, 115.4, 115.1, 108.2, 53.9, 41.1, 34.6, 31.8, 31.6, 29.4, 29.2, 29.1, 26.8, 22.6, 14.2. Calcd for $C_{47}H_{59}NO_2S$ (702.05): C, 80.41; H, 8.47; N, 2.00. Found: C, 79.60; H, 8.35; N, 1.96.

Synthesis of poly[2,7-(9,9-bis(2-ethylhexyl)fluorene)-alt-4,4'-diphenyl(phenylphosphinylidene] (**PFTPO**). According to the synthetic procedure for **PFDSO,** polymerization of **5** with **2** abtained **PFTPO** as a light yellow solid (0.258 g, 77%). ^{1}H NMR (400 MHz, $CDCl_3$) δ [ppm]: 7.85-7.74 (m, 12H), 7.63-7.52 (m, 7H), 2.07 (m, 4H), 0.83-0.76 (m, 18H), 0.58-0.50 (m, 12H). ^{13}C NMR (100 MHz, $CDCl_3$) δ [ppm]: 153.1, 151.6, 145.3, 138.4, 132.7, 132.6, 132.1, 127.2, 127.1, 126.4, 122.9, 120.3, 117.9, 55.2, 44.5, 34.7, 33.8, 28.2, 27.1, 22.7, 14.0, 10.4. Calcd for $C_{47}H_{55}OP$ (666.93): C, 82.64; H, 8.31. Found: C, 80.46; H, 8.26.

Synthesis of poly[2,7-(9-(2-heptylundecyl)-9*H*-carbazole)-alt-4,4'- diphenyl(phenylphosphinylidene] (**PCTPO**). According to the synthetic procedure for **PFDSO,** polymerization of **5** with **2** abtained **PCTPO** as a light yellow solid (0.155g, 78%). ^{1}H NMR (400 MHz, $CDCl_3$) δ [ppm]: 8.21-8.16 (m, 2H), 7.89-7.71 (m, 11H), 7.65-7.46 (m, 6H), 4.68-4.65 (m, 1H), 2.35-2.30 (m, 2H), 1.99-1.95 (m, 2H), 1.26-1.04 (m, 31H), 0.84-0.78 (m, 6H). ^{13}C NMR (100 MHz, $CDCl_3$) δ [ppm]: 157.4, 145.8, 132.8, 132.7, 132.6, 132.2, 132.1, 132.0, 128.7, 128.6, 127.8, 127.7, 127.6, 120.7, 110.4, 110.3, 107.7, 56.6, 33.8, 31.8, 31.7, 29.5, 29.3, 29.2, 26.8, 24.9, 22.6, 14.0. Calcd for $C_{51}H_{64}NOP$ (738.05): C, 83.00; H, 8.74; N, 1.90. Found: C, 81.79; H, 8.90; N, 1.89.

Synthesis of poly[2,7-(4-(1-decylundecyl)-4*H*-benzo[*def*]carbazole)-alt-4,4'-diphenyl(phenylphosphinylidene] (**PBCTPO**). According to the synthetic procedure for **PFDSO,** polymerization of **5** with **2** abtained **PBCTPO** as a light yellow solid (0.178 g, 86%). ^{1}H NMR (400 MHz, $CDCl_3$) δ [ppm]: 8.12 (s, 2H), 7.98-7.75 (m, 14H), 7.62-7.52 (m, 3H), 4.74-4.72 (m, 1H), 2.42-2.39 (m, 2H), 2.09-2.02 (m, 2H), 1.32-1.10 (m, 31H), 0.82-0.78 (m, 6H). ^{13}C NMR (100 MHz, $CDCl_3$) δ [ppm]: 154.0, 151.4, 143.9, 143.5, 140.1, 134.6, 134.5, 132.6, 128.8, 128.7, 128.6, 126.7, 121.4, 121.3, 114.9, 57.9. 48.0, 34.6, 31.8, 31.6, 29.4, 29.3, 29.2, 26.7, 22.6, 14.0. Calcd for $C_{53}H_{64}NOP$ (762.07): C, 83.53; H, 8.47; N, 1.84. Found: C, 81.75; H, 8.49; N, 1.78.

^{1}H NMR spectra of **PFDSO**

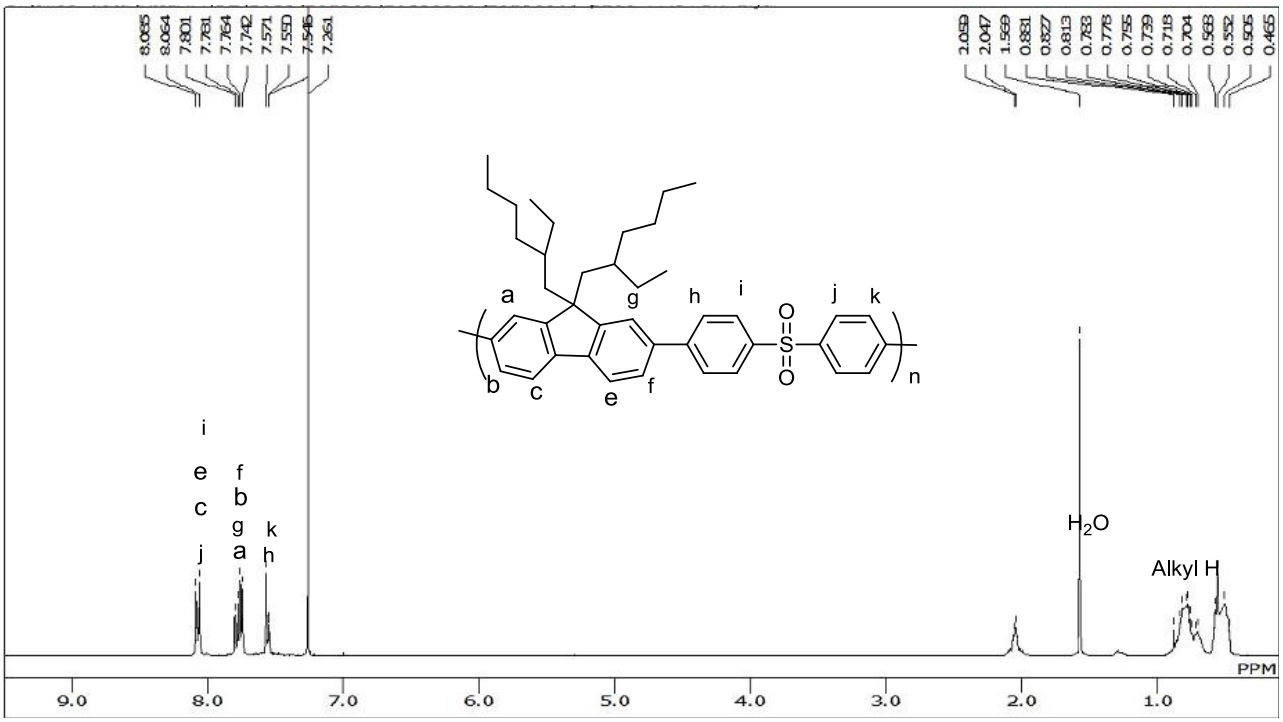

^{13}C NMR spectra of **8**

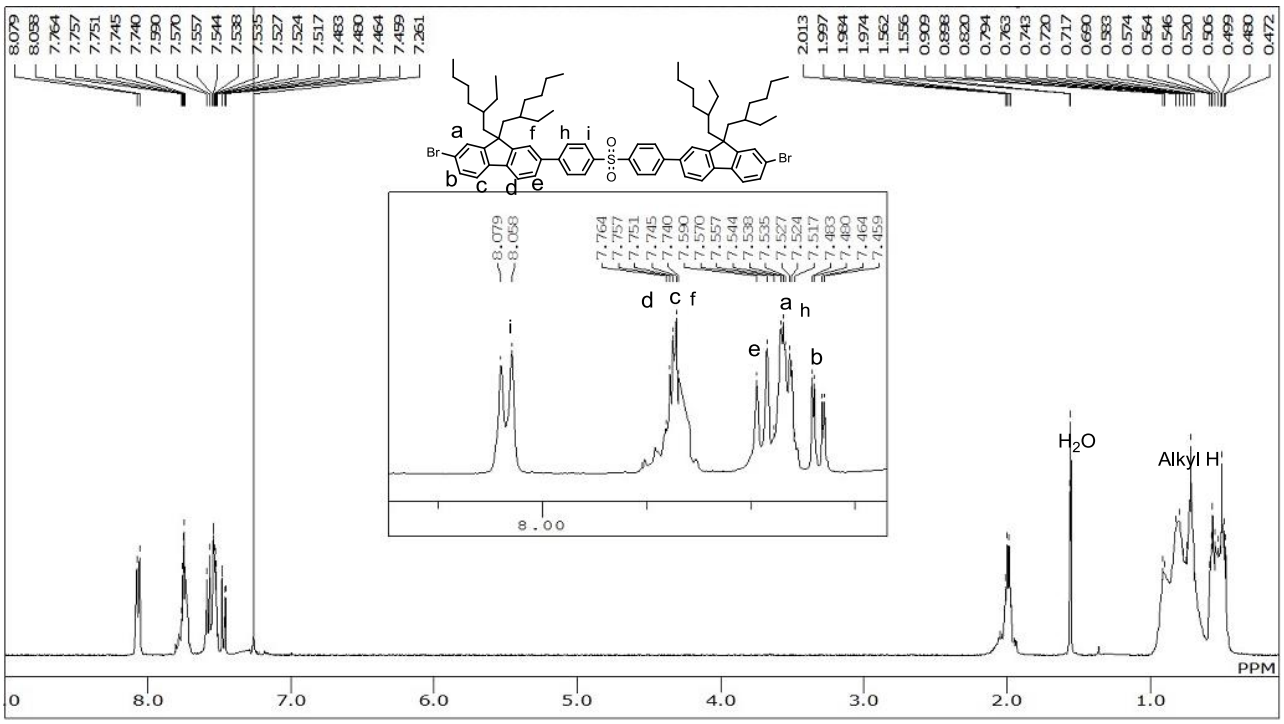

^{1}H NMR spectra of **PDFDSO**

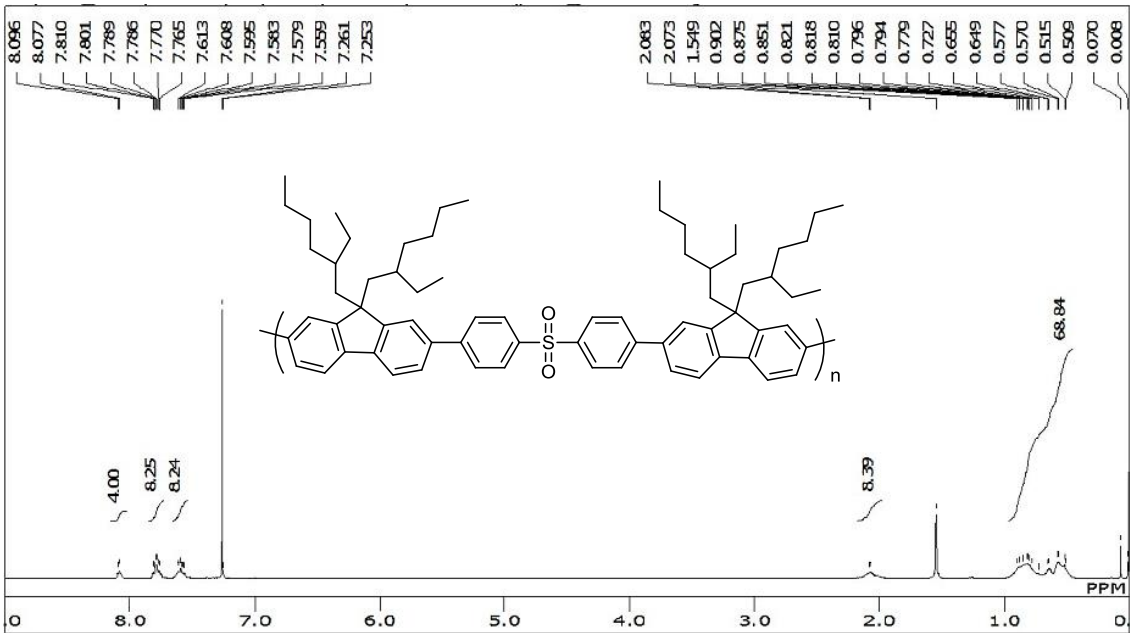

^{1}H NMR spectra of **PCDSO**

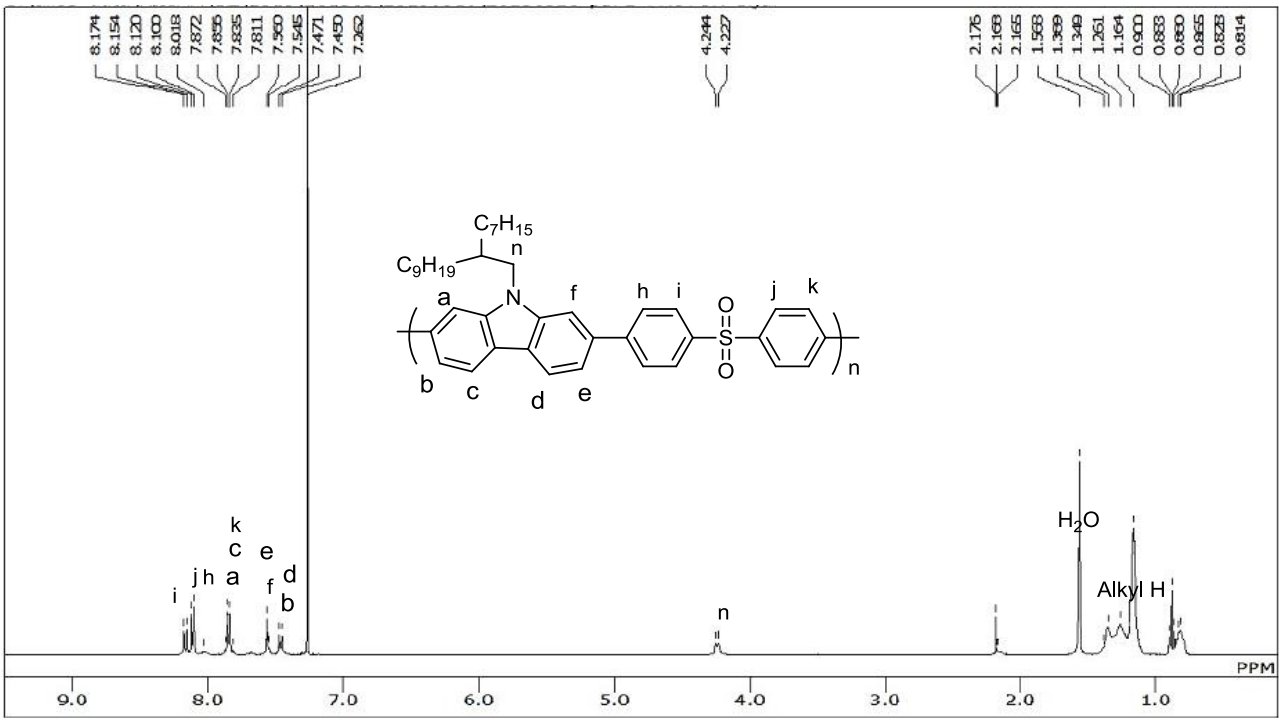

^{13}C NMR spectra of **PCDSO**

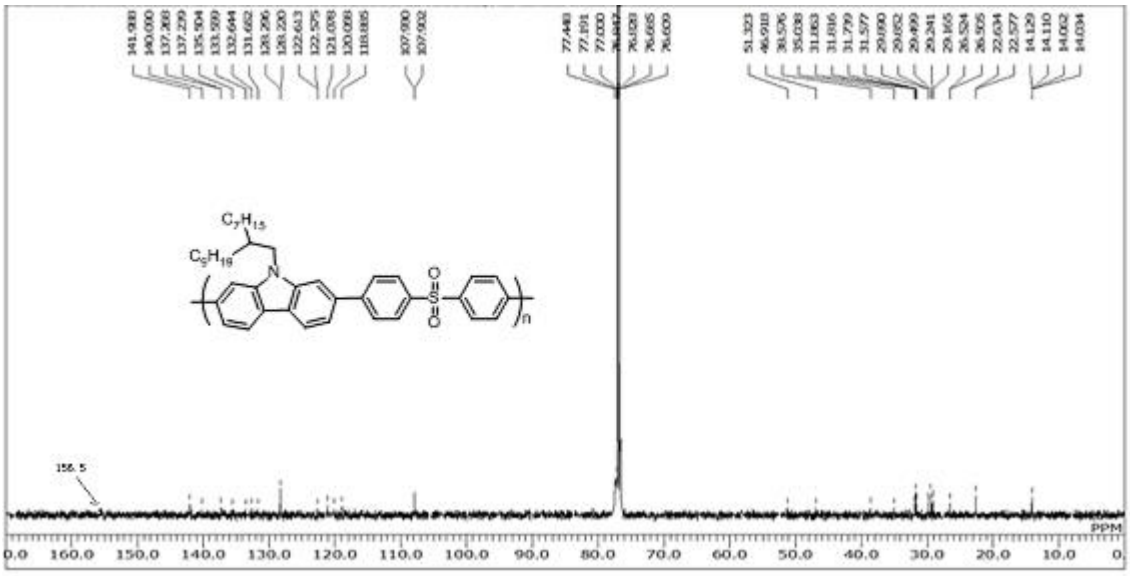

^{1}H NMR spectra of **PBCDSO**

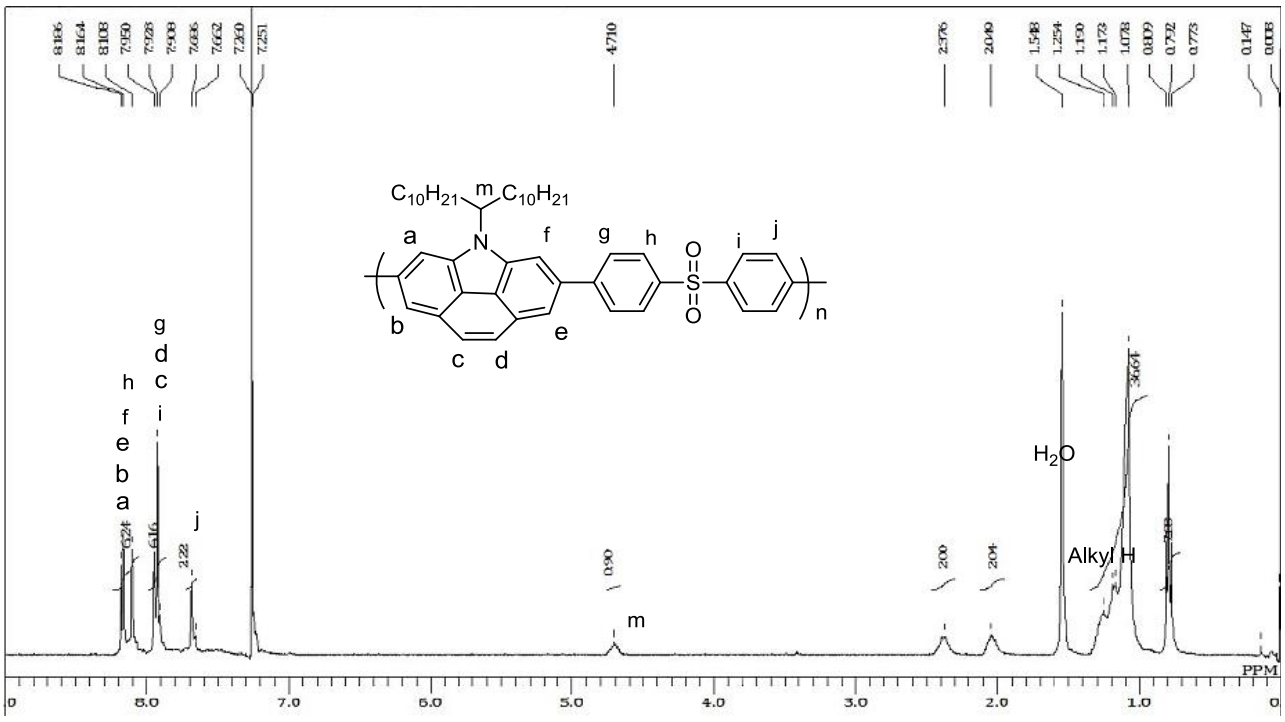

^{13}C NMR spectra of **PBCDSO**

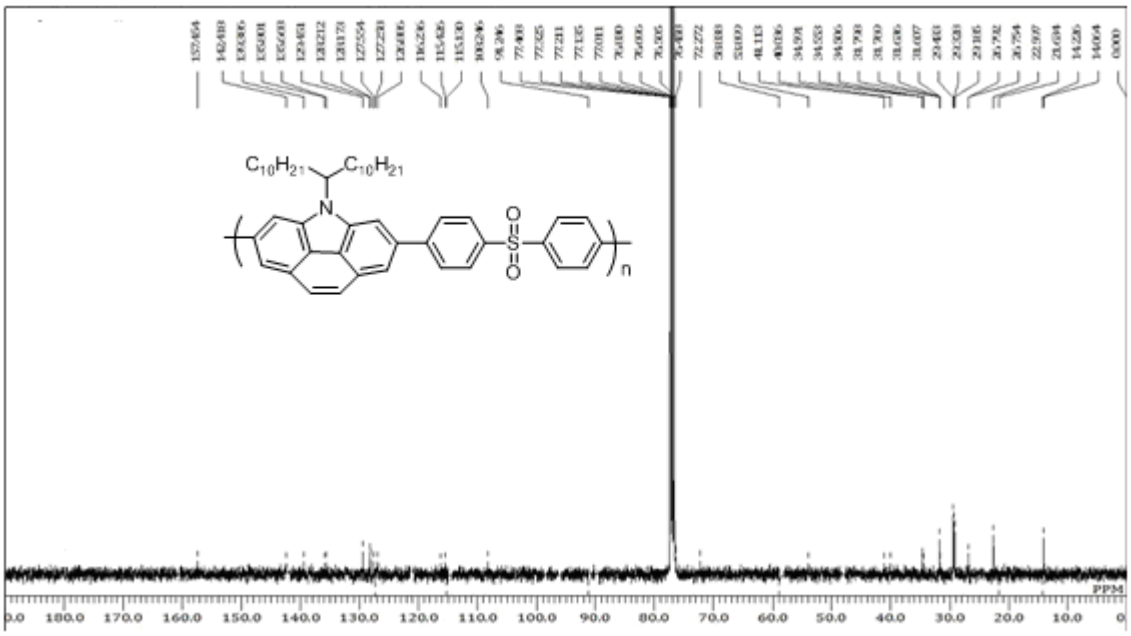

^{1}H NMR spectra of **PCTPO**

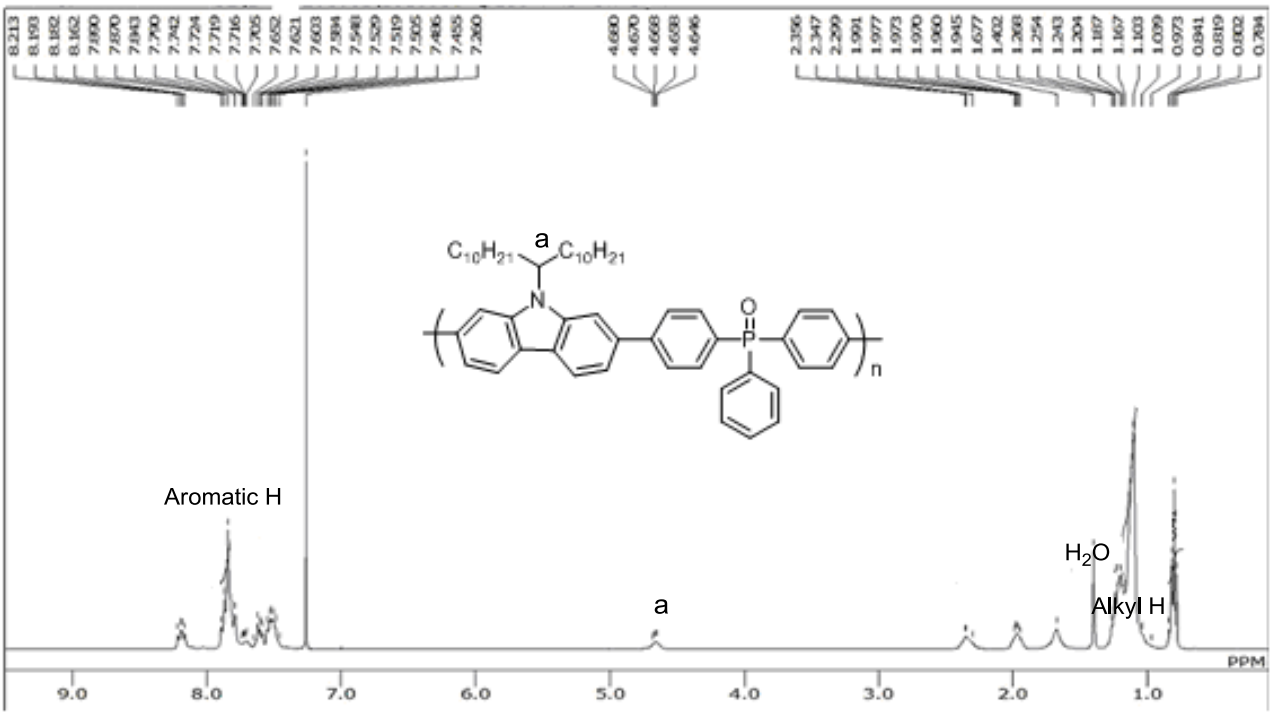

^{1}H NMR spectra of **PFTPO**

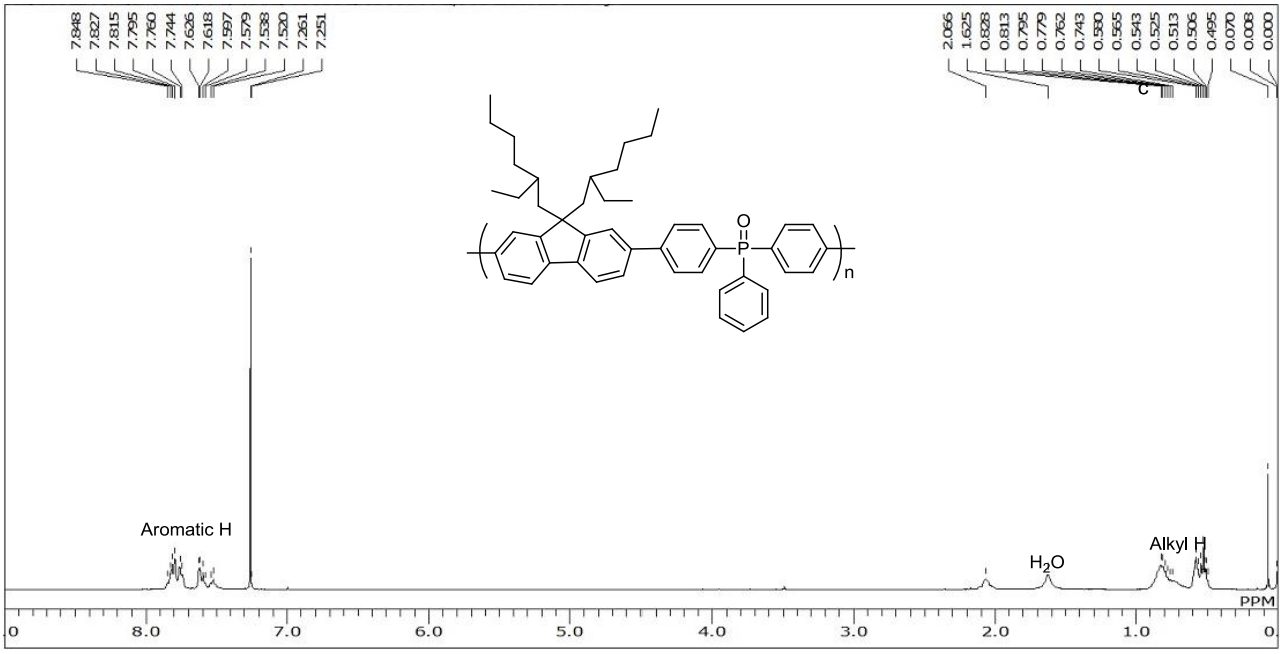

^{1}H NMR spectra of **PBCTPO**

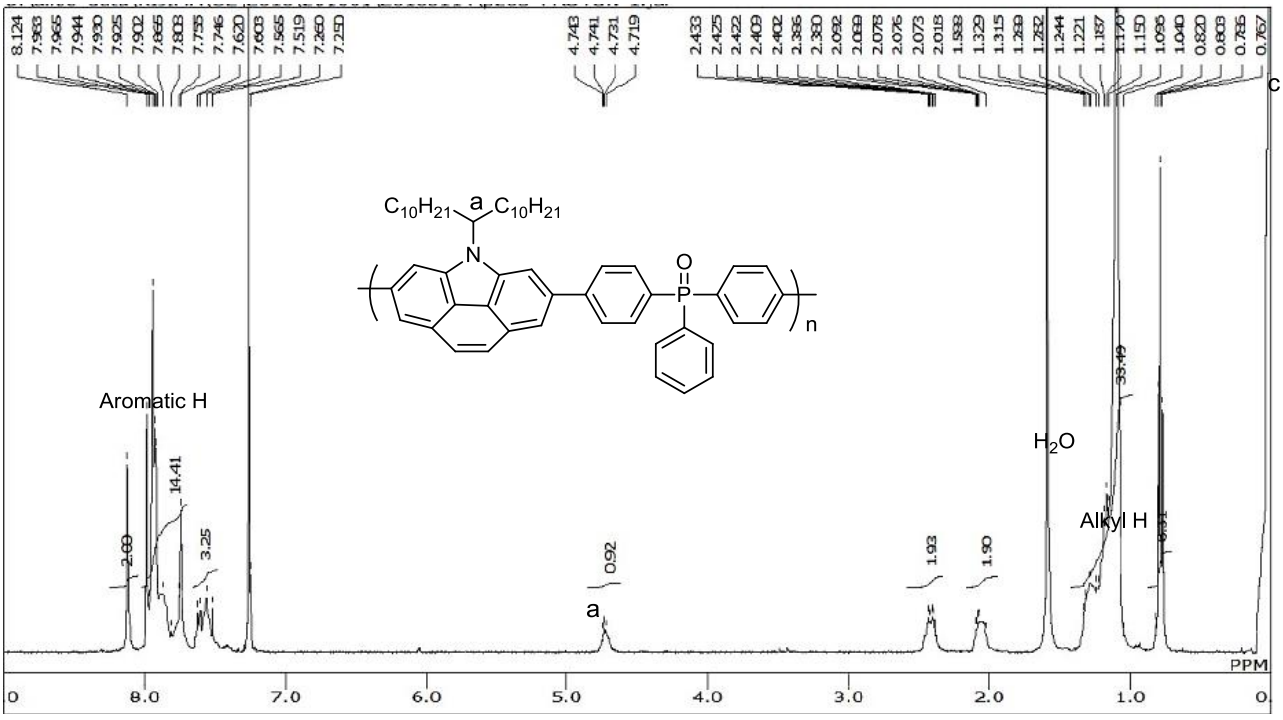

Reference

[1] S. Beaupré, M. Leclerc, Adv. Funct. Mater. 12 (2002) 192-196.

[2] U. Mitschke, P. Bäuerle, J. Mater. Chem. 10 (2000) 1471-1507.

[3] D. Y. Kim, H. N. Cho, C. Y. Kim, Prog. Polym. Sci. 25 (2000) 1089-1139.

[4] A. Pertegás, D. Tordera, J. J. Serrano-Pérez, E. Ortí, H. J. Bolink, J. Am. Chem. Soc. 135 (2013) 18008-18011.

[5] Z. Yu, L. Li, H. Gao, Q. Pei, Sci. China. Chem. 56 (2013) 1075-1086.

[6] Q. Pei, G, Yu, C, Zhang, Y, Yang, A, Heeger, J. Science. 269 (1995) 1086-1088.

[7] E. Bundgaard, F. C. Krebs, Sol. Energy Mater. Sol. Cells. 91 (2007) 954-985.

[8] S. Günes, H. Neugebauer, N. S. Sariciftci, Chem. Rev. 107 (2007) 1324-1338.

[9] M.M. Durban, P.D. Kazarinoff, C.K. Luscombe, Macromolecules. 43 (2010) 6348-6352.

[10] https://zh.wikipedia.org/wiki/File:LG%EC%A0%84%EC%9E%90,_%EA%B9%9C%EB%B9%A1%EC%9E%84_%EC%97%86%EB%8A%94_55%EC%9D%B8%EC%B9%98_3D_OLED_TV_%EA%B3%B5%EA%B0%9C%282%29.jpghttp://www.samsung.com/uk/discover/tv/oled-tv-a-revolution-in/

[11] https://commons.wikimedia.org/wiki/File:Thin_Film_Flexible_Solar_PV_Ken_Fields_1.JPG

[12] https://commons.wikimedia.org/wiki/File:Flexible_display.jpg

[13] J. Ye, Z. Chen, M. K. Fung, C. Zheng, X. Ou, X. H. Zhang, Y. Yuan, C. S. Lee, Chem. Mater. 25 (2013) 2630-2637.

[14] T. Horii, T. Shinnai, K. Tsuchiya, T. Mori, M. Kijima, J. Polym. Sci. Polym. Chem. 50 (2012) 4557-4562.

[15] F. C. Krebs, Org. Electron. 10 (2009) 761-768.

[16] F. C. Krebs, T. Tromholt, M. Jorgensen, Nanoscale. 2 (2010) 873-886.

[17] J. H. Burroughes, D. D. C. Bradley, A. R. Brown, R. N. Marks, K. Mackay, R. H. Friend, P. L. Burns, A. B. Holmes, Nature. 347 (1990) 539-541.

[18] D. Braun, A. J. Heeger, Appl. Phys. Lett. 58 (1991) 1982-1984.

[19] M. Singh, H. M. Haverinen, P. Dhagat, G. E. Jabbour, Adv. Mater. 22 (2010) 673-685.

[20] L. Ma, Z. Xie, J. Liu, J. Yang, Y. Cheng, L. Wang, and F. Wang, Appl. Phys. Lett. 87 (2005) 163502.

[21] L. Romaner, A. Pogantsch, P.S. de Freitas, U. Scherf, M. Gaal, E. Zojer, E. J. W. List, Adv. Funct. Mater. 13 (2003) 597-601.

[22] C. Yang, H. Scheiber, E.J.H. List, J. Jacob, K. Müllen, Macromolecules 39 (2006) 5213-5221.

[23] S. Qiu, L. Liu, B. Wang, F. Shen, W. Zhang, M. Li, and Y. Ma, Macromolecules 38 (2005) 6782-6788.

[24] M. C. Hung, J. L. Liao, S. A. Chen, S. H. Chen, A. C. Su, J. Am. Chem. Soc. 127 (2005) 14576-14577.

[25] U. Mitschke, P. Bäuerle, J. Mater. Chem. 10 (2000) 1471-1507.

[26] D. Neher, Macromol. Rapid Commun. 22 (2001) 1365-1385.

[27] F. B. Dias, J. Morgado, A. L. Maçanita, P. C. Costa, H. D. Burrows, A. P. Monkman, Macromolecules. 39 (2006) 5854-5864.

[28] Yang, J. X, Tao, X. T, Yuan, C. X, Yan, Y. X, Wang, L, Liu, Z.; Ren, Y, Jiang, M. H. J. Am. Chem. Soc. 2005, 127, 3278.

[29] Adhikari, R. M.; Mondal, R.; Shah, B. K.; Neckers, D. C. J. Org. Chem. 2007, 72, 4727.

[30] J. F. Morin, S. Beaupré, M. Leclerc, I. Lévesque, M. D'Iorio, Appl. Phys. Lett. 80 (2002) 341-343.

[31] M. Kijima, R. Koguchi, S. Abe, Chem. Lett. 34 (2005) 900-901.

[32] M. Kijima, IOP Conf. Series: Materials Science and Engineering. 54 (2014) 012017.

[33] P. L. T. Boudreault, S.Beaupré, M. Leclerc, Polym. Chem. 1 (2010) 127-136.

[34] H. Suh, Y. Jin, S. H. Park, D. Kim, J. Kim, C. Kim, J. K. Kim, K. Lee, Macromolecules. 38 (2005) 6285-6289.
[35] J. F. Brière, M. Cô té. J. Phys. Chem. B.108 (2004) 3123-3129.
[36] S. Abe, Y. Nagasaki, M. Kijima. Synth. Met. 123 (2003) 135-136.
[37] N. Blouin, A. Michaud, M. Leclerc, Adv. Mater. 19 (2007) 2295-2300.
[38] R. Koguchi, N. Kobayashi, M. Kijima, Macromolecules. 42 (2009) 5946-5952.
[39] T. Yamamoto, A. Morita, Y. Muyazaki, T. Maruyama, H. Wakayama, Z. H. Zhou, Y. Nakamura, T. Kanbara, S. Sasaki, K. Kubota, Macromolecules. 25 (1992) 1214-1223.
[40] N. Kobayashi, R. Koguchi, M. Kijima, Macromolecules. 39 (2006) 9102-9111.
[41] R. Grisorio, G. P. Suranna, P. Mastrorilli, C. F. Nobile, Org. Lett. 9 (2007) 3149-3152.
[42] N. Kobayashi, R. Koguchi, M. Kijima, Macromolecules. 39 (2006) 9102-9111.
[43] R. Grisorio, G. P. Suranna, P. Mastrorilli, C. F. Nobile, Org. Lett. 9 (2007) 3149-3152
[44] C. Yang, H. Scheiber, E. J. W. List, J. Jacob, K. Müllen, Macromolecules. 39 (2006) 5213-5221.
[45] Z. B. Zhang, M. Fujiki, H. Z. Tang, M. Motonaga, K. Torimitsu, Macromolecules. 35 (2002) 1988-1990.
[46] A. Iraqi, I. Wataru, J. Polym. Sci., Part A: Polym. Chem. 42 (2004) 6041-6051.
[47] J. Pommerehne, H. Vestweber, W. Guss, R. F. Mahrt, H. Bässler, M. Porsch, J. Daub. Adv. Mater. 7 (1995) 551-554.
[48] A. K. Agrawal, S. A. Jenekhe, Chem. Mater. 8 (1996) 579-589.
[49] J. V. Grazulevicius, P. Strohriegl, J. Pielichowski, K. Pielichowski, Prog. Polym. Sci. 28 (2003) 1297-1353.
[50] D. Neher, Macromol. Rapid Commun. 22 (2001) 1365-1385.
[51] Z. C. He, C. Zhang, X. F. Xu, L. J. Zhang, L. Huang, J. W. Chen, H. B. Wu, Y. Cao, Adv. Mater. 23 (2011) 3086-3089.
[52] R.F. He, S.J. Hu, J. Liu, L. Yu, B. Zhang, N. Li, W. Yang, H.B. Wu, J. B. Peng, J. Mater. Chem. 22 (2012) 3440-3446.
[53] J. Ye, Z. Chen, M.K. Fung, C. Zheng, X. Ou, X. Zhang, Y. Yuan, C.S. Lee, Chem. Mater. 25 (2013) 2630-2637.
[54] S. Ren, D. Zeng, H. Zhong, Y. Wang, S. Qian, Q. Fang, J. Phys. Chem. B. 114 (2010) 10374-10383.
[55] H. Alyar, M. Bahat, Z. Kantarcı, E. Kasap, *Comput.* Theor. Chem. 977 (2011) 22-28.
[56] T. Horii, T. Shinnai, K. Tsuchiya, T. Mori, M. Kijima, J. Polym. Sci. Part A: Polym. Chem. 50 (2012) 4557-4562.
[57] Z. Q. Gao, M. Luo, X. H. Sun, H. L. Tam, M. S. Wong, B.X. Mi, P. F. Xia, K. W. Cheah, C.H. Chen, Adv. Mater. 21 (2009) 688-692.
[58] A. W. Grice, D. D. C. Bradley, M. T. Bernius, M. Inbasekaran, W. W. Wu, E. P. Woo, Appl. Phys. Lett. 73 (1998) 629-631.
[59] M. Kijima, R. Koguchi, S. Abe, Chem. Lett. 34 (2005) 900-901.
[60] F. Dierschke, A. C. Grinsdale, and K. Müllen, Synthesis, 16 (2003) 2470-2472..
[61] S. Yrjölä, T. Kalliokoski, T. Laitinen, A. Poso, T. Parkkari, T. Nevalainen, Eur. J. Pharm. Sci. 2013, 48, 9-20.
[62] T. C. Lin, Y. H. Lee, B. R. Huang, C. L. Hu, Y. K. Li, Tetrahedron. 68 (2012) 4935-4949.
[63] Y. Li, J. Ding, M. Day, Y. Tao, J. Lu, M. D'iorio, Chem. Mater. 16 (2004) 2165-2173.
[64] X. W.Chen, W. C. H. Choy, S. He, J. Display Technol. 3 (2007) 110-117.
[65] Q. Pei, G. Yu, C. Zhang, Y. Yang, A. Heeger, 269 (1995) 1086-1088.
[66] T. Ouisse, O. Stéphan, M. Armand, J. C. Leprêtre, J. Appl. Phys. 92 (2002) 2795-2795.

[67] Q. B. Pei, Y. Yang, G. Yu, C. Zhang, A. J. Heeger, J. Am. Chem. Soc. 118 (1996) 3922-3929.
[68] Q. Sun, Y. Li, Q. B. Pei, J. Display Technol. 3 (2007) 211-224.
[69] Y. Cao, G. Yu, A. J. Heeger, C. Y. Yang, Appl. Phys. Lett. 68 (1996) 3218-3220.
[70] L. Edman, M. Pauchard, D. Moses, A. J. Heeger, J. Appl. Phys. 95 (2004) 4357-4361.
[71] B. Chen, Y. H. Li, W. Yang, W. Luo, H. B. Wu, Org. Electron. 12 (2011) 766-773.
[72] L. He, L. Duan, J. Qiao, R. J. Wang, P. Wei, L. D. Wang, Y. Qiu, Adv. Funct. Mater. 18 (2008) 2123-2131.
[73] J. Ye, Z. Chen, M. K. Fung, C. Zheng, X. Ou, X. Zhang, Y. Yuan, C. S. Lee, Chem. Mater. 25 (2013) 2630-2637.
[74] T. H. Huang, J. T. Lin, L. Y. Chen, Y. T. Lin, C. C. Wu, Adv. Mater. 18 (2006) 602-606.
[75] M. Y. Lai, C. H. Chen, W. S. Huang, J. T. Lin, T. H. Ke, L. Y. Chen, M. H. Tsai, C. C. Wu, Angew. Chem. Int. Ed. 47 (2008) 581-585.
[76] S. L. Lin, L. H. Chan, R. H. Lee, M. Y. Yen, W. J. Kuo, C. T. Chen, R. J. Jeng, Adv. Mater. 20 (2008) 3947-3952.
[77] C. Liu, Y. Gu, Q. Fu, N. Sun, C. Zhong, D. G. Ma, J. G. Qin, C. L. Yang, Chem. Eur. J. 18 (2012) 13828-13835.
[78] M. C. Ho, C. H. Chao, C. H. Chen, R. J. Wu and W. T. Whang, Macromolecules. 45 (2012) 3010-3016.
[79] K. L. Chan, M. J. McKiernan, C. R. Towns and A. B. Holmes, J. Am. Chem. Soc. 127 (2005) 7662-7663.

Chapter 3

Synthesis and Photovoltaic Performance of D-A structure Narrow Bandgap Copolymers Based on Benzo[*def*]carbazole

3.1 Background

With the increasing of power consumption, renewable sources have attracted much attention. Solar power is one promising renewable source which has the possible to have a significant impact on lowering the demand for electricity produced by fossil fuels. Polymer solar cells (PSCs) (Fig.2-1) offer great potential as renewable, alternative source for electrical energy due to their light weight, low cost, solution processablity, flexibility, and the synthetic versatility, which can convert solar energy into electrical energy via the photovoltaic effect [1-4]. Although the PSCs are similar to traditional silicon based solar cells in function, the mechanisms of PSCs generated differs significantly.

Fig. 3-1 Application of PSCs [5, 6]

During the past ten years, PSCs have received much attention because of their unique advantages of low cost, light weight, and great potential for the realization of flexible and large-area devices. Typically, bulk heterojunction (BHJ) PSCs (Fig. 3-2) have dramatically improved the cells performance due to the unique merits such as the design and synthesis of novel donor materials, the control and optimization of device fabrication, and the development of new device architectures such as tandem and ternary solar cells. In the BHJ PSCs, blend layer of an electron-donating conjugated polymer and an electron-accepting fullerene derivative with phase separation in nanoscale is sandwiched between cathode and anode [7-9]. Compared to the bilayer device architecture, the BHJ structure can provide a much larger interfacial area due to the formation of interpenetrating network. It should be indicated that the interplay of these components in the heterojunction is among the most important aspects determining the properties of the PSCs. Compete with silicon-based solar cells, the current challenges for PSCs remain to further improve photovoltaic efficiency as well as durability and cost-effectiveness. Conjugated polymers show a potential alternative because (1) the synthesis of polymer is easy and cost-effective, (2) the polymers can be easily cast on a variety of substrates using wet-processing techniques such as spin-casting or even printing technologies, (3) the energy band gap can be easily modified by chemical structure, and (4) the strong absorptivity and high extinction coefficients of these semiconductor films can be achieved, which make them excellent chromophores for optoelectronic applications.

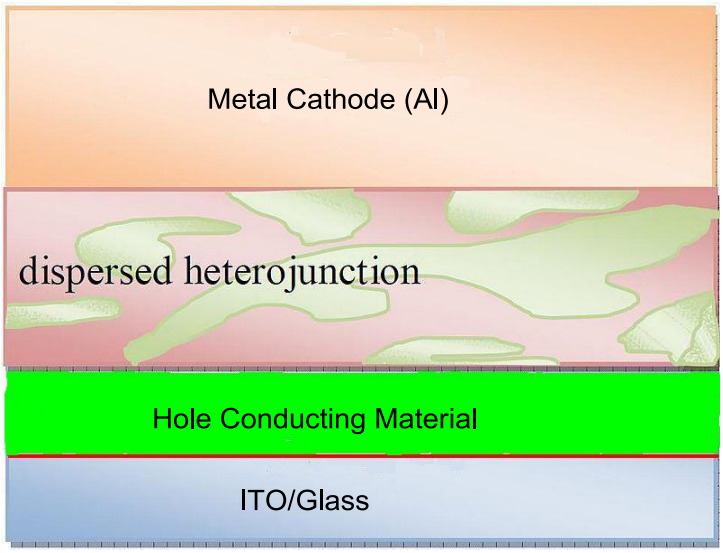

Fig. 3-2 Device architecture of BHJ PSCs [10]

The major objectives of the present study are:

1. Design, syntheses and characterization of new type of D-A-structure narrow bandgap copolymers
2. Clarifications of basic physical properties of these new copolymers
3. Preliminary investigation of the photovoltaic performance of the copolymers based on bulk heterojunction polymer solar cells

In order to obtain high-performance PSCs, it is necessary to design and synthesize conjugated polymers with desired properties, such as sufficient solubility to promise processing a good miscible thin-layer with an n-type material, high hole mobility for efficient charge transport, and narrow bandgap for matching the high photon flux region of the solar spectrum to ensure enough light harvesting, leading to an increase of short-circuit current (J_{sc}) [11-14]. It has been also known for using a polymer whose HOMO energy level is situated close to –5.5 eV [15] could lead to a large open-circuit voltage (V_{oc}) in PSCs devices [16]. Since these complicated factors in relation of trade-off, the developments of new polymers with proper properties of photoabsorption, energy levels, semiconducting, and stability have been a challenging research up to now.

A well known strategy to synthesize narrow bandgap polymers is to construct D-A type conjugated copolymers, which have a polymer backbone consisted of alternating electron donating (D) and electron accepting (A) units. Poly(2,7-carbazole-*alt*-dithienylbenzo thiadiazole) (**PCDTBT**) which was one of the most successful D-A type copolymers due to its deep energy level of HOMO and high stability against oxidation, was shown in Fig.3-3. According to the report, the power conversion efficiencies (PCEs) of **PCDTBT**-based PSCs with the standard devices configuration reached 4.6% [17]. Although the **PCDTBT**-based PSCs showed an outstanding high PCE, the band gap (E_g) of **PCDTBT** was larger than the typical narrow-bandgap copolymers which exhibited high photovoltaic performance [18]. A polycyclic aromatic compound, benzo[*def*]carbazole, is a unique building block with a large π-conjugation system and its electron-donating ability is suggested to be stronger than carbazole [19]. In general, a π-extended planar fused aromatic ring will be helpful for intensifying intermolecular π overlap and thus narrowing π-π stacking distance, which can contribute to enhancing charge carrier mobility. Furthermore, by introducing appropriate

substituents, the bridging nitrogen-atom in benzo[*def*]carbazole works as a center a center for solubilizing functionality and tuning of energy levels of molecular orbital [20]. Therefore, benzo[*def*]carbazole was selected as the donor unit to construct new D-A type copolymers.

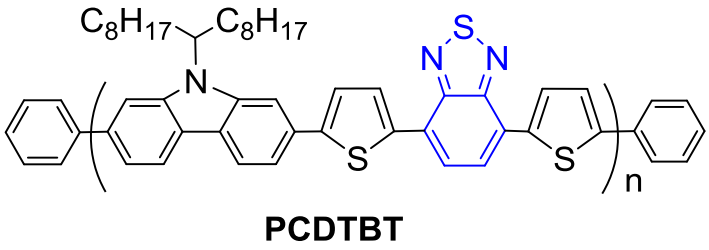

PCDTBT

Fig. 3-3.Chemical structure of **PCDTBT**

In this chapter, three D-A type of benzo[*def*]carbazole-based copolymers poly[4-(1-decylundecyl)-4*H*-benzo[*def*]carbazole-2,6-diyl-thiophene-2,5-diyl-2,1,3-benzothiadiazole-4,7-diyl-thiophene-2,5-diyl] (**PBCDTBT**), poly[4-(1-decylundecyl)-4*H*-benzo[*def*] carbazole-2,6-diyl-thiophene-2,5-diyl-5-(2-ethylhexyl) thieno[3,4-c]-pyrrole-4,6-dione-1,3-diyl-thiophene-2,5-diyl] (**PBCDTTPD**) and poly[4-(1-decylundecyl) -4*H*-benzo[*def*]carbazole-2,6-diyl-thiophene-2,5-diyl-2,5-didecylpyrrolo-[3,4-*c*]pyrrole-1,4-dione-3,6-diyl-th iophene-2,5-diyl] (**PBCBTDPP**), as shown in Fig. 3-4, were designed, synthesized and characterized. In this study, benzo[*def*]carbazole was chosen as the D unit, while benzothiadiazole (**BT**) having electronegative heterocyclic system, thienopyrrole-4,6-dione (**TPD**) having electron withdrawing imino-bridged system, and diketopyrrolopyrrole (**DPP**) having electron withdrawing pyrazolone system were selected as the typical A unit. The effects of the different A segment on the absorption spectra, energy levels, and the photovoltaic performances of the copolymers were also investigated.

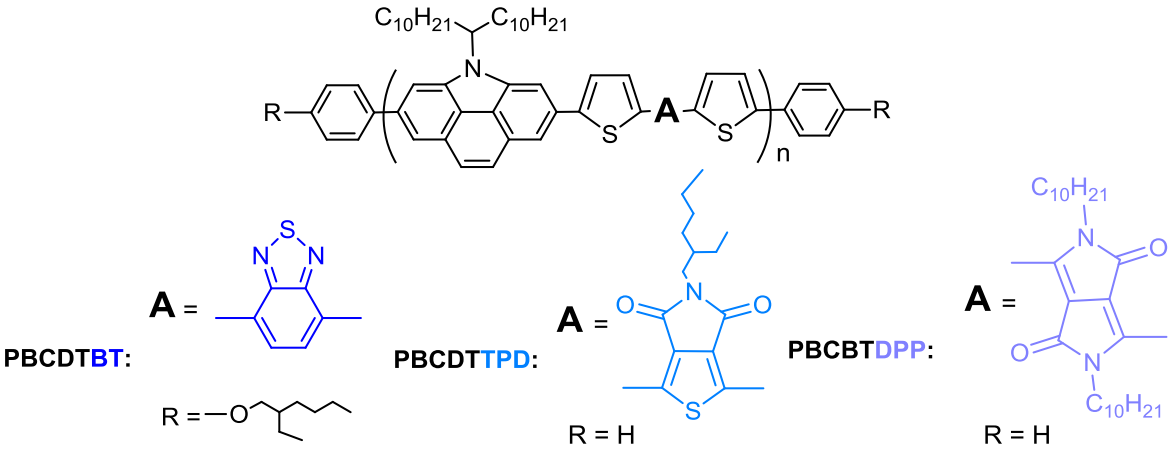

Fig. 3-4 Chemical structures of **PBCDTBT**, **PBCDTTPD** and **PBCBTDPP**

3.2 Results and Discussion

3.2.1 Synthesis

Scheme 3-1 showed the general synthetic routes toward the monomers and polymers. Coupling of **1** and bis(pinacolato)diboron with $PdCl_2$(dppf) as the catalyst was to synthesize the diboronic ester **2.** The dibromination of **3** was performed to give **4** by the procedure reported previously [21]. The alkyl group was introduced into N-position of **5** giving **6** by using K_2CO_3 and the corresponding alkyl bromide in the presence of catalytic amount of 18-crown-6. The dibromination of **6** was carried out with NBS, giving **7**. **PBCDTBT**, **PBCDTTPD**, and **PBCBTDPP** were synthesized by Suzuki coupling polymerization of **2** with the corresponding three acceptor units. For stabilization of the copolymers, an end-capping with phenyl or alkoxyphenyl was performed.

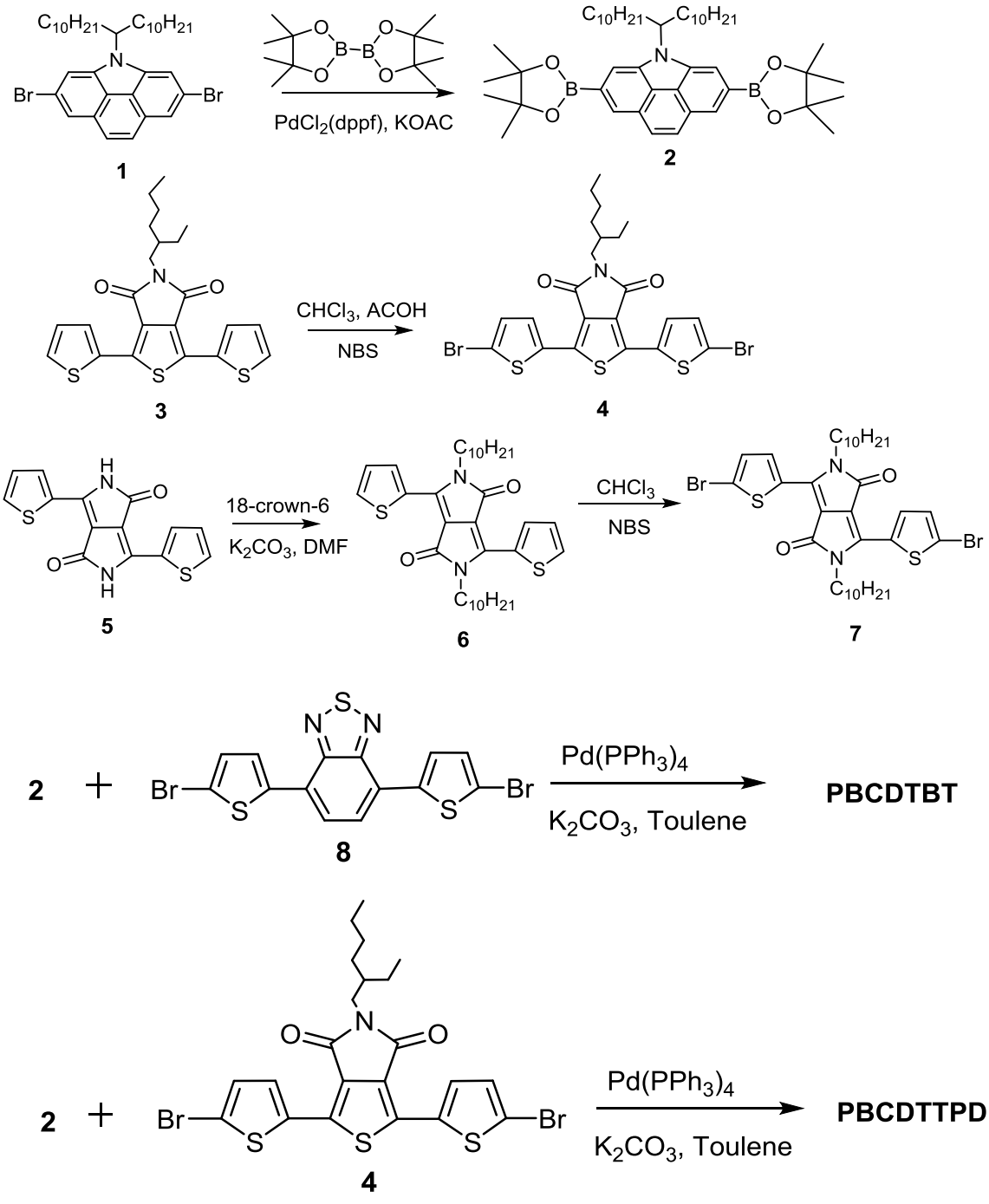

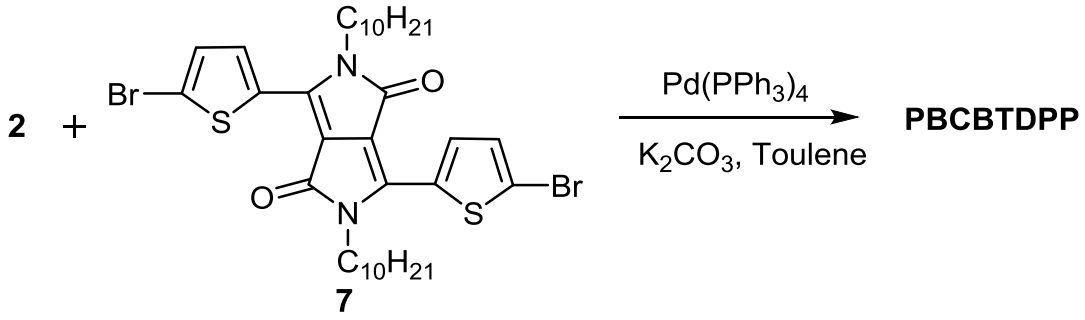

Scheme 3-1 Synthetic routes of **PBCDTBT**, **PBCDTTPD** and **PBCBTDPP**

3.2.2 Solubility and thermal stability

These copolymers showed good solubility in common organic solvents such as $CHCl_3$, o-dichlorobenzene, and chlorobenzene. All of the copolymers were identified by NMR and elemental analyses. The results of gel permeation chromatography (GPC) were summarized in Table 3-1. They showed good processability to make thin cast films. The M_n and M_w/M_n of **PBCDTBT**, **PBCDTTPD**, and **PBCBTDPP** were about 10 kg/mol and about 1, which were comparable each other and not so high but enough to investigate their basic properties and to examine basic characteristics of BHJ PSCs. The TGA results are shown in Fig.3-5. These polymers showed that temperature of 5 wt % loss in the TGA was around 350 °C, which suggeste that the thermal stability of these copolymers were good for making organic devices as well as the carbazole-based copolymers [22].

Table 3-1 GPC and TGA results of the polymers.

Polymer	M_n (kg mol^{-1})	M_w (kg mol^{-1})	M_w/M_n	T_d (°C)[a]
PBCDTBT	9.0	9.3	1.04	362
PBCDTTPD	7.0	7.5	1.03	326
PBCBTDPP	10.7	18.0	1.68	371

[a]Temperature of 5% weight loss determined by TGA under an argon atmosphere.

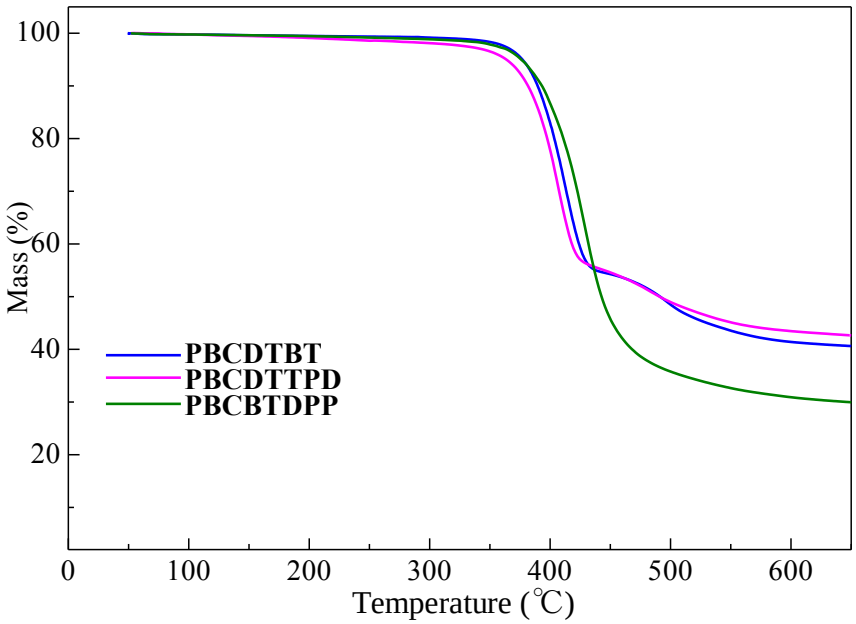

Fig. 3-5 TGA curves of **PBCDTBT**, **PBCDTTPD** and **PBCBTDPP**

3.2.3 Optical properties.

The UV-vis absorption spectra of dilute solution and thin films state of **PBCDTBT**, **PBCDTTPD** and **PBCBTDPP** were investigated, and the results are shown in Fig. 3-6. The UV-vis spectra data for all polymers are summarized in Table 3-2.

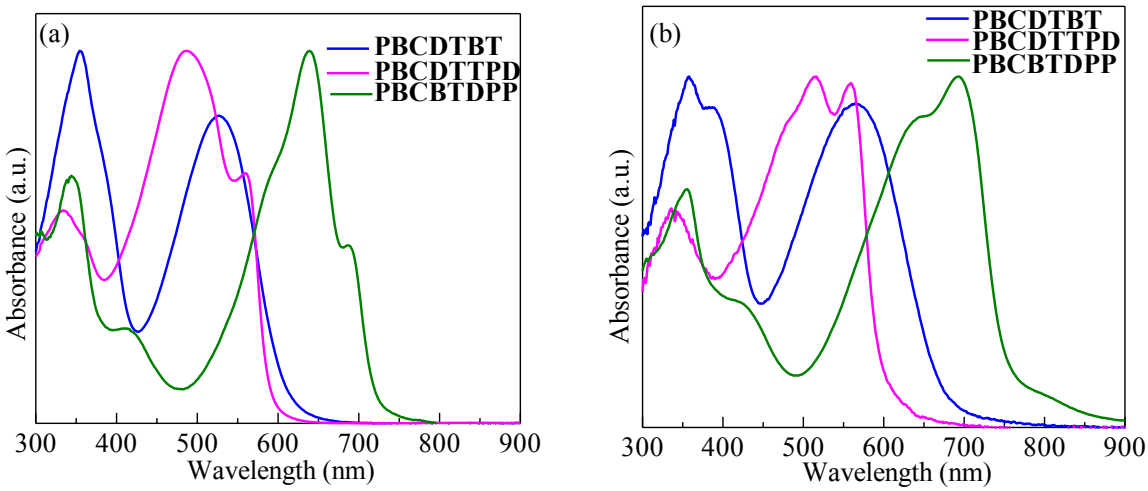

Fig. 3-6 UV-vis spectra of **PBCDTBT**, **PBCDTTPD** and **PBCBTDPP** in $CHCl_3$ (a) and film state (b)

All of the polymers in $CHCl_3$ exhibited two major absorption bands in the ranges of 300-400 and 450-750 nm, as shown in Fig. 3-6a. The bands at longer wavelength corresponds to the intramolecular charge transfer (CT) transition between the D and A units and the other at the shorter wavelength could be attributed to localized π-π* transition. The absorption maximum (λ_{max}) values in wavelength of these polymers were in order from longest to shortest of **PBCBTDPP, PBCDTBT, PBCDTTPD**. The **DPP** unit is found to have the strongest D-A effect in the series of benzocarbazole copolymers due to the degree of the red-shifts of D-A bands,

Table 3-2 Absorption spectrum data, HOMO-LUMO energy gaps, and the energy levels of the polymers.

Polymer	Abs. λ_{max} (nm)		E_g^{opt} (eV)	E_{HOMO} (eV)	E_{LUMO}[a] (eV)
	$CHCl_3$	film			
PBCDTBT	355, 527	358, 564	1.93	–5.22	–3.29
PBCDTTPD	337, 486	355, 516, 559	2.11	–5.34	–3.23
PBCBTDPP	344, 638	356, 694	1.68	–5.31	–3.63

[a] $E_{LUMO} = E_g^{opt} + E_{HOMO}$

The absorption spectra of three polymers in thin film state are shown in Fig 3-6b. The shape of the absorption bands in thin film state was similar to that in solution. Compared with the absorption maxima in solution, there were red-shifted by 37-63 nm in film state due to increase of coplanarity of polymer chains by alignment on a planar substrate and enhancement of π-π stacking of the planar units as well as the highly planar polymers in the solid film state [23]. The E_g^{opt} were estimated to be 1.68, 1.93, and 2.11 eV for **PBCDTBT**, **PBCDTTPD** and **PBCBTDPP**, respectively, from the absorption edges of the films. The difference of the E_g^{opt} of **PBCDTBT**, **PBCDTTPD** and **PBCBTDPP** affected by the D-A interaction suggests that light harvesting capabilities along with E_g^{opt} can be tuned by the D-A segments in the backbone of polymer, which is one of the efficient ways to design the PSCs materials by changing D and A.

The energy levels of HOMO (E_{HOMO}) and LUMO (E_{LUMO}) of **PBCDTBT**, **PBCDTTPD** and **PBCBTDPP** are summarized in Table 3-2. The E_{HOMO} of **PBCDTBT**, **PBCDTTPD** and **PBCBTDPP** were found to situate in the range from −5.34 to −5.22 eV, which would be moderately deep to offer relatively high V_{oc} when BHJ PSCs are constructed, accordingly the E_{LUMO} of these copolymers were situated from −3.63 to −3.23 eV suitable for efficient charge separation from copolymer to $PC_{70}BM$. These data indicate that the acceptor segments differently introduced in three polymers considerably affect on E_{LUMO} but little affect on E_{HOMO}. The E_{LUMO} of **PBCBTDPP** was –3.63 eV, which was deeper than those of **PBCDTBT** (–3.29 eV) and **PBCDTTPD** (–3.23 eV). The results suggest that the electron-accepting ability of the A units is in an order of **DPP** > **BT** ≈ **TPD**.

3.2.4 Photovoltaic Properties

These new copolymers could be expected to be good donor materials in PSCs, because **PBCDTBT**, **PBCDTTPD** and **PBCBTDPP** have the deep-lying E_{HOMO} and narrow band gaps. Therefore, the intrinsic photovoltaic properties of PSCs was carried out using **PBCDTBT**, **PBCDTTPD** and **PBCBTDPP** as the electron donors and $PC_{70}BM$ selected as an electron acceptor materials with a BHJ PSC device configuration of ITO/ PEDOT:PSS (40 nm)/ polymer:$PC_{70}BM$/ LiF (1 nm)/ Al (80 nm). $CHCl_3$ was chosen as the solvent to obtain the blended polymer active layer. BHJ PSCs based on various blend ratios of copolymers (**PBCDTBT**, **PBCDTTPD** and **PBCBTDPP**) and $PC_{70}BM$ were prepared and characterized.

The ratios of the polymers:$PC_{70}BM$ were changed from the optimal ratios, PCE dates as summarized in Table 3-3, and the surface morphologies were shown in Fig.3-7. The blend ratios of **PBCDTBT**:$PC_{70}BM$ at 1:3, **PBCDTTPD**:$PC_{70}BM$ at 1:3, and **PBCBTDPP**:$PC_{70}BM$ at 1:4 gave the optimal values for PSCs performances. The values of V_{oc}, J_{sc}, FF and PCE of the devices are summarized in Table 3-4. Fig, 3-8 showed the current density-voltage (*J*-*V*) curves for these devices measured under irradiation of AM 1.5 solar-simulated light (100 mW cm^{-2}).

Table 3-3 Characteristics of **PBCDTBT**, **PBCDTTPD** and **PBCBTDPP**-based PSCs[a]

Polymer	Polymer:$PC_{70}BM$ (weight ratio)	BHJ Thickness (nm)	J_{sc} (mA/cm^2)	V_{oc}(V)	FF	PCE (%)
PBCDTBT	1:4	64	5.63	0.68	0.32	1.20
PBCDTBT	1:3	61	6.41	0.67	0.33	1.42
PBCDTBT	1:2	69	5.52	0.69	0.30	1.14
PBCDTTPD	1:4	65	1.92	0.74	0.53	0.76
PBCDTTPD	1:3	64	2.52	0.77	0.50	0.98
PBCDTTPD	1:2	64	2.38	0.81	0.43	0.84
PBCDTTPD	1:1	64	2.29	0.90	0.36	0.75
PBCBTDPP	1:4	61	2.10	0.70	0.51	0.75
PBCBTDPP	1:3	65	2.17	0.69	0.48	0.72

[a] The average value calculated from the results of three PSCs with device structure of ITO/ PEDOT:PSS (40 nm)/ copolymer:$PC_{70}BM$/ LiF (1 nm)/ Al (80 nm).

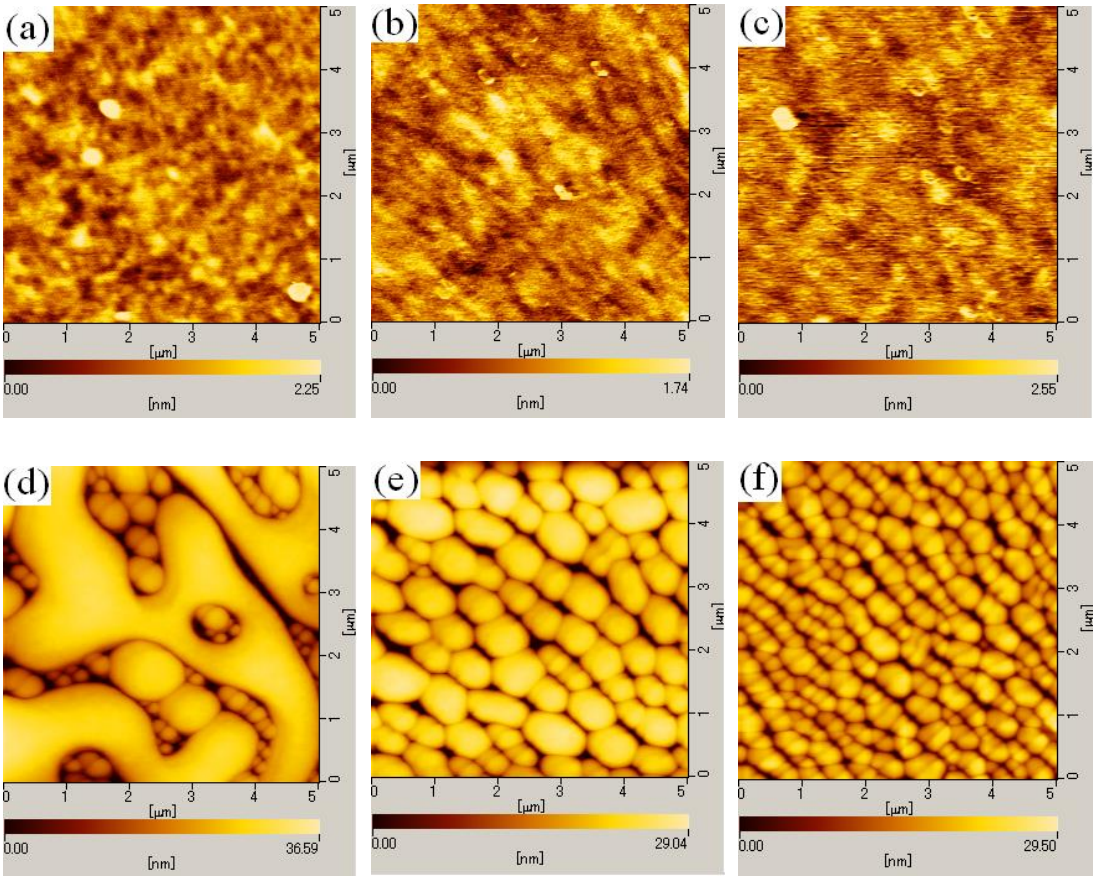

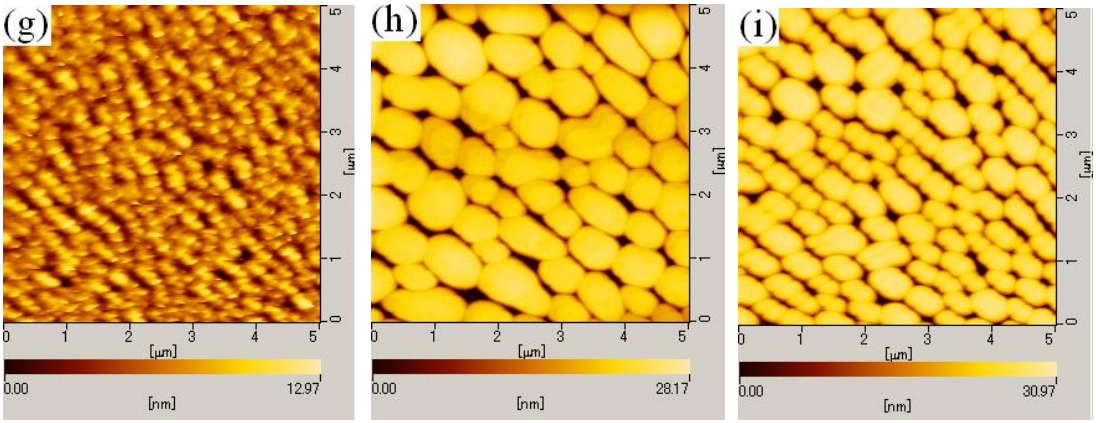

Fig 3-7. AFM images of the blend films of **PBCDTBT**:$PC_{70}BM$ (a) (1:4), (b) (1:3), (c) (1:2), **PBCDTTPD**:$PC_{70}BM$ (d) (1:4), (e) (1:3), (f) (1:2), (g) (1:1) and **PBCBTDPP**:$PC_{70}BM$ (h) (1:4), (i) (1:3).

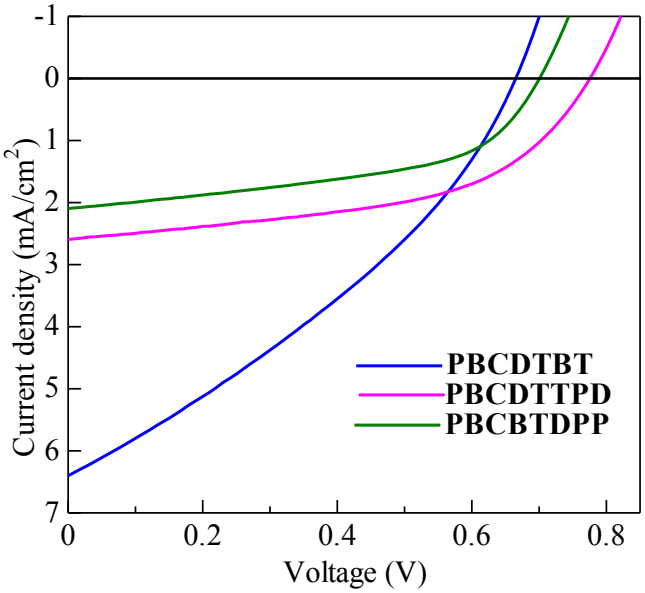

Fig. 3-8 *J*–*V* curves of BHJ solar cell of **PBCDTBT:**$PC_{70}BM$ (1:3), **PBCDTTPD:**$PC_{70}BM$ (1:3) and **PBCBTDPP:**$PC_{70}BM$ (1:4) irradiation of AM 1.5 solar-simulated light (100 mW cm^{-2}).

The V_{oc} values of the copolymer-$PC_{70}BM$-OPV devices were in the order of largeness; **PBCDTTPD** (V_{oc}= 0.77 V) > **PBCBTDPP** (V_{oc}= 0.70 V) > **PBCDTBT** (V_{oc}= 0.67 V). This order could result from E_{HOMO} in shallow order of the polymers: **PBCDTTPD** (–5.34 eV) < **PBCBTDPP** (–5.31 eV) < **PBCDTBT** (–5.22 eV), since V_{oc} is related to difference between E_{LUMO} of an acceptor ($PC_{70}BM$) and E_{HOMO} of a donor (copolymers) [24].

Table 3-4 Characteristics of **PBCDTBT**, **PBCDTTPD** and **PBCBTDPP**-based PSCs[a]

Polymer	Polymer:$PC_{70}BM$ (weight ratio)	BHJ Thickness (nm)	J_{sc} (mA/cm^2)	V_{oc} (V)	FF	PCE (%)
PBCDTBT	1:3	61	6.41	0.67	0.33	1.42
PBCDTTPD	1:3	64	2.52	0.77	0.50	0.98
PBCBTDPP	1:4	61	2.10	0.70	0.51	0.75

[a] All the data are an average value obtained from independent three PSC devices. The device structure: ITO/

PEDOT:PSS (40 nm)/ polymer:$PC_{70}BM$/ LiF (1 nm)/ Al (80 nm).

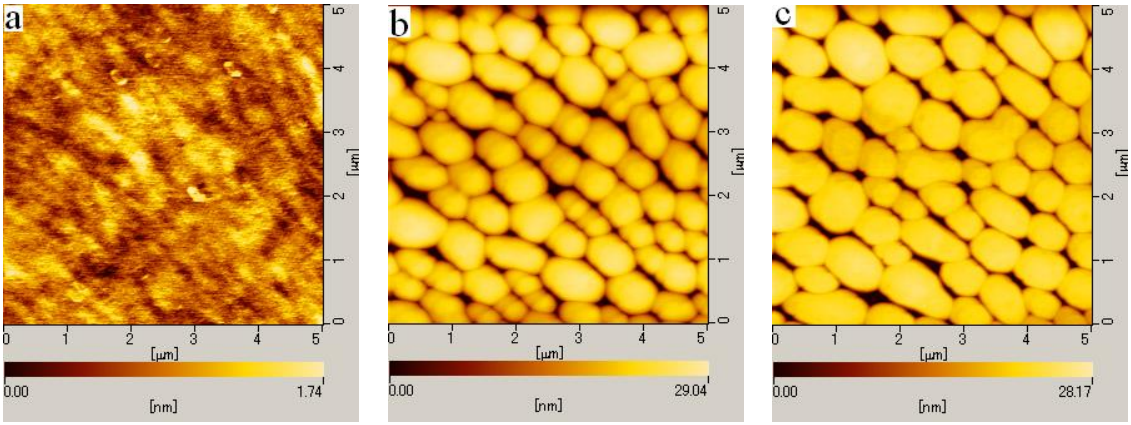

Fig. 3-9 AFM images of the blend films of (a) **PBCDTBT**:$PC_{70}BM$ (1:3), (b) **PBCDTTPD**:$PC_{70}BM$ (1:3), and (c) **PBCBTDPP**:$PC_{70}BM$ (1:4).

It has been proven that the morphology of blend films of the copolymers and $PC_{70}BM$ is a determining factor for photovoltaic properties. The phase separation in nanoscale which assists in forming an interpenetrating network between the donor and acceptor materials lead to efficient charge separation and carrier transport [25]. Thus, surface morphologies of the spin coating films were investigated by AFM, and the images are shown in Fig. 3-9. The blend film of **PBCDTBT**:$PC_{70}BM$ (1:3) showed smooth surface and well intimate mixing in nanoscale(Fig. 3-9a), meanwhile, a rough surface and pronounced phase separation in microscale were observed for **PBCDTTPD**:$PC_{70}BM$ (1:3) and **PBCBTDPP**:$PC_{70}BM$ (1:4) (Fig. 3-9b,c). Large globular domains in microscale were observed in the blend films of **PBCDTTPD**:$PC_{70}BM$ (1:3) and **PBCBTDPP**:$PC_{70}BM$ (1:4), which certainly reduced total area of heterojunction interface for exciton dissociation. As a results, the PSCs devices with phase separation in nanoscale led to the higher J_{sc} than **PBCDTTPD**:$PC_{70}BM$ (1:3) and **PBCBTDPP**:$PC_{70}BM$ (1:4) device with phase separation in microscale. These results suggest that that **PBCDTTPD** and **PBCBTDPP** were incompatible with $PC_{70}BM$ in the films cast from the $CHCl_3$ solutions, which might caused by steric hindrance of the side chain and polar amino- and imino structures in the A unit.

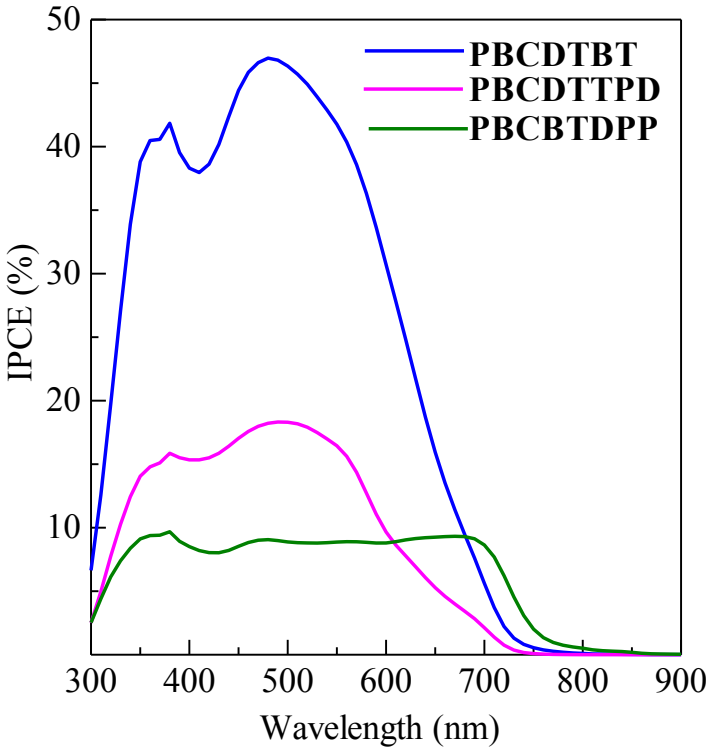

Fig. 3-10 IPCEs of the devices of **PBCDTBT**:$PC_{70}BM$ (1:3), **PBCDTTPD**:$PC_{70}BM$ (1:3), and **PBCBTDPP**:$PC_{70}BM$ (1:4)

Fig 3-10 shows the incident photon to current conversion efficiencies (IPCEs) curves of the devices of **PBCDTBT**:$PC_{70}BM$ (1:3), **PBCDTTPD**:$PC_{70}BM$ (1:3), and **PBCBTDPP**:$PC_{70}BM$ (1:4). All of the devices were found to show sensitization over the whole visible light region, which are consistent with the absorption spectra of the polymers. The **PBCDTTPD**:$PC_{70}BM$ (1:3) (maximum IPCE = 19 % at 490 nm) and **PBCBTDPP**:PC70BM (1:4) (maximum IPCE = 10 % at 380 nm)based BHJ PSCs displayed lower IPCE response than that of PSCs of **PBCDTBT**:$PC_{70}BM$ (1:3) (maximum IPCE = 47 % at 480 nm). The **PBCDTBT**:$PC_{70}BM$ (1:3) device showed higher IPCE response, which was attributed to phase separation in nanoscale, that should increase area of heterojunction interface for exciton dissociation.

3.3 Summary

In this work, three types of D-A copolymers, **PBCDTBT**, **PBCDTTPD** and **PBCBTDPP,** which consisted of the π-extended D of benzo[*def*]carbazole and three typical A, **BT**, **TPD**, and **DPP**, were successfully synthesized by Suzuki cross-coupling polymerization. These copolymers showed excellent solubility of **PBCDTBT**, **PBCDTTPD** and **PBCBTDPP** in most organic solvent along with good film-forming ability due to the long branched alkyl-chains at N-position of D unit. The strong intramolecular charge transfer band of the D and A units lead to UV-vis spectra measurements showed that these thin films covered the whole visible light absorption (from 300 to 800 nm). The benzo[*def*]carbazole unit with a high donor ability was used to narrow the band gap of the copolymers, however, the E_g of **PBCDTBT**, **PBCDTTPD** and **PBCBTDPP** were similar to those of corresponding carbazole-**TBT**, -**TTPD** and -**TDPP** [26, 27, 28]. Compared to the corresponding carbazole-based coplymers, the E_{HOMO} values of **PBCDTBT** and **PBCDTTPD** were shallower [27, 28], these tendency

has been observed similarly in the case of benzocarbazole-based homopolymers [29]. On the other side, **PBCBTDPP** exceptionally showed a deep-lying $E_{HOMO.}$ Preliminary evaluation of the **PBCDTBT:**$PC_{70}BM$ (1:3) based BHJ PSCs exhibited PCE of 1.42 %, which was the highest value after optimization. The moderate PCE was owe to immiscibility of the polymer and $PC_{70}BM$ in the film state after thin film forming, which reduce efficiency of charge separation of exciton and carrier transport paths. Practically, the morphology of **PBCDTTPD**:$PC_{70}BM$ (1:3) and **PBCBTDPP**:$PC_{70}BM$ (1:4) showed pronounced phase separation in microscale, which lead to the PCE values lower than 1 %. Therefore, improvement of the miscibility of the copolymers with $PC_{70}BM$ should be an imperative solution to increase the performance of PSCs.

3.4 Experimental

3.4.1 General method and instrumentation

Column chromatography was performed using a silica gel (Kanto Chem., 60 N, 63–120 mm). UV-Vis measurements of the polymer samples in $CHCl_3$ and in a form of a thin film coating on a quartz glass were performed using a Shimadzu UV-1800 spectrophotometer (Hitachi). NMR spectra were recorded on a JEOL JNM-ECS 400 spectrometer.^{1}H and ^{13}C chemical shifts are given in units of δ (ppm) relative to δ (TMS) = 0.00 and δ($CDCl_3$) = 77.0 ppm, respectively. The atomic force microscopy (AFM) measurement of the surface morphology of samples was conducted on a Nanocute (SII NanoTechnology Inc.) in tapping mode. The number-average molecular weight (M_n) and the weight-average molecular weight (M_w) of the polymers were estimated by Shimadzu LCsolution GPC using polystyrene standards in $CHCl_3$. Thermogravimetric analysis (TGA) was performed under argon at a heating rate of 10 °C min^{-1} with a Seiko EXSTAR7000. HOMO energy levels of polymers were estimated by photoelectron yield spectroscopy (PYS) using an AC-3 spectrometer (Riken Keiki). Elemental analyses were carried out with a Perkin-Elmer type 2400 apparatus.

3.4.2 Fabrication and measurement of solar cell devices

The solar cells were fabricated in the configuration of ITO/PEDOT:PSS/polymers:$PC_{70}BM$/LiF/Al. The patterned ITO (conductivity: 10 Ω/square) glass was precleaned by ultrasonication in acetone and successively in ethanol. The precleaned ITO glass was treated in an ultraviolet-ozone chamber. A thin layer (40 nm) of PEDOT:PSS was spin-coated on the ITO at 3000 rpm and air-dried at 110 °C for 10 min on a hot plate. The substrate was transferred to a glovebox and redried at 110 °C for 10 min on a hot plate under N_2 atmosphere. Solutions of the polymers and $PC_{70}BM$ at various blending ratios in $CHCl_3$ were subsequently spin-coated on the PEDOT:PSS layer. The BHJ layers were dried at 110 °C for 10 min. LiF (1 nm) and Al (80 nm) were deposited on the BHJ layer with conventional thermal evaporation at the chamber pressure lower than 5×10^{-4} Pa, which provided the devices with an active area of 2×5 mm^2. The thickness of BHJ and PEDOT:PSS layers were measured using an automatic microfigure measuring instrument (Surfcorder ET200, Kosaka Laboratory Ltd.). The current density-voltage (J-V) curves were measured using an ADCMT 6244 DC voltage current source/monitor under AM 1.5 solar-simulated light irradiation of 100 mW cm^{-2} (P_{in}) (OTENTO-SUN III, Bunkoh-Keiki Co., Ltd.). The PCEs of a solar cells based on the polymers were determined by the equation of PCE = ($J_{sc} \times V_{oc} \times$ FF)/ (P_{in}), where J_{sc}, V_{oc}, and FF are short-circuit current, open-circuit voltage and fill factor. These organic photovoltaic parameters were calculated at the average of the measured results of three PSCs. The incident photon to current conversion efficiencies (IPCEs) were measured using an SM-250 system (Bunkoh-Keiki Co., Ltd.).

3.4.3 Materials

Reagents and solvents were purchased from Kanto Chemical, Tokyo Chemical Industry, Aldrich and Nacalai Tesque Inc. 5-(2-ethylhexyl)-1,3-di-2-thienyl-4*H*-thieno[3,4-*c*] pyrrole-4,6-dione **3** [30] and 4,7-bis(5-bromo-2-thienyl)-2,1,3-benzothiadiazole **8** [31] were synthesized according to the procedures reported previously. 2,6-Dibromo-4-(1-decylundecyl)-4*H*-benzo[*def*]carbazole **1** was synthesized following our another report [29]. The other solvents and all commercially available reagents were used without further purification.

3.4.4 Synthesis of monomers and polymers

Synthesis of 2,6-bis(4,4,5,5-tetramethyl-1-3-2-dioxaborolan-2-yl)-4-(1-decylundecyl)-4H-benzo[def]carbazole (**2**). A mixture of **1** (1.07 g, 1.71 mmol), potassium acetate (1.18 g, 12 mmol), bis(pinacolato)diboron (1.04 g, 4.12 mmol), and 1,1'-bis(diphenylphosphino)ferrocene]dichloropalladium(II) ($PdCl_2$(dppf)) (0.086g, 0.24 mmol) in dioxane (30 mL) was stirred at 80 °C for one day under argon atmosphere. After cooling to ambient temperature, the mixture solution was mixed with water. After extraction with dichloromethane, drying over $MgSO_4$ and the solvent evaporation, the crude product was purified by column chromatography using hexane/dichloromethane (1:1, v/v) as an eluent to give a pure white solid (1.1g, 90 %). ^{1}H NMR (400 MHz, $CDCl_3$) δ [ppm]: 8.26 (s, 2H), 8.02 (s, 2H), 7.97 (s, 2H), 4.80-468 (br, 1H), 2.42-2.38 (m, 2H), 2.06-2.01 (m, 2H), 1.47 (s, 24H), 1.26-1.11 (m, 32H), 0.88-0.82(m, 6H). ^{13}C NMR (100 MHz, $CDCl_3$) δ [ppm]: 138.6, 132.3, 127.5, 126.3, 123.7, 121.8, 114.2, 83.8, 57.7, 34.6, 31.8, 31.6, 29.5, 29.4, 29.3, 29.2, 26.8, 24.9, 22.6, 14.1.

Synthesis of 1,3-bis(5-bromothiophen-2-yl)-5-(2-ethylhexyl)-5H-thieno[3,4-c] pyrrole-4,6-dione (**4**). Excess N-bromosuccinimide (NBS) (0.45 g, 2.5 mmol) was added to the mixture of **3** (0.43 g, 2.07 mmol) in chloroform (19 mL), followed by addition of acetic acid (1.2 mL). The solution was kept at ambient temperature for whole night. After extraction with dichloromethane from water, drying over $MgSO_4$ and the solvent evaporation, the crude product was purified by column chromatography (silica gel, dichloromethane/hexane, 1:4, as eluent) to afford a yellow solid (0.55 g, 94 %).^{1}H NMR (400 MHz, $CDCl_3$) δ [ppm]: 7.66 (d, J= 4.4 Hz 2H), 7.08 (d, J= 4.4 Hz 2H), 3.55 (d, J= 7.2 Hz 2H), 1.84-1.81 (m, 1H), 1.33-1.27 (m, 8H), 0.92-0.87 (m, 6H). ^{13}C NMR (100 MHz, $CDCl_3$) δ [ppm]: 162.7, 135.4, 133.7, 131.1, 129.8, 128.8, 116.7, 42.6, 38.3, 30.6, 28.5, 27.5, 23.9, 23.0, 14.1.

Synthesis of 2,5-didecyl-3,6-di(thiophen-2-yl)pyrrolo[3,4-c]pyrrole-1,4(2H,5H)-dione (**6**). A mixture of **5** (0.12 g, 0.4 mmol), potassium carbonate (0.18 g, 1.32 mmol), 1-Bromodecane (0.29 g, 1.3 mmol) and 18-crown-6 (0.001 g, 0.013 mmol) in DMF (2 mL) was stirred at 80 °C for 12 h, and then cooled to ambient temperature slowly. The precipitates were collected by filtration and were redissolved in chloroform (20 mL). The mixture solution was mixed with water. After extraction with dichloromethane, drying over $MgSO_4$ and the solvent evaporation, the crude product was purified by column chromatography (silica gel, chloroform:hexane, 1:1, as eluent) to yield a dark reddish brown solid (0.15g, 64 %). ^{1}H NMR (400 MHz, $CDCl_3$) δ [ppm]: 8.92 (d, J= 5.2 Hz 2H), 7.64 (d, J= 5.2 Hz 2H), 7.28 (t, J= 5.2 Hz 2H), 4.07 (t, J= 8 Hz 4H), 1.75-1.73 (m, 4H), 1.41-1.25 (m, 28H), 0.89-0.85(m, 6H). ^{13}C NMR (100 MHz, $CDCl_3$) δ [ppm]: 161.3, 140.0, 135.2, 130.6, 129.8, 128.6, 107.6, 42.2, 31.8, 30.2, 29.5, 29.4, 29.3, 29.2, 26.8, 22.6, 14.1.

Synthesis of 3,6-bis-(5-bromo-thiophen-2-yl)-2,5-didecyl-pyrrolo[3,4-c]pyrrole-1,4-dione (**7**). N-bromosuccinimide (0.11 g, 0.58 mmol) was added to the mixture of **6** (0.15 g, 0.26 mmol) in chloroform

(48 mL), which was covered with aluminum foil. The reaction solution was stirred for two days at ambient temperature. After extraction with dichloromethane, drying over $MgSO_4$ and the solvent evaporation, the crude product was purified by column chromatography using an eluent of dichloromethane:hexane (1:1, v/v) to yield a dark reddish brown solid (0.12 g, 63 %). ^{1}H NMR (400 MHz, $CDCl_3$) δ [ppm]: 8.68 (d, J= 4.8 Hz 2H), 7.24 (d, J= 4.8 Hz 2H), 3.98 (t, J= 7.6 Hz 4H), 1.73-1.70 (m, 4H), 1.40-1.25 (m, 28H), 0.89-0.86(m, 6H).

Synthesis of poly[4-(1-decylundecyl)-4H-benzo[def]carbazole-2,6-diyl-thiophene-2,5-diyl-2,1,3-benzothiadiazole-4,7-diyl-thiophene-2,5-diyl] (**PBCDTBT**). Suspension of **2** (0.147 g, 0.2mmol), **8** (0.091 g, 0.2 mmol), tetrakis(triphenylphosphine) palladium ($Pd(PPh_3)_4$, 12 mg) and aqueous K_2CO_3 (2 M, 0.5 mL) in 2 mL of toluene was heated reflux with vigorous stirring for 72 h under an argon atmosphere. The solution was added **2** (0.02 mmol) and stirred for 2 h, and then 1-bromo-4-[(2-ethylhexyl)oxy]-benzene (0.02 mmol) was added and refluxed for whole night to finish the end-capping reaction. After the reaction mixture was cooled to ambient temperature, the resultant precipitate was firstly precipitated from methanol/HCl aq, and reprecipitated from methanol/NH_3 aq and from methanol, respectively. The polymer was successively washed and extracted with acetone, hexane and chloroform by Soxhlet extraction. The chloroform extract was again precipitated from methanol. The final product was dried under vacuum overnight, giving a dark red solid (0.040 g, 27 %). ^{1}H NMR (400 MHz, $CDCl_3$) δ [ppm]: 8.12-8.10 (m, 2H), 8.09-8.03 (m, 2H), 7.94-7.71 (br, 4H), 7.60-7.47 (br, 4H), 4.75 (br, 1H), 2.49-2.47 (br, 2H), 2.13-2.12 (br, 2H), 1.48-0.91 (br, 40 H), 0.90-0.79 (br, 6H). $C_{49}H_{57}N_3S_3$ (735.61): Calcd. C 75.25, H 7.33, N 5.36; Found. C 74.42, H 7.71, N 5.23.

Synthesis of poly[4-(1-decylundecyl)-4H-benzo[def]carbazole-2,6-diyl-thiophene-2,5-diyl-5-(2-ethylhexyl)thieno[3,4-c]pyrrole-4,6-dione-1,3-diyl-thiophene-2,5-diyl] (**PBCDTTPD**). Under an argon atmosphere, a suspension of **2** (0.118 g, 0.16 mmol), aqueous K_2CO_3 (2M, 0.45 mL), **4** (0.094 g, 0.16 mmol) and $Pd(PPh_3)_4$ (10 mg) in 1.5 mL of toluene was heated reflux with vigorous stirring for 72 h. Then, bromobenzene (1.5 μL, 0.016 mmol) was added and stirred for 2 h, phenylboronic acid (3.9 mg, 0.016 mmol) was added and the reaction refluxed for whole night to finish the end-capping reaction. After the reaction solution was cooled to ambient temperature, the resultant precipitate was precipitated from methanol/HCl aq, and reprecipitated from methanol/NH_3 aq and from methanol, respectively. The polymer was successively washed and extracted with acetone, hexane and chloroform by Soxhlet extraction. The chloroform extract was again precipitated from methanol. The final product was dried under vacuum overnight, giving a deep red solid (0.052 g, 38 %). ^{1}H NMR (400 MHz, $CDCl_3$) δ [ppm]: 8.07 (br, 2H), 7.84-7.51 (m, 8H), 4.85 (br, 1H), 3.85-3.49 (m, 2H), 2.37-2.04 (br, 4H), 1.48-0.72 (br, 52H). $C_{57}H_{72}N_2O_2S_3$ (864.70): Calcd. C 74.95, H 7.95, N 3.07; Found. C 72.96, H 7.76, N 2.29.

Synthesis of Poly[4-(1-decylundecyl)-4H-benzo[def]carbazole-2,6-diyl-thiophene-2,5-diyl-2,5-didecylpyrrolo[3,4-c]pyrrole-1,4-dione-3,6-diyl-thiophene-2,5-diyl] (**PBCBTDPP**). According to procedure of the synthesis of **PBCDTTPD,** starting with **2** (0.14 mmol, 0.09 g) and **7** (0.14 mmol, 0.09 g) to afford a deep blue solid (0.121 g, 93 %). ^{1}H NMR (400 MHz, $CDCl_3$) δ [ppm]: 9.11-9.10 (m, 2H), 8.10-7.90 (m, 2H), 7.83-7.41 (m, 6H), 4.74-4.71 (m, 1H), 4.26-4.21 (m, 4H), 2.45-2.43 (m, 2 H), 1.44-1.14 (br, 46 H), 0.96-0.80 (br, 12H). $C_{69}H_{97}N_3O_2S_3$ (1063.28): Calcd. C 77.84, H 9.18, N 3.95; Found. C 72.82, H 8.46, N 3.11.

^{1}H NMR spectra of **PBCDTBT**

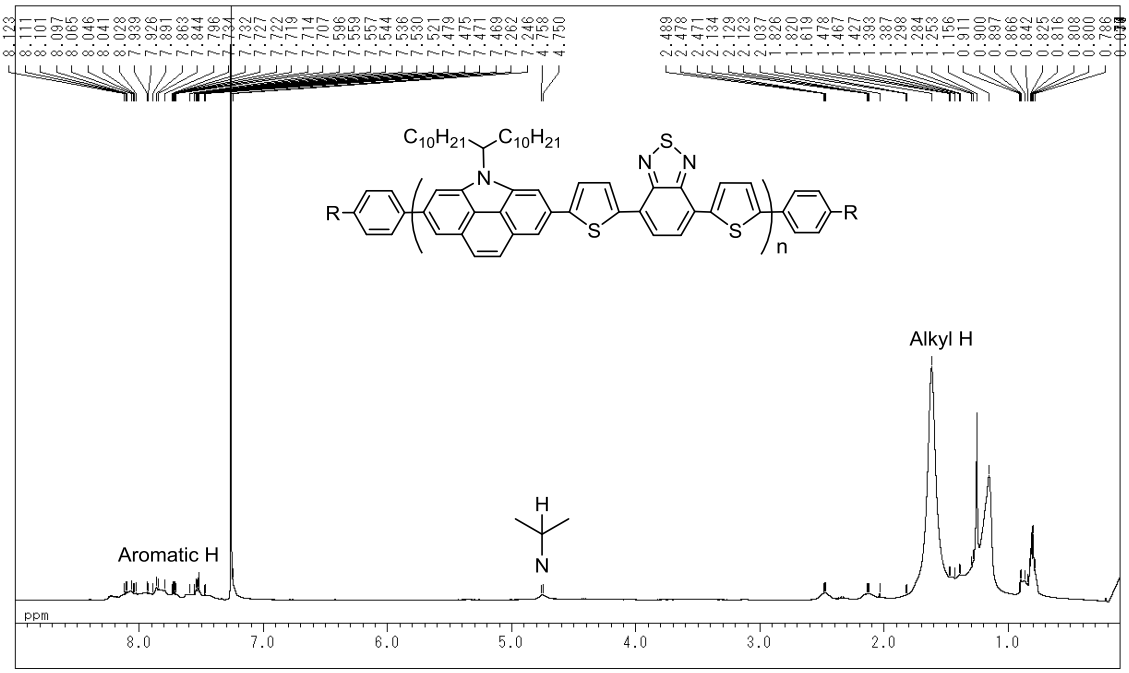

^{1}H NMR spectra of **PBCDTTPD**

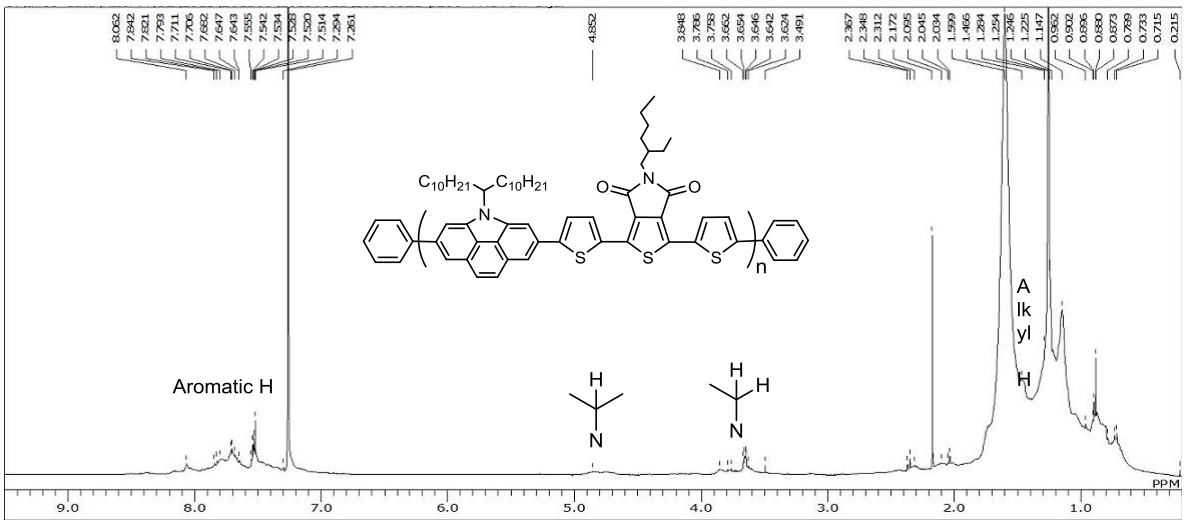

^{1}H NMR spectra of **PBCBTDPP**

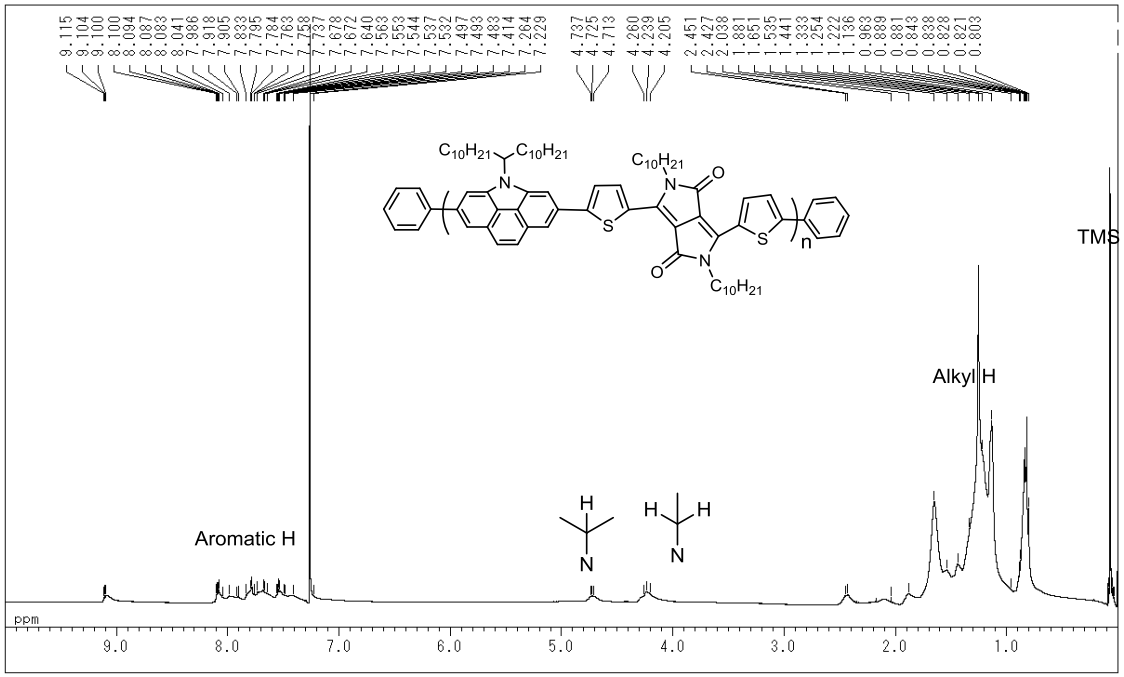

References

[1] G. Li, R. Zhu, Y. Yang, Nat. Photonics. 6 (2012) 153-161.

[2] G. Dennlen, M. C. Scharber, C. Brabec, J. Adv. Mater. 21 (2009) 1323-1338.

[3] H. Zhou, L. Yang, W. You, Macromolecules. 45 (2012) 607-632.

[4] K. M. Coakley, M. D. McGehee, Chem. Mater. 16 (2004) 4533-4542.

[5] https://en.wikipedia.org/wiki/File:SolarFachwerkhaus.jpg

[6] https://en.wikipedia.org/wiki/File:Ombri%C3%A8re_SUDI_-_Sustainable_Urban_Design_%26_Innovation.jpg

[7] S. Shaheen, C. J. Brabec, N. S. Sariciftci, F. Padinger, T. Fromherz, J. C. Hummelen, Appl. Phys. Lett. 78 (2001) 841-843.

[8] J. Chen, Y. Cao, Acc. Chem. Res. 42 (2009) 1709-1718.

[9] F. Huang, K. S. Chen, H. L. Yip, S. K. Hau, O. Acton, Y. Zhang, J. Luo, A. K. Y. Jen, J. Am. Chem. Soc. 131 (2009) 13886-13887.

[10] https://en.wikipedia.org/wiki/File:Fig_4_sketch_of_dispersed_junction_photovoltaic_cell.JPG.

[11] J. S. Wu, Y. J. Cheng, M. Dubosc, C. H. Hsieh, C. Y. Chang, C. S. Hsu, Chem. Commun. 46 (2010) 3259-3261.

[12] Z. Deng, L. Chen, F. Wu, Y. Chen, J. Phys. Chem. C. 118 (2014) 6038-6045.

[13] L. Wang, Y. Fu, L. Zhu, G. Cui, F. Liang, L. Guo, X. Zhang, Z. Xie, Z. Su, 52 (2011) 1748-5174.

[14] H. Zhou, L. Yang, S. Stoneking, W. You, ACS. Appl. Mater. Interfaces. 2 (2010) 1377-1383.

[15] A. J. Heeger, Chem. Soc. Rev. 39 (2010) 2354-2371.

[16] S. M. Park, Y. Yoon, C. W. Jeon, H. Kim, M. J. Ko, D. K. Lee, J. Y. Kim, H. J. Son, S. K. Kwon, Y. H. Kim, B. S. Kim, J. Polym. Sci., Part A: Polym. Chem. 52 (2014) 796-803.

[17] S. Wakim, S. Beaupré, N. Blouin, B.R. Aich, S. Rodman, R. Gaudiana, Y. Tao, M. Leclerc, J. Mater. Chem. 19 (2009) 5351-5358.

[18] L. Bian, E. Zhu, J. Tang, W. Tang, F. Zhang, Prog. Polym. Sci. 37 (2012) 1292-1331.

[19] F. Wu, L. Chen, H. Wang, Y. Chen, J. Phys. Chem. 117 (2013) 9581-9589.

[20] H. Chen, C. He, G. Yu, Y. Zhao, J. Huang, M. Zhu, H. Liu, Y. Guo, Y. Li, Y. Liu, J. Mater. Chem. 22 (2012) 3696-3698.

[21] Y. Q. Yang, H. Park, S. H. Lee, D. H. Kim, Y. S. Lee, Synth. Met. 176 (2013) 70-77.

[22] E. Zhou, J. Cong, S. Yamakawa, Q. Wei, M. Nakamura, K. Tajima, C. Yang, K. Hashimoto, Macromolecules. 43 (2010) 2873-2879.

[23] K. Lu, C. A. Di, H. X. Xi, Y. Q. Liu, G. Yu, W. F. Qiu, H. J. Zhang, X. K. Gao, Y. Liu, T. Qi, C. Y. Du, D. B. Zhu, J. Mater. Chem. 18 (2008) 3426-3432.

[24] B. Minnaert, M. Burgelman, 15 (2007)741-748.

[25] L. M. Chen, Z. R. Hong, G. Li, Y. Yang, Adv. Mater. 21 (2009) 1434-1449.

[26] N. Blouin, A. Michaud, M. Leclerc, Adv. Mater. 19 (2007) 2295-2300.

[27] K. W. Song, M. H. Choi, J. Y. Lee, D. K. Moon, J. Ind. Eng. Chem. 20 (2014) 290-296.

[28] O. Kwon, J. Jo, B. Walker, G.C. Bazen, J. H. Seo, J. Mater. Chem. A. 1 (2013) 7118-7124.

[29] Z. M. Geng, K. Shibasaki, M. Kijima, Synth. Met. 213 (2016) 57-64.

[30] X. Guo, R. P. Ortiz, Y. Zheng, M. G. Kim, S. Zhang, Y. Hu, G. Lu, A. Facchetti, T.J. Marks, J. Am. Chem Soc. 133 (2011) 13685-13697.

[31] D. Patra, D. Sahu, H. Padhy, D. Kekuda, C. W. Chu, H. C. Lin, J. Polym. Sci. Part A: Polym. Chem. 48 (2010) 5479-5489.

Chapter 4

Conclusion

Chapter 4 Conclusion

In this thesis work, the motivation for this thesis was the synthesis, characterization and the testing of new, environmentally stable materials based on carbazole for blue-light emitting and photovoltaic applications.

In chapter 2 first section, a new series of N-alkyl and N-phenyl substituted poly(carbazole)s having an 4,5-ethenylene bridge, poly(4*H*-benzo[*def*]carbazole)s, were synthesized. Derivatives of poly(carbazole)s having an 4,5-ethylene bridge were also synthesized for comparison. These polymers were prepared from corresponding dibromo monomers by Ni(0)-catalyzed Yamamoto polycondensation. All of the polymers had good solubility in common organic solvents, enough high molecular weights to make thin films, amorphous nature in the solid state, and good thermal stability showing about 400 °C of temperature at 5 wt% loss in TGA. The band gaps of these homopolymers were in the range of 2.77-3.15 eV which were appropriate for bluish light emissions. The absorption and emission maxima of these homopolymers in $CHCl_3$ were in the ranges of 361-396 and 419-456 nm, respectively. The CIE(x, y) values of these polymers in $CHCl_3$ were almost identical to (0.15, 0.05) in the region of deep blue. In film state, CIE values poly(benzocarbazole)s (0.19, 0.21) shifted toward greenish blue but in the region of blue. The shift of the PL color is ascribed to the stronger intermolecular interaction between the larger planar units of poly(benzocarbazole)s as suggested in the XRD results. All of the polymers showed good fluorescence quantum efficiencies in $CHCl_3$. The energy levels of highest occupied molecular orbital of the poly(benzocarbazole)s were shallower than those of corresponding 4,5-ethylene bridged poly(carbazole)s. It is considered that poly(benzocarbazole)s have potential to be applied in OLEDs as blue-light emitting materials.

In second section, Three types of donor-acceptor copolymers were designed and synthesized by combination of an electron donor unit of carbazole/fluorene sequences and an electron acceptor azine unit such as 1,2,4,5-tetrazine and 1,3,5-triazine. They were well soluble in common organic solvents with the number average molecular weight (M_n) of 7.5, 7.0 and 14.5 kg mol^{-1}, respectively, and have good thermal stability showing about at 370 °C with 5 wt% loss in TGA. These copolymers exhibited intense blue photoluminescence with emission peak maxima at 438, 437 and 421 nm in $CHCl_3$, and 495, 451 and 422 nm in the film state, respectively. All of the polymers exhibited good fluorescence quantum efficiencies in $CHCl_3$ (Φ_{fl} = 0.62, 0.63, 0.97). Energy levels of the highest occupied molecular orbital and lowest unoccupied molecular orbital energy levels estimated by cyclic voltammetry were to be –5.47, –5.83, –6.0 eV and –2.70 –2.85, –2.88 eV, respectively. We fabricated the OLEDs devices that have a configuration of ITO/ PEDOT:PSS/ copolymer/ LiF/ Al using these polymers as the emitting layer materials, and investigated their EL performances for the first time. **PF-triAz** based OLEDs devices showed maximum brightness and the maximum current efficiencies were 536 cd/m^2 and 0.35 cd/A, respectively. According to above results, these D-A copolymers have a great potential to be applied in OLEDs as the blue-light emitting materials.

In third section, a new series of donor-π-acceptor type carbazole/fluorene-based copolymers with sulfone/phosphine oxide unit as electron acceptor to break π-conjugation in main chain for obtaining high efficiency and pure-blue emitting materials were designed and synthesized. All of these copolymers showed good solubility in common organic solvents, enough high molecular weights to make thin films, and good thermal stability showing about 380 °C of temperature at 5 wt% loss in TGA. The electroluminescence properties of these copolymers were investigated by fabricating light-emitting electrochemical cells devices that have a configuration of ITO/ PEDOT:PSS/ copolymer:ionic liquid/ Al. The device based on **PDFDSO** exhibited pure blue electroluminescence maximum centered at 434 nm with CIE coordinates of (0.17, 0.10), and maximum luminance and current efficiency have reached 1080 cd m^{-2} and 1.96 cd A^{-1} at 12.5 V. To our

knowledge, this result overall in one of the best reported blue polymer LECs, which suggests that it is an effective way for blue emission polymers by controlling the π-conjugation.

In chapter 3, three type of narrow bandgap copolymers by combination of a donor unit of benzo[*def*]carbazole with an acceptor unit of benzothiadiazole, thienopyrrole-4,6-dione, and 1,4-diketopyrrolopyrrole were successfully synthesized. Basic properties of these copolymers were investigated for the applications in bulk heterojunction polymer solar cells. Absorption spectra showed that these copolymers exhibited broad absorption bands in UV and visible regions from 350 to 800 nm with optical band gaps in the range of 1.68-2.11 eV, which overlapped with the major region of the solar spectrum. All of the copolymers showed energy levels of the highest occupied molecular orbital in the range of –5.22 eV to –5.34 eV, which could provide good air stability and high open circuit voltages in photovoltaic applications. Initial performances of these copolymers in bulk heterojunction photovoltaic devices showed power conversion efficiencies about 1 % under irradiation of AM 1.5 solar-simulated light (100 mW cm^{-2}). Benzo[*def*]carbazole is a kind of effective donor segment for the design of D-A type polymer solar cells according to initial performances of these copolymers.

Publications

List of publications

1) ZhongMin Geng, Masashi Kijima. Synthesis and Characterization of Fluorene-Based Polymers Having Azine Unit for Blue Light Emission. International Letters of Chemistry, Physics and Astronomy. 62 (2015) 21-28.
2) ZhongMin Geng, Kosuke Shibasaki, Masashi Kijima. Blue Photoluminescence N-substituted Poly(4*H*-benzo[*def*]carbazole)s. Synthetic Metal 213 (2016) 57-64.
3) ZhongMin Geng, Takeshi Yasuda, Masashi Kijima. Synthesis and Intrinsic Photovoltaic Properties of a Series of Narrow Bandgap D-A-Copolymers Based on Benzo[def]carbazole. Polymer (submitted for publication).
4) ZhongMin Geng, Gou Satou, Kazuhiro Marumoto, Masashi Kijima. D-π-A Polysulfones for Blue Electroluminescence. J. Mater. Chem. C (will be submit).

Patent, Oral Presentation and Posters

1) 木島 正志, 耿 忠民，佐野 夏博. <発光材料、発光素子> 特許 2015-096609, 2015, 05, 11.
2) ZhongMin Geng, Masashi Kijima. Synthesis and Characterization of Polycarbazoles Having Triazine Side Groups for OLEDs. International Workshop on Science and Patents (IWP) 2013, (Sep.5 2013, University of Tsukuba, Japan). IWP074.
3) ZhongMin Geng, Masashi Kijima. Synthesis and Characterization of Polymers Having Sulfone Unit for Blue Electroluminescence. International Workshop on Science and Patents (IWP) 2014, (Sep.5 2014, University of Tsukuba, Japan). IWP29.
4) ZhongMin Geng, Masashi Kijima. Efficient Blue Luminescence Donor Acceptor Type Copolymers Having Diphenylsulfone Unit. 2015. Polymer Preprints, Japan Vol. 64, No. 1. 2Pb062. The Society of Polymer Scienece, Japan (SPSJ), 64th SPSJ Annual Meeting. (May 27-29, 2015, Sapporo Convention Center Japan).
5) ZhongMin Geng, Gou Satou, Kazuhiro Marumoto, Masashi Kijima. Synthesis and Characterization of Polymers Having Phosphine Oxide unit for Blue Light Emitting Devices. International Workshop on Science and Patents (IWP) 2015, (Sep.4 2015, University of Tsukuba, Japan). IWP01.

Acknowledgements

This dissertation could not have been completed without the inspiration and assistance of many people. First and foremost, I would like to express my sincere gratitude to my doctoral advisor Professor Masashi Kijima for taking me as his PhD student in Materials Science. I want to thank him for his instruction, understanding and encouragement through the great three years. This work would not have been possible without his able guidance. I have learned not only a great number of concepts concerning the present thesis and science in general from him, but also a great deal about life.

I also gratefully acknowledge Professor Hiromasa Goto (University of Tsukuba) for inviting to give poster and oral presentations at IWP, which gave me a chance to communicate with others.

I would like to express my appreciation to Professor Kazuhiro Marumoto (University of Tsukuba) and Mr Sato Go. Under his help, I can successfully to fabricate OLEDs and LECs devices, and investigate the electroluminescent properties of all the devices.

I would also like to thank Professor Takeshi Yasuda (Photovoltaic Materials Unit, National Institute for Materials Science (NIMS)) for investigating photovoltaic properties of polymers applied in polymer solar cells, and enriching the knowledge of photovoltaic cells.

I also thank Professor Junpei Kuwabara(University of Tsukuba) for for attending my doctor examination and checking my doctor thesis.

I am very grateful to all the present and past members of Kijima lab for a lot of valuable discussions, help and enjoyment. I would like to thank Satoshi Kato, Tomohiro Okura, Kaito Suzuki, Takafumi Watanabe, Yasuyuki Kimura, Takeshi Shimada, Mari Watanabe, Hidenori Amano, Shinnosuke Okabe, Kazuya Yamada, Roan Ito, Yuki Okuda and Peng Wenli for all their help and for all the past time we experienced; Mr Fukuhara Toshi and Mr Shibasaski Kosuke for all the discussions from labwork to afterwork and all his generous help.

In addition, I would like to thank Chemical Analysis Division, Research Facility Center for Science and Technology, University of Tsukuba, for facilities of the NMR, elemental analysis, and TGA.

Finally, I am deeply indebted to my parents, my wife and my daughter for their love and support for the past three years.